

# **INAUGURAL-DISSERTATION**

submitted to the

Combined Faculties for the Natural Sciences and for Mathematics

of the Ruperto-Carola University of Heidelberg, Germany

for the degree of

Doctor of Natural Sciences

presented by

M.Sc. Sebastian Specht

born in Berlin

Oral examination: 22 July 2010



**The Small Heat Shock Protein Hsp42 Controls The  
Spatio-Temporal Organization Of Aggregated  
Proteins In *Saccharomyces Cerevisiae***

Referees: 1. Prof. Dr. Bernd Bukau  
2. Prof. Dr. Elmar Schiebel



## Summary

Stress-induced protein aggregation represents a major threat for cell survival and is also associated with various human disorders and cellular aging. The primary cellular response to aberrant protein conformations is the refolding of misfolded proteins by molecular chaperones or their elimination by AAA+ proteases. Once this first line of defense has been overrun, aggregated proteins are directed to specific compartments, thus protecting the cellular environment from potentially deleterious protein conformations. Organizing protein aggregates might also facilitate the recruitment of protein quality control components, thereby increasing the efficiency of aggregate removal in a subsequent phase. In *Saccharomyces cerevisiae* application of mild stress (37°C) results, upon inhibiting proteasomal degradation, in partitioning of misfolded proteins between two distinct compartments (Kaganovich, 2008). More mobile misfolded proteins, which are ubiquitylated and likely represent substrates for proteasomal degradation, are sequestered at the JUNQ (juxtannuclear quality control) compartment. Terminally aggregated, insoluble proteins are sorted to the peripheral IPOD (insoluble protein deposit) compartment that also harbors amyloidogenic proteins.

To gain further insight into the spatio-temporal organization of misfolded proteins in *Saccharomyces cerevisiae*, I analyzed the localization of stress-induced protein aggregates by employing various fluorescent reporter proteins that either misfold upon stress application or bind to aggregated proteins. Since little is known about cellular factors involved in the sorting of misfolded proteins, I performed a candidate approach and focused on the *Saccharomyces cerevisiae* small heat shock proteins (sHsps), namely Hsp26 and Hsp42. I identified Hsp42 as an essential factor in the formation of IPOD-like inclusions. In *hsp42Δ* cells misfolded proteins do not accumulate in peripheral inclusions, but seem to be re-directed to the JUNQ. As Hsp42 localizes specifically to IPOD-like inclusions, but is absent from the JUNQ compartment, the lack of peripheral aggregation foci is a direct effect of missing Hsp42, thus illuminating a novel function of sHsps in controlling the cellular sorting of damaged proteins. In contrast, the second *Saccharomyces cerevisiae* sHsp, Hsp26, does not affect aggregate sorting and is present in both JUNQ and IPOD-like compartments. Transferring the elongated N-terminal domain (NTD) of Hsp42 to Hsp26 enables Hsp26 partially to replace Hsp42 function in aggregate sorting. In contrast, Hsp42 deleted of its NTD is not able to restore the occurrence of peripheral inclusions in *hsp42Δ* cells. The NTD is thus a key determinant in contributing functional specificity to Hsp42. My data suggest that Hsp42 acts as an adaptor protein that co-aggregates efficiently with misfolded proteins. The sHsp might link such

complexes via its NTD to further, so far unknown, sorting factors. Thereby, protein inclusions might be directed to the actin cytoskeleton, which I demonstrate to be crucial for aggregate sorting to JUNQ and IPOD-like compartments. Nonetheless, Hsp42 function is restricted to amorphous aggregates, because the localization of amyloidogenic proteins to IPOD-like inclusions does not depend on Hsp42. Comparing the mobility and stability of aggregated proteins deposited at the JUNQ in wild-type and *hsp42Δ* cells revealed the JUNQ compartment of *hsp42Δ* cells to have a moderate increase in substrate mobility and be solubilized more rapidly by Hsp104. These findings suggest that the Hsp42-dependent sorting to IPOD-like compartments retards substrate resolubilization, thereby potentially reducing substrate load of the quality control system.

I also analyzed the spatio-temporal organization of protein aggregates in cells with intact proteasomal degradation during sublethal heat-stress and a subsequent recovery phase allowing for aggregate solubilization. Heat shock generates multiple aggregation foci that are distributed throughout the cell. Sorting of aggregated proteins to JUNQ and IPOD-like deposition sites does not occur upon return to physiological growth conditions. Instead, protein disaggregation takes places *in situ* and does not require an intact actin cytoskeleton. My data thus demonstrate that the applied stress condition has a profound impact on the organization of misfolded proteins.

Moreover, my findings disclose functional divergence of the *Saccharomyces cerevisiae* sHsps in the refolding and organization of heat shock-generated protein aggregates. Incorporation of Hsp26 facilitates the reactivation of aggregated proteins. In contrast, Hsp42 is not influencing protein refolding, but serves as a sorting factor essential for the persistence of protein inclusions in the cellular periphery.

## Zusammenfassung

Stress-induzierte Proteinaggregation stellt eine starke Gefährdung der Zellviabilität dar und ist mit verschiedenen menschlichen Krankheiten und Zellalterung assoziiert. Der erste zelluläre Schutzwall gegen anomale Proteinkonformationen besteht in der Rückfaltung der missgefalteten Proteine durch molekulare Chaperone und deren Elimination durch AAA+ Proteasen. Sobald der erste Schutzwall seine Funktion nicht mehr erfüllt, werden aggregierte Proteine zu bestimmten Orten im Zytosol geleitet. Dieser Prozess stellt den zweiten zellulären Schutzwall dar. Die Ablagerung von Proteinaggregaten in speziellen Kompartimenten schützt die zelluläre Umgebung vor potentiell gefährlichen Proteinstrukturen. Die Ablagerung könnte auch die Rekrutierung der Proteinqualitätskontrollmaschinerie erleichtern, wodurch ein späterer Aggregatabbau gefördert werden würde. In *Saccharomyces cerevisiae* führt die Applikation von mildem Hitzestress, bei gleichzeitiger Inhibition von proteasomalem Proteinabbau, zur Ablagerung von missgefalteten Proteinen in zwei unterschiedlichen Kompartimenten, einem juxt nuklearen JUNQ (juxt nucleolar quality control) und einem perivakuolären IPOD (insoluble protein deposit) Kompartiment (Kaganovich *et al.*, 2008). Der JUNQ enthält mobilere missgefaltete Proteine, die ubiquityliert sind und wahrscheinlich Substrate für proteasomalen Abbau darstellen. Der IPOD hingegen scheint terminal aggregierte, unlösliche Proteine zu beherbergen, einschließlich amyloidogener Proteine.

Um ein besseres Verständnis der räumlich-zeitlichen Organisation von missgefalteten Proteinen in *Saccharomyces cerevisiae* zu erlangen, habe ich die Lokalisation von stress-induzierten Proteinaggregaten verfolgt. Dafür habe ich von verschiedenen fluoreszenten Reportern Gebrauch gemacht, die entweder nach Stressapplikation selbst aggregieren oder an Proteinaggregate binden. Da wenig über zelluläre Faktoren bekannt ist, welche in der Ablagerung missgefalteter Proteine eine Rolle spielen, habe ich einen gerichteten Ansatz gewählt und mich auf die kleinen Hitzeschockproteine (sHsps) von *Saccharomyces cerevisiae*, Hsp26 und Hsp42, konzentriert. So habe ich Hsp42 als einen essentiellen Faktor für die Bildung IPOD-ähnlicher Strukturen identifiziert. In *hsp42Δ* Zellen akkumulieren missgefaltete Proteine nicht in peripheren Ablagerungen, sondern werden zum JUNQ dirigiert. Da Hsp42 ausschließlich in IPOD-ähnlichen Ablagerungen anzutreffen ist, nicht aber in JUNQ Kompartimenten, scheint das Fehlen peripherer Aggregatablagerungen in *hsp42Δ* Zellen eine direkte Konsequenz der Abwesenheit Hsp42s zu sein. Somit konnte eine neuartige Rolle der sHsps in der Aggregatablagerung aufgezeigt werden. Im Gegensatz dazu beeinflusst das zweite sHsp in *Saccharomyces cerevisiae*, Hsp26, die Aggregatablagerung

nicht. Hsp26 ist sowohl im JUNQ als auch in IPOD-ähnlichen Kompartimenten anzutreffen. Transferiert man die elongierte N-terminale Domäne (NTD) von Hsp42 auf Hsp26, so kann Hsp26 teilweise die Hsp42 Funktion in der peripheren Aggregatablagerung übernehmen. Im Gegensatz dazu kann eine NTD-deletierte Hsp42 Mutante nicht die periphere Aggregatablagerung in *hsp42Δ* Zellen wiederherstellen. Somit ist eine Schlüsselrolle der NTD in der Funktion von Hsp42 aufgezeigt. Man kann spekulieren, dass Hsp42 als Adaptorprotein fungiert, welches mit Substraten effizient coaggregiert. Die daraus resultierenden Komplexe könnten durch die Hsp42 NTD an bisweilen nicht identifizierte Sortierfaktoren gekoppelt werden. Dadurch könnten Proteinaggregate an das Aktinzytoskelet gebunden werden, welches ich als essentielle Komponente für die Aggregatablagerung in JUNQ und IPOD-ähnlichen Kompartimenten identifiziert habe.

Vergleicht man die Mobilität und Stabilität missgefalteter Proteine im JUNQ von wildtyp und *hsp42Δ* Zellen, so wird für *hsp42Δ* JUNQ Kompartimente eine moderate Erhöhung der Substratmobilität und schnellere Auflösung durch Hsp104 ersichtlich. Somit scheinen die Hsp42-abhängigen IPOD-ähnlichen Ablagerungen zu einer verlangsamten Solubilisierung von Substraten zu führen, was eine verringerte Substratmenge für die Proteinqualitätskontrollmaschinerie nach sich ziehen könnte. Hsp42 spielt jedoch nur eine Rolle in der Organisation amorpher Aggregate, da die Ablagerung von amyloidogenen Aggregaten in IPOD-ähnlichen Kompartimenten nicht von Hsp42 abhängt.

Des Weiteren habe ich die räumlich-zeitliche Organisation von Proteinaggregaten während eines subletalen Hitzeschocks und anschließender Erholungsphase, welche Aggregatsolubilisierung erlaubt, in Zellen mit intaktem proteasomalem Proteinabbau untersucht. Der Hitzeschock generiert multiple Aggregate, welche in der gesamten Zelle verteilt sind. Die Ablagerung missgefalteter Proteine in JUNQ und IPOD-ähnlichen Kompartimenten ist nach der Rückkehr zu physiologischen Temperaturen nicht zu beobachten. Stattdessen findet die Proteindisaggregation *in situ* statt, wofür kein intaktes Aktinzytoskelet vonnöten ist. Folgerichtig wird das Schicksal missgefalteter Proteine von der Stressart bestimmt.

Darüber hinaus habe ich eine funktionale Divergenz der *Saccharomyces cerevisiae* sHsps in der Rückfaltung und Organisation Hitzeschock-generierter Proteinaggregate entdeckt. Die Integration von Hsp26 beschleunigt die Reaktivierung aggregierter Proteine nach Hitzeschock. Im Gegensatz dazu beeinflusst Hsp42 die Proteinrückfaltung nicht, dient aber als Sortierungsfaktor, welcher für den fortdauernden Aufenthalt von Proteinaggregaten in der zellulären Peripherie zuständig ist.

With A Dedication To My Beloved Parents

# Table of Contents

<i>SUMMARY</i> .....	<i>I</i>
<i>ZUSAMMENFASSUNG</i> .....	<i>III</i>
<i>DEDICATION</i> .....	<i>V</i>
<i>TABLE OF CONTENTS</i> .....	<i>VI</i>
<i>LIST OF FIGURES</i> .....	<i>X</i>
<i>LIST OF TABLES</i> .....	<i>XII</i>
<b>1. INTRODUCTION</b> .....	<b>1</b>
<b>1.1 Protein aggregation</b> .....	<b>1</b>
1.1.1 Causes of protein aggregation .....	1
1.1.2 Identity of protein aggregates .....	2
<b>1.2 Sequestration of aggregates</b> .....	<b>3</b>
1.2.1 Inclusion bodies in bacteria.....	4
1.2.2 Aggregate sequestration in yeast.....	5
1.2.3 Aggresomes in mammalian cells .....	6
<b>1.3 Protein refolding</b> .....	<b>7</b>
1.3.1 Molecular chaperones .....	7
1.3.2 Hsp70-Hsp104/ClpB bichaperone system .....	8
1.3.2.1 The Hsp70 chaperones .....	8
1.3.2.2 The Hsp104/ClpB chaperones.....	9
1.3.3 Small heat shock proteins .....	10
1.3.3.1 The <i>S. cerevisiae</i> small heat shock proteins .....	13
<b>1.4 Protein degradation</b> .....	<b>14</b>
1.4.1 Protein breakdown in prokaryotes .....	14
1.4.2 The 26S proteasome in eukaryotes .....	15
1.4.3 Autophagy.....	16
<b>1.5 Asymmetric inheritance of damaged proteins</b> .....	<b>17</b>
1.5.1 Unequal aggregate inheritance in bacteria .....	17
1.5.2 Biased aggregate segregation in yeast.....	18
1.5.3 Unequal partitioning of protein inclusions in mammalian cells.....	19
<b>2. AIMS OF THE THESIS</b> .....	<b>21</b>
<b>3. MATERIALS</b> .....	<b>22</b>
<b>3.1 General equipment</b> .....	<b>22</b>
<b>3.2 Microscopic equipment</b> .....	<b>22</b>
3.2.1 Confocal microscopy .....	22
3.2.2 Peltier element .....	23

<b>3.3</b>	<b>Software</b> .....	<b>23</b>
<b>3.4</b>	<b>Expendable items</b> .....	<b>24</b>
<b>3.5</b>	<b>Primers, plasmids, and strains</b> .....	<b>24</b>
3.5.1	Primers.....	24
3.5.2	Plasmids.....	27
3.5.2.1	Bacterial plasmids / Expression plasmids.....	27
3.5.2.2	Yeast shuttle vectors.....	27
3.5.2.3	Yeast integration / knock-out vectors.....	28
3.5.3	Bacterial strains.....	28
3.5.4	<i>S. cerevisiae</i> strains.....	29
<b>3.6</b>	<b>Chemicals</b> .....	<b>30</b>
3.6.1	General chemicals.....	30
3.6.2	Column materials.....	30
3.6.3	Inhibitors.....	30
3.6.4	Media.....	30
3.6.5	DNA and protein size standards.....	30
<b>3.7</b>	<b>Kits</b> .....	<b>31</b>
<b>3.8</b>	<b>Antibodies</b> .....	<b>31</b>
<b>3.9</b>	<b>Enzymes and miscellaneous proteins</b> .....	<b>31</b>
<b>3.10</b>	<b>Growth media and antibiotics</b> .....	<b>32</b>
3.10.1	Bacterial media.....	32
3.10.2	Yeast media.....	32
<b>3.11</b>	<b>Antibiotics</b> .....	<b>33</b>
<b>4.</b>	<b><i>METHODS</i></b> .....	<b>33</b>
<b>4.1</b>	<b>Molecular biology methods</b> .....	<b>33</b>
4.1.1	Molecular cloning.....	33
4.1.2	Agarose gel electrophoresis.....	33
4.1.3	Preparation of chemically competent cells and transformation.....	34
4.1.4	Polymerase chain reaction (PCR).....	34
4.1.4.1	Colony PCR.....	35
<b>4.2</b>	<b>Protein purification</b> .....	<b>35</b>
4.2.1	Purification of Hsp26.....	36
4.2.2	Purification of Hsp42.....	37
4.2.3	Purification of CFP- and YFP-luciferase.....	39
<b>4.3</b>	<b>Protein analysis</b> .....	<b>41</b>
4.3.1	Bradford colorimetric protein quantification method.....	41
4.3.2	Gel-electrophoresis with SDS-PAGE.....	41
4.3.2.1	Coomassie Blue staining of gels.....	42
4.3.2.2	Silver stain of protein bands in SDS-polyacrylamide gels.....	43
4.3.3	Western blotting of SDS-PAGE gels.....	44
4.3.3.1	Wet blotting technique.....	44
4.3.3.2	Semi-dry blotting technique.....	45
4.3.3.3	Immunodetection of immobilized proteins.....	46
4.3.3.4	Quantification of Western blot signals.....	46
4.3.4	Solubility assay of luciferase aggregates.....	46
<b>4.4</b>	<b><i>In vitro</i> work</b> .....	<b>47</b>
4.4.1	Malate dehydrogenase (MDH) prevention of aggregation assay.....	47

4.4.2	CFP-luciferase and YFP-luciferase prevention of aggregation assay .....	48
4.4.3	Monitoring the aggregation rate of CFP-luciferase and YFP-luciferase by measuring the FRET signal .....	48
<b>4.5</b>	<b>Yeast work.....</b>	<b>49</b>
4.5.1	Transformation of <i>S. cerevisiae</i> cells .....	49
4.5.2	Deletion of genes in the <i>S. cerevisiae</i> genome.....	50
4.5.3	Isolation of genomic DNA from <i>S. cerevisiae</i> .....	50
4.5.4	Chromosomal fluorescent protein tagging .....	50
4.5.5	MG132, latrunculin A, benomyl, and cycloheximide treatment .....	50
4.5.6	Thermotolerance analysis .....	51
4.5.7	Serial dilution spot tests .....	51
4.5.8	Preparation of <i>S. cerevisiae</i> cell extracts for Western blotting .....	51
4.5.9	<i>In vivo</i> luciferase assay with <i>S. cerevisiae</i> .....	52
<b>4.6</b>	<b>Microscopy .....</b>	<b>52</b>
4.6.1	Image acquisition .....	52
4.6.2	Image processing and data analysis .....	52
4.6.3	Fluorescence Loss in Photobleaching (FLIP) .....	53
4.6.4	Immunofluorescence.....	53
<b>5.</b>	<b><i>RESULTS</i>.....</b>	<b>54</b>
5.1	Monitoring the fate of protein aggregates in yeast cells using fluorescent reporters.....	54
5.2	The small heat shock protein Hsp42 affects the organization of protein aggregates.....	58
5.3	Hsp42 localizes exclusively in IPOD-like compartments.....	62
5.4	The N-terminal domain of Hsp42 is crucial for aggregate sorting .....	65
5.5	Localization of amorphous but not of amyloidogenic aggregates to the IPOD depends on Hsp42	70
5.6	The JUNQ compartment of hsp42Δ cells exhibits moderate changes in dynamics and stability...	72
5.7	Aggregate sequestration depends on the actin cytoskeleton .....	75
5.8	Monitoring organization of misfolded proteins upon severe heat stress using fluorescent reporters .....	81
5.9	Following severe heat stress mCherry-VHL is not sorted to specific compartments .....	86
5.10	Protein disaggregation does not rely on specific deposition sites.....	87
5.11	sHsps affect the refolding and organization of heat shock-induced aggregated proteins.....	89
5.12	Misfolded proteins accumulate at the nucleus in hsp42Δ cells irrespective of the aggregate load	97
5.13	The actin cytoskeleton does not play a role in protein disaggregation.....	100
5.14	Protein inclusions are inherited asymmetrically .....	102
5.15	sHsps do not accelerate the velocity of thermal luciferase aggregation <i>in vitro</i> .....	104
<b>6.</b>	<b><i>DISCUSSION</i>.....</b>	<b>108</b>
6.1	The small heat shock protein Hsp42 controls the spatio-temporal organization of misfolded proteins in <i>S. cerevisiae</i> .....	108

6.2 Stress conditions determine the organization of aggregated proteins..... 111

7. *REFERENCES*..... 114

8. *ABBREVIATIONS*..... 126

9. *ACKNOWLEDGEMENTS*..... 128

## List of Figures

Figure 1.1. Protein aggregation.....	3
Figure 1.2. Aggregate sequestration.....	5
Figure 1.3. Protein disaggregation in the yeast cytosol by the sHsp – Hsp70 – Hsp104 system. ....	8
Figure 1.4 Number of sHsp representatives in different organisms. ....	11
Figure 1.5 Functions of the sHsp domains. ....	12
Figure 1.6 Structure and domain localizations of <i>S. cerevisiae</i> Hsp26. ....	13
Figure 1.7. Comparison between pro- and eukaryotic proteases.....	16
Figure 5.1 Hsp104-mCFP provides wild-type like thermotolerance.....	54
Figure 5.2 Outline of the experimental setup.....	55
Figure 5.3 Spatio temporal organization of protein aggregates.....	57
Figure 5.4 Different substrates are sorted to the same compartments.....	58
Figure 5.5 Hsp42 is essential for the targeting of misfolded proteins to peripheral compartments. ....	59
Figure 5.6 Hsp42 is essential for the targeting of misfolded proteins to peripheral compartments. ....	60
Figure 5.7 The lack of peripheral inclusions in hsp42Δ cells is directly caused by missing Hsp42. ....	61
Figure 5.8 In hsp42Δ cells mCherry-VHL foci form exclusively at the nucleus. ....	61
Figure 5.9 Hsp42 localizes exclusively to IPOD-like compartments.....	63
Figure 5.10 Hsp26-mCitrine exhibits WT-like luciferase refolding after heat shock. ....	64
Figure 5.11 Hsp42 domain deletion and Hsp26 – Hsp42 domain swap constructs.....	66
Figure 5.12 The N-terminal domain of Hsp42 mediates sorting of misfolded proteins to peripheral inclusions..	68
Figure 5.13 The N-terminal domain of Hsp42 mediates sorting of misfolded proteins to peripheral inclusions..	68
Figure 5.14 The N-terminal domain of Hsp42 mediates sorting of misfolded proteins to peripheral inclusions..	69
Figure 5.15 Hsp42 does not affect the localization of amyloidogenic aggregates. ....	71
Figure 5.16 The JUNQ compartment of hsp42Δ cells exhibits an increased exchange rate with the cytosolic mCherry-VHL pool.....	72
Figure 5.17 mCherry-VHL aggregation foci are more rapidly resolved in the hsp42Δ strain. ....	73
Figure 5.18 mCherry-VHL aggregation foci are more rapidly resolved in the hsp42Δ strain. ....	74
Figure 5.19 Disintegration of protein inclusions requires Hsp104-mediated protein disaggregation. ....	75
Figure 5.20 Microtubule-independent effects of benomyl prevent aggregate sorting of misfolded mCherry-VHL into JUNQ and IPOD-like compartments. ....	77
Figure 5.21 The actin cytoskeleton is required for aggregate compartmentalization.....	79
Figure 5.22 Latrunculin A treatment does not reduce cell viability.....	79
Figure 5.23 Actin cytoskeleton is not altered in hsp42Δ cells at both physiological and folding stress conditions. ....	80
Figure 5.24 Outline of the experimental setup for heat shock treatment followed by a recovery period.....	81
Figure 5.25 Spatio-temporal organization of heat shock-induced protein aggregates. ....	82
Figure 5.26 Spatio-temporal organization of heat shock-induced protein aggregates. ....	83
Figure 5.27 Hsp104-mCFP co-localizes with mCitrine-luciferase. ....	84

---

Figure 5.28 A translation inhibitor does not change the spatio-temporal organization of mCitrine-luciferase aggregates. ....	84
Figure 5.29 Reactivation of aggregated mCitrine-luciferase is completed within 30 min and dependent on the presence of Hsp104. ....	85
Figure 5.30 Spatio-temporal organization of heat shock-induced protein aggregates in hsp104Δ cells. ....	85
Figure 5.31 Following heat shock mCherry-VHL is not sorted to distinct compartments. ....	87
Figure 5.32 Reactivation of protein aggregates does not require sorting to specific deposition sites. ....	88
Figure 5.33 Reactivation of protein aggregates does not require sorting to specific deposition sites. ....	89
Figure 5.34 Small heat shock proteins influence refolding, but not degradation, of heat shock-induced protein aggregates. ....	90
Figure 5.35 Small heat shock proteins influence the organization of heat shock-induced protein aggregates. ....	92
Figure 5.36 Small heat shock proteins influence the organization of mCitrine-luciferase aggregates. ....	93
Figure 5.37 Small heat shock proteins influence the organization of endogenous yeast aggregates stained by Hsp104-mCFP. ....	94
Figure 5.38 mCitrine-luciferase solubility as well as Hsp104 expression levels are not altered in hsp42Δ cells. ....	95
Figure 5.39 The altered distribution of protein aggregates in hsp42Δ cells is directly caused by missing Hsp42. ....	95
Figure 5.40 Hsp42 is essential for the persistence of protein inclusions in the cellular periphery. ....	96
Figure 5.41 Juxtannuclear accumulation of protein inclusions in hsp42Δ cells occurs irrespective of the aggregate load. ....	98
Figure 5.42 Aggregation foci accumulate rapidly at the nucleus in hsp42Δ cells during blocked proteasomal degradation. ....	99
Figure 5.43 The actin cytoskeleton is not required for protein disaggregation. ....	102
Figure 5.44 Aggregation foci are inherited asymmetrically. ....	103
Figure 5.45 Hsp26 influences the thermal aggregation of malate dehydrogenase. ....	105
Figure 5.46 sHsps do not accelerate the velocity of luciferase aggregation. ....	106
Figure 6.1 Model of the Hsp42-dependent sorting of misfolded proteins during prolonged stress conditions. ...	109

## List of Tables

Table 1. Primers used in this study. ....	24
Table 2. Bacterial plasmids for protein expression. ....	27
Table 3. Yeast shuttle vectors used in this study.....	27
Table 4. Yeast integration / knock-out vectors used in this study.....	28
Table 5. Bacterial strains used in this study. ....	28
Table 6. Yeast strains used in this study. ....	29
Table 7. Basic PCR amplification protocols .....	35
Table 8. Composition of the separating SDS-gel.....	41
Table 9. Composition of the stacking SDS-gel .....	42

# 1. Introduction

## 1.1 *Protein aggregation*

Proteins depend entirely on their correct three-dimensional structure for proper function. Certain conditions however lead to misfolding and protein aggregation, causing cellular dysfunction. As a consequence aging and a wide range of deleterious human diseases, including neurodegeneration and cancer, are associated with aggregation. Understanding formation and processing of aggregates is therefore of primary importance. To counteract protein misfolding cells have developed a protein quality control network comprising molecular chaperones and proteases, which will be described later in paragraphs 1.3 and 1.4.

### 1.1.1 Causes of protein aggregation

The protein folding process starts once the nascent polypeptide chain emerges from the ribosomal exit tunnel. Since this channel can only accommodate extended chains or at most helical structures (Ban *et al.*, 1999), the nascent chain reaches the cytoplasm in a linear conformation, exposing hydrophobic residues towards the aqueous environment of the cell. Folding of the nascent chain into its unique three-dimensional structure requires selection of a single structure out of a vast repertoire of constellations that are sterically available but incorrect. The permanent exposure of hydrophobic patches during the folding process can result in adopting aberrant conformations, which can complex to form aggregates. However, also correctly folded proteins are at constant risk of generating non-native conformations, because the energy barriers that separate native from aberrant folds are usually small. In this light it is not surprising that protein misfolding and aggregation have several causes. Mutations, for example, might disturb protein folding and, as a consequence, result in aggregation. Various diseases, including type II diabetes, Huntington's disease, familial forms of Parkinson's disease, and Alzheimer disease, are caused by mutations occurring in the aberrant proteins themselves (Powers *et al.*, 2009; Chiti and Dobson, 2006). Also mutations in components of the protein quality control network can have devastating consequences. As an example, mutated human small heat shock protein  $\alpha$ -crystallin induces cataract, which is caused by denaturing lens protein normally kept soluble by the chaperone. Moreover, aggregation can be caused by the lack of oligomeric assembly partners, leading to the exposure of hydrophobic patches normally buried at the interface of the complexes. In addition, protein aggregation results from erroneous translation (e.g. premature termination)

and environmental stress conditions such as thermal or oxidative stress. Heat shock, for example, perturbs the tertiary structure of numerous polypeptides, causing quantitative aggregation of cellular proteins. While heat-induced unfolding processes are often reversible (Parsell *et al.*, 1994), oxidative stress induces several irreversible reactions, including radical-induced fragmentation of the polypeptide backbone or replacement of specific amino acid side chains by carbonyl groups (Nystrom, 2005), both leading to misfolding and aggregate formation. Also aging seems to promote protein aggregation by the accumulation of oxidized and nitrated intracellular proteins (Erjavec *et al.*, 2007; Squier, 2001), which are thermodynamically unstable and assume partially unfolded tertiary structures that readily form aggregates. As a consequence cellular dysfunction occurs and senescent animals have a reduced ability to withstand physiological stresses (Squier, 2001).

### **1.1.2 Identity of protein aggregates**

Characteristic of all the different causes of aggregation is the inappropriate exposure of hydrophobic patches, which are normally buried within the inner core of the folded protein or at the interface with other subunits (Wetzel, 1994). These patches pose a risk for the cell, because they can interact with and trap native proteins, thus disturbing specific cellular functions (Nucifora *et al.*, 2001). When the exposed hydrophobic patches of monomeric proteins agglutinate, aggregates are formed, which are characterized by their poor solubility in aqueous or detergent solvents, aberrant localization, and non-native secondary structure (Kopito, 2000; Fink, 1998). Originally, the aggregation process was considered to be either unspecific, leading to the formation of amorphous structures, or, in case of amyloid fibrils, highly specific through the formation of cross  $\beta$ -sheets in prefibrils (Figure 1.1). However, bacterial inclusion bodies have recently been demonstrated to contain amyloid-like structures (de Groot *et al.*, 2009). Intermolecular  $\beta$ -sheets were shown to be contained within both amorphous and amyloidogenic aggregates. Nonetheless, proportionally the highest  $\beta$ -sheet content is found in amyloid fibrils, in which they run perpendicular to the fibril axis (Fandrich, 2007; Chiti and Dobson, 2006; Dobson, 2003). An important determinant of aggregate morphology is the cause of the unfolding process. Heat shock, for example, leads to co-aggregation of diverse protein species, thereby restricting specificity of the resulting inclusions. If aggregation is mainly driven by a single misfolded protein species, as would be the case during overproduction of recombinant proteins in bacteria, highly organized aggregates are generated in the form of inclusion bodies. Such divergent aggregation pathways could explain the finding that distinct proteins form discrete inclusions (Rajan *et al.*,

2001). Moreover, a single protein species has been shown to form aggregates of different morphologies, depending on the type of denaturing condition (Ben-Zvi and Goloubinoff, 2002).

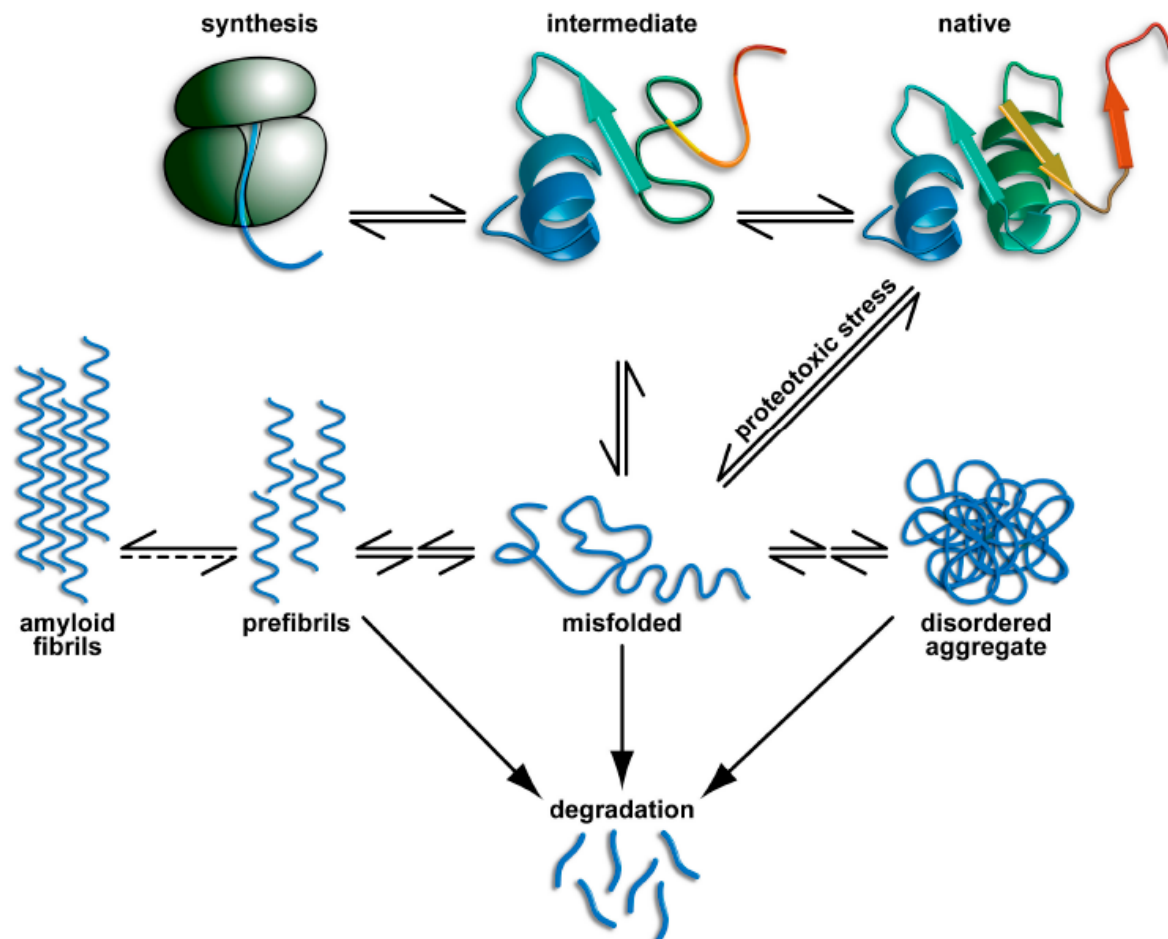


**Figure 1.1. Protein aggregation.**

Nascent polypeptides as well as natively folded proteins can misfold. Non-native polypeptides might be (re-) folded to the native state by molecular chaperones. Otherwise, misfolded protein species might form prefibrillar structures, which ultimately form amyloid fibrils. Alternatively, misfolded monomeric proteins can complex to form disordered aggregates. All aberrant protein conformations except amyloid fibrils can be degraded. For details see text. (Tydmers *et al.*, submitted for publication).

## 1.2 Sequestration of aggregates

Protein aggregates are formed when the first line of defense, the cell's molecular chaperones and proteolytic systems, is overwhelmed by excessive production of unfolded polypeptides. As the second line of defense against protein damage, aggregated proteins are directed to specific compartments, which protects the cellular environment from potentially deleterious protein conformations. Organizing protein aggregates might also facilitate the recruitment of protein quality control components, thereby increasing the efficiency of aggregate removal in a subsequent phase (Kaganovich *et al.*, 2008; Wigley *et al.*, 1999). In agreement with such a

cytoprotective role of sequestering misfolded proteins into large, microscopically visible aggregates, there is now emerging evidence that conformational diseases result from intermediate oligomeric forms of misfolded proteins, but not from large aggregates (de Groot *et al.*, 2009; Arrasate *et al.*, 2004). The toxicity of these early aggregates seems to result from the perturbation of essential processes by co-aggregating with cellular components which eventually leads to apoptotic or necrotic cell death (Stefani and Dobson, 2003). The process of aggregate sequestration appears to be evolutionary ancient as it is observed from bacteria to mammals.

### **1.2.1 Inclusion bodies in bacteria**

Heterologous protein expression in *E. coli* allows producing proteins of commercial interest in large quantities. However, many overproduced proteins form insoluble aggregates in inclusion bodies. Although efficient refolding protocols have been established, aggregation of a variety of target proteins constitutes a major bottleneck in the purification of heterologously produced proteins, because the recovery is usually low and the procedure requires adaptation for each target protein (de Groot *et al.*, 2009). Protein aggregation thus narrows the spectrum of protein-based drugs that are available in the biotechnology market (Ventura and Villaverde, 2006). Besides overproduction of heterologous proteins, inclusion bodies are formed from endogenous proteins, particularly under stress conditions (Laskowska *et al.*, 2004; Gragerov *et al.*, 1991). A recent report even monitored the existence of inclusion bodies in wild-type cells cultivated at physiological temperatures in the absence of protein overproduction (Lindner *et al.*, 2008). Microscopically, inclusion bodies share a common amorphous appearance, regardless of the target protein (Carrio and Villaverde, 2005). They can be nearly 1  $\mu\text{m}$  in diameter and are very dense refractive particles that can be found in both the cytoplasmic and periplasmic space of bacteria. As mentioned earlier (Paragraph 1.1.2), the amorphous microscopic appearance is undermined by the discovery of extended, intermolecular  $\beta$ -sheet conformations, which are very similar to the cross- $\beta$  sheets present in amyloids (Doglia *et al.*, 2008; Morell *et al.*, 2008). In many inclusion bodies, however, disordered conformations are detected and, in some cases, native-like secondary structure (de Groot *et al.*, 2009; de Groot and Ventura, 2006; Garcia-Fruitos *et al.*, 2005). Usually one to two copies of inclusion bodies are present per cell, which are located at the cellular poles, mid-, or quarter-cell positions (Lindner *et al.*, 2008; Laskowska *et al.*, 2004; Gragerov *et al.*, 1991). Interestingly, the pole-localized inclusions are preferentially found at the old cell pole. This particular localization suggests an active energy-driven transport process. However, a

recent report has shown nucleoid-exclusion as the main cause of polar localization, indicating a rather passive mechanism for aggregate sequestration (Figure 1.2, *left*) (Winkler *et al.*, 2010). The localization of inclusion bodies has consequences for their inheritance during cell division, as will be discussed later (Paragraph 1.5.1)

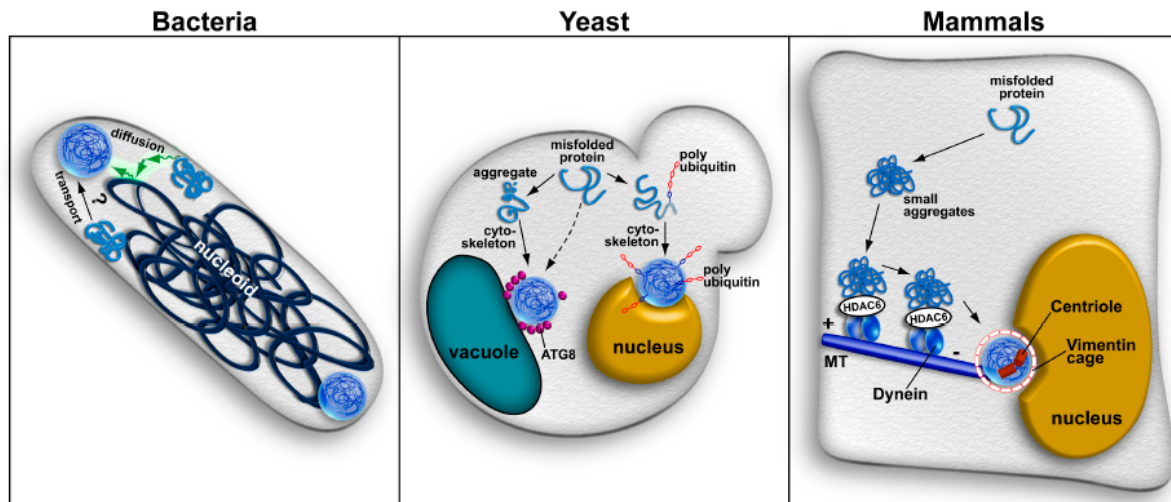


**Figure 1.2. Aggregate sequestration.**

(*Left*) Bacteria form inclusion bodies preferentially at the cellular poles. This might occur through an active transport or a passive nucleoid occlusion process. (*Middle*) In yeast, poly-ubiquitylated misfolded proteins are sequestered at the perinuclear JUNQ compartment, while insoluble protein inclusions are deposited at the perivacuolar IPOD compartment. (*Right*) Mammalian cells transport peripheral microaggregates along microtubules to the pericentriolar aggresome, which is ensheathed by the intermediate filament vimentin. For details see text (Tydmers *et al.*, submitted for publication).

## 1.2.2 Aggregate sequestration in yeast

Exposing yeast to severe heat stress leads to the accumulation of multiple foci distributed throughout the cell. These aggregates are localizing randomly and can mostly be resolubilized with the help of molecular chaperones, once the stress conditions are removed (Parsell *et al.*, 1994). However, also terminally misfolded protein species form in yeast, including oxidatively damaged proteins (Nystrom, 2005), amyloidogenic proteins such as yeast prions (Edskes *et al.*, 1999; Patino *et al.*, 1996), or polyQ-rich model proteins (e.g. Htt103Q) (Meriin *et al.*, 2002; Krobitsch and Lindquist, 2000). The aggregation behavior of these proteins is diverse. For example, oxidatively damaged proteins such as carbonylated species form visible aggregation foci in the cytoplasm only in aged yeast cells or after application of oxidative stress (Erjavec and Nystrom, 2007). It is unknown whether these foci form randomly or at distinct localizations. The observation that carbonylated proteins are inherited asymmetrically in an actin-dependent process suggests interplay between the actin cytoskeleton and the inclusions. When studying the localization of amorphous and amyloidogenic aggregates a recent study has described partitioning of misfolded proteins between two distinct

compartments (Figure 1.2, *middle*) (Kaganovich *et al.*, 2008). Upon inhibition of proteasome-mediated degradation, soluble misfolded proteins were partitioned to the JUNQ (juxtannuclear quality control) compartment, which localized to an indentation of the nucleus close to the endoplasmic reticulum. Ubiquitylation seemed to be a prerequisite for targeting to the JUNQ, where also proteasomes were concentrated. Non-diffusible, insoluble misfolded proteins were partitioned to the perivacuolar IPOD (insoluble protein deposit), which also harbored amyloidogenic proteins such as polyQ expanded Huntington (Htt103Q) or the yeast prion protein Rnq1. Interestingly, poly-ubiquitylation of Rnq1 re-targeted it to the JUNQ. In contrast, impairing ubiquitylation of misfolding substrates through deletion of the E2 pair *ubc4/5* resulted in deposition at the IPOD. Use of a microtubule-depolymerizing drug inhibited aggregation sequestration at the two distinct compartments, suggesting a role for the microtubule cytoskeleton in this process.

### 1.2.3 Aggresomes in mammalian cells

In mammalian cells inhibition of proteasomal activity or overexpression of certain proteins such as misfolded cystic fibrosis transmembrane conductance regulator (CFTR) (Johnston *et al.*, 1998), parkin (Junn *et al.*, 2002), or huntingtin (Waelter *et al.*, 2001) results in the formation of a single inclusion called the aggresome, which localizes to a pericentrosomal indentation of the nucleus. Preformed microaggregates from the cellular periphery are transported to the centrosome on the microtubule cytoskeleton in a process mediated by dynein/dynactin complexes (Figure 1.2, *right*) (Johnston *et al.*, 2002). As a consequence, microtubule-depolymerizing drugs inhibit aggresome formation (Kopito, 2000). Although the aggresome is membrane-free, it might be stabilized by ensheathing in a cage of the intermediate filament vimentin. Poly-ubiquitylation is generally considered a prerequisite for substrate recognition and transport to aggresomes. However, some aggresomal substrates have been shown not to be ubiquitylated, leaving the possibility that other signals are responsible for transport to aggresomes (Garcia-Mata *et al.*, 2002; Kopito, 2000). The microtubule-associated deacetylase HDAC6 has been demonstrated to be a major player in aggresome formation (Kawaguchi *et al.*, 2003). It binds simultaneously to ubiquitylated misfolded protein and dynein motors, thereby enabling transport of misfolded cargo along microtubules. The E3 ubiquitin ligase parkin that promotes the proteasomal degradation of several substrates (Kahle and Haass, 2004), is believed to recognize and ubiquitylate non-native proteins, herewith marking it for HDAC6-mediated transport to aggresomes. Moreover, HDAC6 binding of aberrant proteins promotes a protective cellular response mediated by

dissociation of a repressive HDAC6/HSF1 (heat-shock factor 1) / Hsp90 complex and subsequent HSF1 activation, thus upregulating the expression of molecular chaperones. Immunohistochemical analysis indicates that aggresomes are enriched in molecular chaperones, including Hsc70, the Hsp40 proteins Hdj1 and Hdj2, and the chaperonin TriC/TCP (Garcia-Mata *et al.*, 1999; Wigley *et al.*, 1999). Also the presence of both 19S and 26S proteasome subunits in aggresomes has been reported (Anton *et al.*, 1999; Wigley *et al.*, 1999; Wojcik *et al.*, 1996). Thus, the refolding and degradative machineries are present at the aggresome.

### **1.3 Protein refolding**

Maintaining the integrity of proteins is of fundamental importance for life. For that reason cells have developed a sophisticated machinery of folding helpers, the so-called molecular chaperones, which guide *de novo* protein folding and help sustaining the native fold.

#### **1.3.1 Molecular chaperones**

The observation that the level of many chaperones is elevated under heat shock conditions led to the term ‘heat shock protein’ (Hsp) (Ellis, 1987). This upregulation already suggested that they are required for the protection of proteins during severe stress conditions. The unfolding and subsequent exposure of hydrophobic stretches to the environment is acted against by Hsps, which have evolved to bind to these stretches and assist proteins to regain their native state. Hsps exist in several evolutionary conserved families, which are named according to the apparent molecular weight of a typical member, e.g. Hsp110, Hsp100, Hsp90, Hsp70, Hsp60, or Hsp40. The Hsps have diverse functions: i) they prevent unfolded proteins from interacting with each other by binding to them (e.g. small heat shock proteins and Hsp90 family members) (Haslbeck *et al.*, 1999b); ii) Hsps assist folding processes (e.g. Hsp60 and Hsp70 chaperones) (Weibezahn *et al.*, 2004); iii) they have the remarkable ability to dissolve already formed protein aggregates to release polypeptide chains for refolding or degradation (Hsp100 family members) (Sanchez and Lindquist, 1990). However, the Hsp100s require cooperation with the Hsp70 and Hsp40 chaperones to dissolve aggregates (Ben-Zvi and Goloubinoff, 2002; Glover and Lindquist, 1998).

### 1.3.2 Hsp70-Hsp104/ClpB bichaperone system

Aggregation has for a long time been seen as the dead-end state of proteins. In 1990, however, the group of Lindquist discovered the Hsp104 protein in yeast, which belongs to the Hsp100 family of chaperones (Sanchez and Lindquist, 1990). Hsp104 (*S. cerevisiae*) / ClpB (*E. coli*) has the ability – together with the Hsp70 chaperone system – to solubilize even large protein aggregates. Notably, each chaperone component on its own has only limited (Hsp70) or no (Hsp104) disaggregation activity. Following a mild pre-heat treatment this bi-chaperone system enables organisms to survive a normally lethal heat shock, a phenomenon referred to as thermotolerance (Queitsch *et al.*, 2000; Sanchez and Lindquist, 1990). The viability of cells under such severe stress conditions is threatened by the quantitative loss of proteins via aggregation and requires Hsp104/ClpB -dependent reactivation of lost protein material. The Hsp70–Hsp104/ClpB system is conserved in most eubacteria, parasitic protozoa, yeast, and plants, but only exists in the mitochondria of higher eukaryotes (Weibezahn *et al.*, 2005).

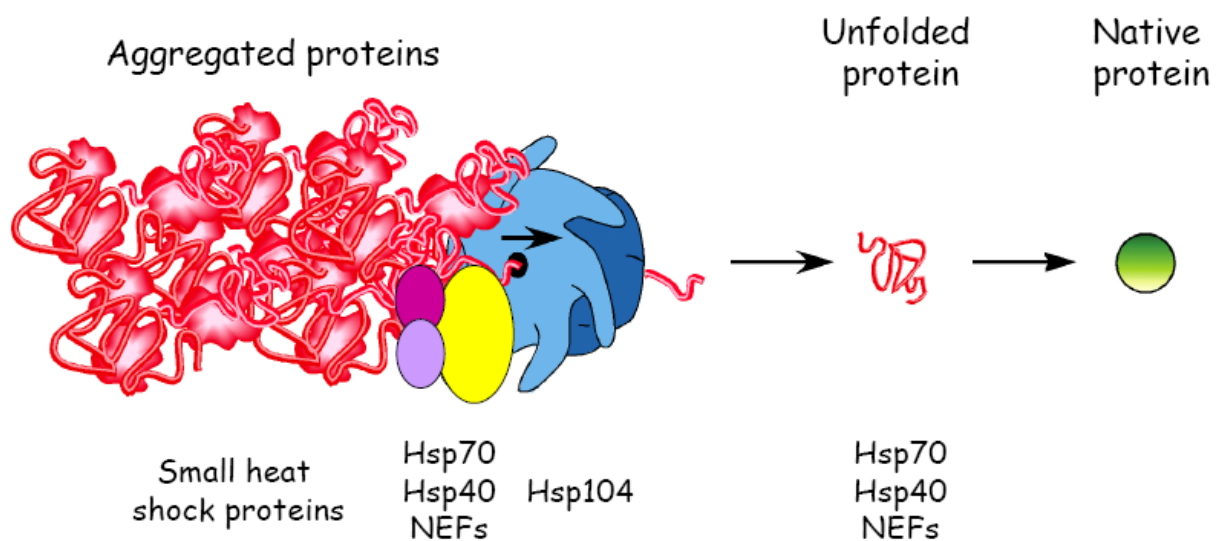


**Figure 1.3. Protein disaggregation in the yeast cytosol by the sHsp – Hsp70 – Hsp104 system.**

sHsps co-aggregate with non-native polypeptides, thus facilitating access of the refolding machinery. Hsp70 delivers, with help of its co-chaperones, individual polypeptide chains to the central pore of Hsp104, which threads them in a one-by-one fashion upon ATP consumption. The solubilized, but still non-native, polypeptide is taken over and folded to its native state by Hsp70. For details see text. Modified from (Weibezahn *et al.*, 2004).

#### 1.3.2.1 The Hsp70 chaperones

Hsp70 family members participate under non-stress conditions in a number of cellular processes, as diverse as folding of newly synthesized proteins, assisting translocation through membranes, activity control of regulatory proteins, disassembly of protein complexes, and facilitating proteolytic degradation of certain substrate proteins (Dragovic *et al.*, 2006; Cotto

and Morimoto, 1999). The Hsp70 proteins exist in two functional states: the ATP- and the ADP-state (Weibezahn *et al.*, 2004). In the ATP-bound state substrates are bound with low affinity and dissociate rapidly. Once ATP is hydrolyzed, Hsp70 proteins bind substrate tightly (Pierpaoli *et al.*, 1997; Theyssen *et al.*, 1996; McCarty *et al.*, 1995). Hsp70s assist folding of proteins by repeated cycles of binding and release of their substrates. *In vivo* Hsp70s interact with members of the Hsp40 protein family (e.g. *S. cerevisiae* Ydj1), which accelerate the speed of the hydrolysis reaction. The release of ADP and binding of ATP reverses Hsp70s to the low affinity state and, thus, completes the functional cycle of substrate binding and release. Therefore, a number of Hsp70 members interact with nucleotide exchange factors including bacterial GrpE or the yeast Fes1 and Sse1 (Dragovic *et al.*, 2006; Raviol *et al.*, 2006; Kabani *et al.*, 2002; Liberek *et al.*, 1991) to accelerate the speed of substrate release. Hsp70s are thought to bind and release their substrates repeatedly, with each cycle inducing local conformational changes, ultimately resulting in a correctly folded protein (McCarty *et al.*, 1995; Szabo *et al.*, 1994; Schroder *et al.*, 1993).

### 1.3.2.2 The Hsp104/ClpB chaperones

Hsp104/ClpB is a member of the superfamily of AAA+ (ATPase associated with various cellular activities) proteins that are responsible for a broad variety of cellular functions such as proteolysis and protein disaggregation (Ogura and Wilkinson, 2001). Aggregated proteins can be resolubilized by the Hsp70 chaperone system only in the presence of cognate Hsp104/ClpB (Glover and Lindquist, 1998; Parsell *et al.*, 1994), as could be concluded from their species-specific cooperation (Weibezahn *et al.*, 2004; Patino *et al.*, 1996). The exact mode of interplay is however not well understood. Hsp70 is required for restricting access of degradative or non-processive systems to the aggregates and substrate transfer to the central pore of Hsp104/ClpB, which assembles into a hexameric ring (Haslberger *et al.*, 2008). Disaggregation is achieved by continuous extraction of single unfolded polypeptide chains from an aggregate through pore-located aromatic residues, which thread substrate upon ATP consumption (Haslberger *et al.*, 2008; Lum *et al.*, 2004; Weibezahn *et al.*, 2004). The shuffling of substrates involves the Hsp104/ClpB -specific M-domain that is lacking in other AAA+ family members (Haslberger *et al.*, 2007). Hsp104/ClpB possesses remarkable flexibility during the threading process. Once folded domains are encountered, Hsp104/ClpB adopts a resting state and polypeptide is released (Haslberger *et al.*, 2008). The partial threading is beneficial, because it results in higher refolding yields by preventing non-productive interactions of different unfolded peptide segments that would otherwise be

produced upon complete substrate threading. Hsp70s are thought to take over translocated polypeptides, preventing reassociation of solubilized, but still non-native, proteins with aggregates, thereby efficiently promoting substrate refolding (Weibezahn *et al.*, 2005). Alternatively, translocated polypeptide might be degraded by components of the protein quality network.

### 1.3.3 Small heat shock proteins

The Hsp70-Hsp104/ClpB bi-chaperone system is assisted by small heat shock proteins (sHsps) (Figure 1.3). sHsps constitute the most widespread type of molecular chaperones, but at the same time also the most poorly conserved family (Haslbeck *et al.*, 2005a). They are found in all three kingdoms of life with prokaryotes and single-celled eukaryotes usually possessing one to two sHsps (Kappe *et al.*, 2002). Higher eukaryotes in turn also have a higher number of genes encoding sHsp proteins (e.g. humans possess 10) (Figure 1.4). One hallmark of sHsps is a small monomer size ranging from 12 to 43 kDa. In their native state the majority of sHsps forms dynamic oligomers of 12 to >32 subunits (Cheng *et al.*, 2008), which mainly form hollow spheres with openings (White *et al.*, 2006; Haley *et al.*, 1998; Kim *et al.*, 1998) or cylindrical complexes (van Montfort *et al.*, 2001b). Another hallmark of sHsps is the presence of a conserved, ~100 amino acids long  $\alpha$ -crystallin domain, whose name derives from the most renowned member of the sHsp family, the vertebrate eye lens  $\alpha$ -crystallin (Horwitz, 1992).  $\alpha$ -crystallin, in conjunction with human Hsp27, is associated with a variety of neurodegenerative disorders, including Alzheimer's and Creutzfeldt-Jakob disease (Krueger-Naug *et al.*, 2002; Lowe *et al.*, 1992; Renkawek *et al.*, 1992). Knock-out mice deficient in  $\alpha$ -crystallin develop cataracts (Brady *et al.*, 1997). The  $\alpha$ -crystallin domain in sHsps is flanked by a short C-terminal extension and an N-terminal arm. While the  $\alpha$ -crystallin domain mediates dimerization of sHsp monomers, the C-terminal extension establishes oligomer formation through contacts with adjacent  $\alpha$ -crystallin domains (Figure 1.5) (van Montfort *et al.*, 2001b; Kim *et al.*, 1998). The N-terminal domain is both of divergent sequence and variable length (from 24 residues in *C. elegans* Hsp12.2 to 247 residues in *S. cerevisiae* Hsp42) (Haslbeck *et al.*, 2004a; Candido, 2002), and is also required for oligomerization (Haslbeck *et al.*, 2004b). Recent data suggest that mainly the N-terminal domain is responsible for substrate binding by assuming different geometries that allow a broad range of substrates to interact (Jaya *et al.*, 2009; Cheng *et al.*, 2008). But also regions of the  $\alpha$ -crystallin domain and C-terminal extension form contacts with misfolded proteins, such that there is no unique binding site in sHsps (Jaya *et al.*, 2009).

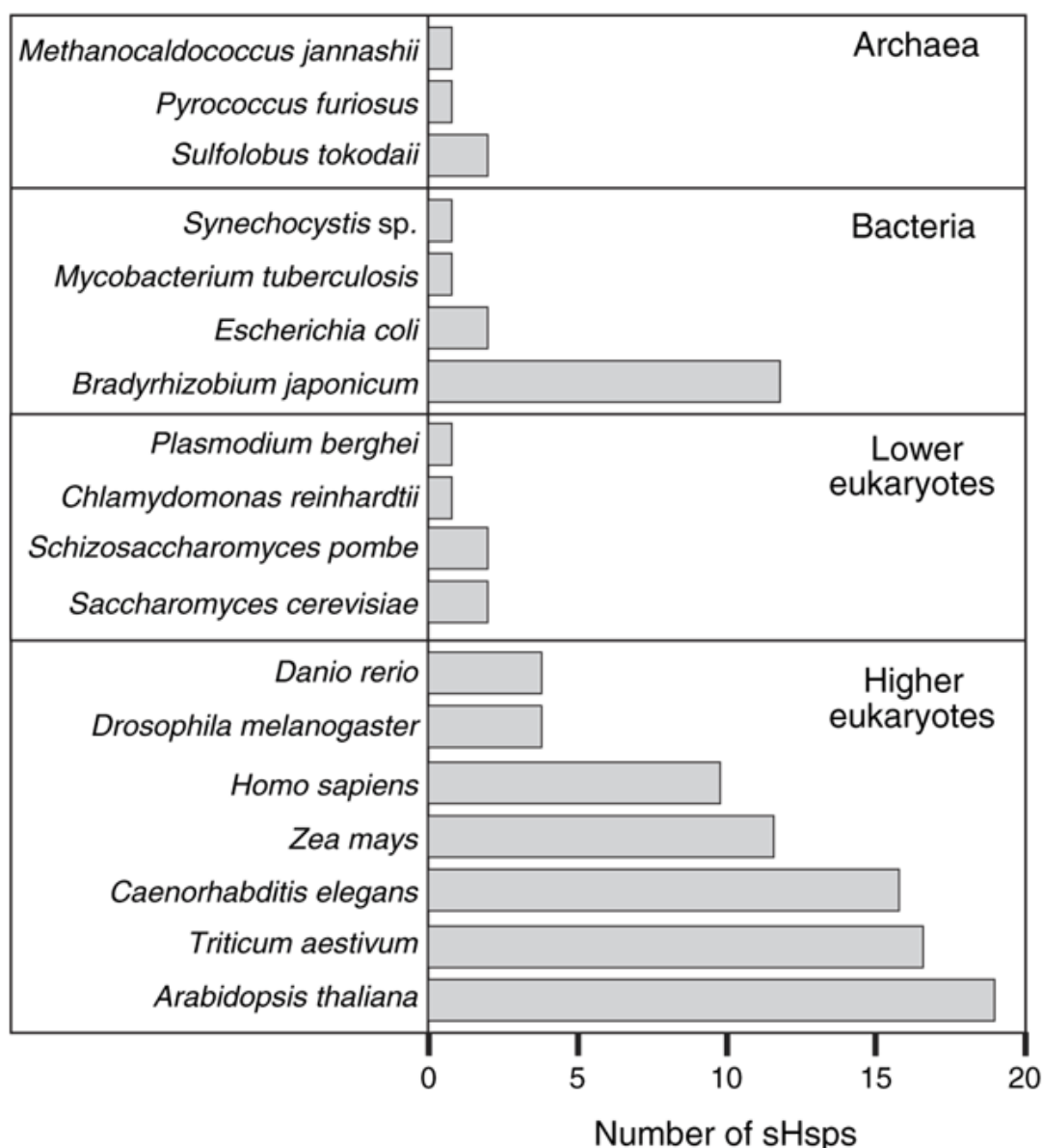


**Figure 1.4 Number of sHsp representatives in different organisms.**

sHsps are found in all three kingdoms of life. However, an increasing number of sHsp representatives is observed from prokaryotes to higher eukaryotes. Rhizobia are an exception to this trend (Haslbeck *et al.*, 2005a).

The expression of sHsps is induced by various stress types including high temperature, oxidative stress, heavy metals, and ischemic injury. Nonetheless, sHsps are constitutively expressed in specific tissues of many different organisms (Cheng *et al.*, 2008). At physiological temperatures most sHsp molecules are only partially active while stress conditions, such as elevated temperature, activate them. Also post-translational modifications, in particular phosphorylation of mammalian sHsps, might be a trigger to switch on their activity according to cellular demands (Koteiche and McHaourab, 2003; Gaestel, 2002). Conditions favoring substrate denaturation shift an equilibrium of numerous sHsps between

high order quaternary structures and dimers towards the dimeric form, suggesting the latter as the substrate-binding conformation (Van Montfort *et al.*, 2001a; van Montfort *et al.*, 2001b; Haslbeck *et al.*, 1999b). For other sHsps increased temperatures result in more rapid subunit exchange which also facilitates binding to sub-oligomeric species (Liu *et al.*, 2006; Friedrich *et al.*, 2004). Electron microscopic studies have identified sHsp/substrate complexes as having a large, regular, globular morphology (Stromer *et al.*, 2003; Ehrnsperger *et al.*, 1999; Haslbeck *et al.*, 1999b; Ehrnsperger *et al.*, 1997), which is influenced by substrate and sHsp identities (Basha *et al.*, 2004; Stromer *et al.*, 2003). When non-native polypeptides exceed sHsp concentration, larger complexes form that are less well defined. Consequently, even oligomers that dissociate into dimers upon activation re-associate with substrate proteins to form large complexes.

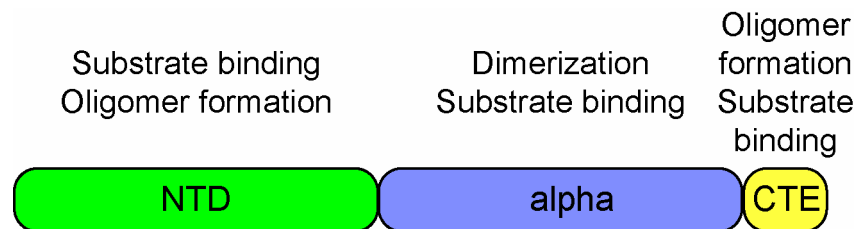


**Figure 1.5 Functions of the sHsp domains.**

Sequence diagram and assigned functions of the sHsp domains are depicted. The length of the N-terminal domain (NTD) varies from 24 residues in *C. elegans* Hsp12.2 to 247 residues in *S. cerevisiae* Hsp42. The NTD is required for oligomerization and the main substrate binding site. Nonetheless, also regions of the  $\alpha$ -crystallin domain (alpha) and C-terminal extension (CTE) form contacts with misfolded proteins, such that there is no unique binding site in sHsps. The  $\alpha$ -crystallin domain moreover mediates dimerization of sHsp monomers, while the CTE establishes oligomer formation through contacts with adjacent  $\alpha$ -crystallin domains.

Under heat-shock conditions a substantial fraction of the cytosolic protein pool is maintained in a soluble state by sHsps (Basha *et al.*, 2004; Haslbeck *et al.*, 2004a). sHsps bind tightly to misfolded protein species, resulting in the formation of sHsp/substrate complexes that do not release bound proteins spontaneously, thereby creating a reservoir of misfolded proteins during stress conditions (Haslbeck *et al.*, 2005a). sHsps thus separate binding of non-native proteins from the refolding process (Franzmann *et al.*, 2008). Also in the presence of sHsps substrates form aggregates, which are of altered composition. Intercalation of sHsps decreases the number of hydrophobic contacts between substrate molecules and increases the accessibility of the protein refolding machinery. Consequently, substrates coupled to sHsps can be reactivated more easily by the Hsp70-Hsp104/ClpB bi-chaperone system, thereby enhancing protein disaggregation efficiency *in vivo* and development of thermotolerance (Figure 1.3) (Ratajczak *et al.*, 2009; Mogk *et al.*, 2003; Lee *et al.*, 2000).

### 1.3.3.1 The *S. cerevisiae* small heat shock proteins

Two distinct sHsps have been described in *S. cerevisiae*, namely Hsp26 and Hsp42. Both chaperones are thought to assemble into oligomers of 24 subunits (Figure 1.6) (Haslbeck *et al.*, 2004a; Haslbeck *et al.*, 1999b). Hsp26 dissociates into dimers at temperatures  $>40^{\circ}\text{C}$ . This change in quaternary structure is accompanied by a change in activity, because Hsp26 is an efficient chaperone only at elevated temperatures. Interestingly, an Hsp26 mutant that does not dissociate into dimers at elevated temperatures and does not exchange subunits still exhibits chaperone activity identical to wild-type (WT) protein (Franzmann *et al.*, 2005). This implies that oligomer dissociation and rate of subunit exchange cannot be a major determinant for chaperone activity of Hsp26.

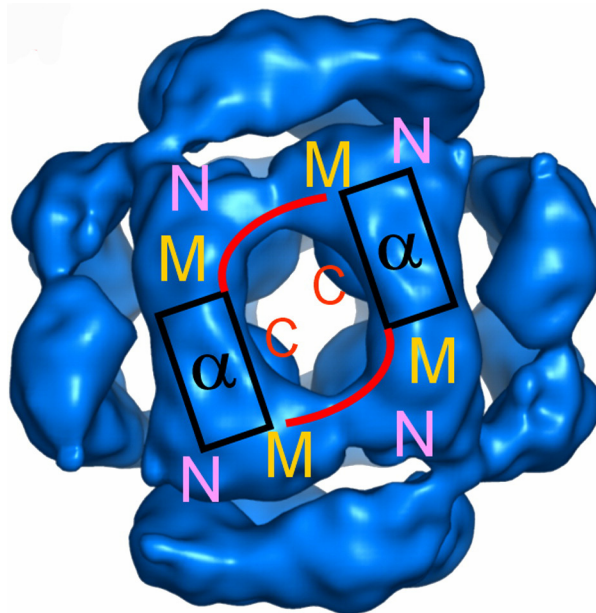


**Figure 1.6 Structure and domain localizations of *S. cerevisiae* Hsp26.**

Structure of Hsp26 as revealed by cryo-electron microscopy. The 24 subunits of Hsp26 are arranged in a porous shell with tetrahedral symmetry. The subunits form elongated, asymmetric dimers. Each subunit contains an N-terminal region (N), a globular middle domain (M), the  $\alpha$ -crystallin domain ( $\alpha$ ), and a C-terminal extension (C). Twelve of the C-termini form contacts which are inserted into the interior of the shell, while the other 12 C-termini form contacts on the surface. Hinge points between the domains allow a variety of assembly contacts, providing the flexibility required for formation of supercomplexes with nonnative proteins. For more information see text (White *et al.*, 2006).

The intrinsic capability of Hsp26 to sense heat stress is a feature of a distinct part of the N-terminal region, the so-called middle domain. The temperature-dependent changes in the middle domain are only local and do not have major consequences for the overall Hsp26 quaternary geometry, but allow for efficient substrate binding (Franzmann *et al.*, 2008). In contrast to Hsp26, Hsp42 is constitutively active as a chaperone and does not undergo structural changes in response to heat shock. Hsp42 is 5–10 times more abundant than Hsp26 in the yeast cytosol (Haslbeck *et al.*, 2004a). Moreover, higher ratios, compared to Hsp42, between Hsp26 and substrate are needed to suppress the aggregation of substrate proteins

(Haslbeck *et al.*, 2004a; Stromer *et al.*, 2003). Nonetheless, previous studies have demonstrated that Hsp26 renders aggregates more accessible to the protein refolding machinery (Hsp104/ Ssa1/Ydj1) and cells lacking Hsp26 have been shown to be impaired in the disaggregation of heat-aggregated luciferase (Cashikar *et al.*, 2005; Haslbeck *et al.*, 2005b). Hsp26 thus plays a vital role in the reactivation of non-native proteins. The spectrum of client proteins of Hsp26 and Hsp42 is 90 % identical. The substrates belong to a broad subset of biochemical pathways and cellular mechanisms, indicating a general protective function of sHsps for proteome stability in *S. cerevisiae* (Haslbeck *et al.*, 2004a). *hsp26,42Δ* strains are viable, but display increased amounts of insoluble proteins. Elevated temperatures in the *hsp26,42* deletion strain also induce a morphology that resembles cells undergoing dehydration, aging, or cytoskeleton and cell wall damages (Haslbeck *et al.*, 2004a).

#### **1.4 Protein degradation**

Besides chaperone-mediated (re-)folding of non-native polypeptides, the cellular quality control machinery battles misfolded and aggregated protein species by removing them from the cytosol. In prokaryotes this occurs via AAA<sup>+</sup> proteases, while in eukaryotes the 26S proteasome and autophagy clear aberrant proteins.

##### **1.4.1 Protein breakdown in prokaryotes**

In bacteria, general and regulated proteolysis is mainly carried out by ring-forming, ATP-dependent members of the Hsp100/Clp family of proteins, a subfamily of the AAA<sup>+</sup> proteins. In *E. coli*, these are ClpA and ClpX, which associate with the diffusible peptidase ClpP (ClpAP, ClpXP), HslU, which associates with HslV (HslUV), and the membrane anchored AAA<sup>+</sup> protease FtsH. The peptidases of these systems are compartmentalized in stable oligomeric rings and, as a consequence, only unfolded polypeptides can be processed by this architecture (Figure 1.7). Therefore, the AAA<sup>+</sup> partner has to bind to the protease subunit, provide substrate unfolding, and subsequent threading of the substrate protein into the catalytic center of the associated peptidase (Ishikawa *et al.*, 2001; Ortega *et al.*, 2000; Singh *et al.*, 2000; Weber-Ban *et al.*, 1999). Apart from the quality control functions of these proteolytic systems, they are also involved in regulatory pathways. Hence, they have to recognize folded proteins, a task accomplished by interacting with special adaptor proteins, which transfer their substrate specificity to the interacting AAA<sup>+</sup> protein (Schmidt *et al.*, 2009; Mogk *et al.*, 2007; Dougan *et al.*, 2002).

### 1.4.2 The 26S proteasome in eukaryotes

Protein degradation in eukaryotes is achieved by two major systems. It was long believed that the lysosomal apparatus was the only site of protein breakdown. Lysosomes / vacuoles (in yeast) contain multiple acidic proteases (cathepsins) and other hydrolases that digest proteins. It has now been established that the bulk of polypeptides in eukaryotic cells is hydrolyzed by the proteasome, which degrades cytosolic, nuclear, and ER-resident proteins (Goldberg, 2003). Most substrates are first poly-ubiquitylated by a series of enzymes, which attach ubiquitin via an isopeptide bond, and then degraded by the 26S proteasome, a 2000 kDa ATP-dependent proteolytic machinery (Goldberg, 1995; Ciechanover, 1994). This large structure is composed of the central 20S (700 kDa) proteasome, in which proteins are degraded, and two 19S complexes, which provide substrate specificity and regulation (Lee and Goldberg, 1998). The 20S core particle, similar to bacterial proteases, is composed of four heptameric rings that form a hollow cylinder, in which proteolysis occurs (Figure 1.7). The two inner  $\beta$ -rings form the central chamber containing the proteolytic sites facing the central cavity. Substrates processed by the 20S complex are completely degraded in a highly processive fashion into small peptides of 3–20 residues that are further hydrolyzed to amino acids by other peptidases (Kisselev *et al.*, 1998). The interior chamber is enclosed on either end by narrow pores in the center of the outer  $\alpha$ -rings. These pores are gated channels normally maintained in a closed state, and their access is controlled by the 19S particle, which locates at either end of the 20S complex (Benaroudj *et al.*, 2003; Groll *et al.*, 2000). This organization ensures that protein digestion is isolated from the surrounding cytosol (Goldberg, 2003). Before entering the 20S proteasome, substrates must be unfolded and translocated, a task carried out by the 19S particle. The base of each 19S complex contains six AAA+ proteins that promote the ATP-dependent unfolding and threading of substrates into the proteolytic chamber of the 20S proteasome.

26S proteasomes often co-localize with aggregates and inhibition of proteasomal activity can cause aggregate formation or a delay in the removal of preexisting aggregates (Bedford *et al.*, 2008; Martin-Aparicio *et al.*, 2001; Johnston *et al.*, 1998). However, *in vitro* proteasomes have failed to degrade amyloidogenic aggregates (Venkatraman *et al.*, 2004; Verhoef *et al.*, 2002). Moreover, *in vivo* activity of the ubiquitin-proteasome system is impaired in the presence of such aggregates either via irreversible sequestration of proteasomes or other effects not understood yet (Bennett *et al.*, 2005; Holmberg *et al.*, 2004; Bence *et al.*, 2001). These data point to a minor role of 26S proteasomes in removal of aggregated protein species. Effects of proteasomal inhibition on aggregate fate might thus be indirect by increasing the

amount of misfolded proteins and disturbing other components of the protein quality control network.

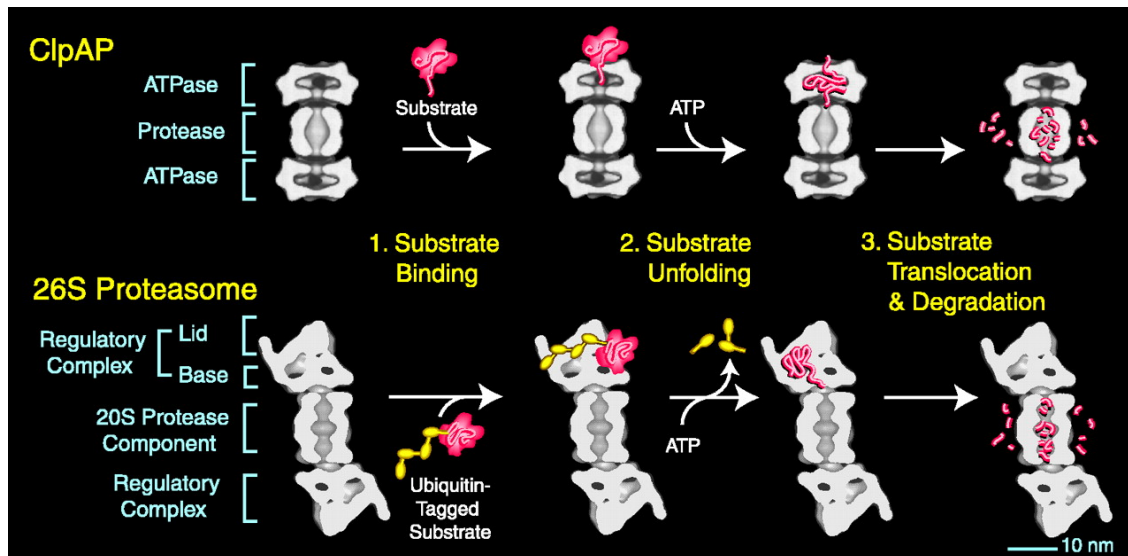


**Figure 1.7. Comparison between pro- and eukaryotic proteases.**

The upper panel shows the degradation path controlled by the bacterial AAA+ chaperone ClpA and its associated protease ClpP. The lower panel describes degradation mediated by the eukaryotic proteasome. For details see text. Adapted by Tessarz from (Wickner *et al.*, 1999).

### 1.4.3 Autophagy

Macroautophagy is a mechanism by which cytosolic components are sequestered in autophagosomes and degraded when autophagosomes fuse with lysosomes. Recently, macroautophagy emerged to be involved in the elimination of misfolded and aggregated proteins from the mammalian cytosol (Kirkin *et al.*, 2009a; Nakatogawa *et al.*, 2009; Rubinsztein, 2006). While the proteasome protects cells against proteotoxicity by degrading soluble monomeric misfolded proteins, it is impaired by oligomers of non-native proteins (Iwata *et al.*, 2005). Autophagy then serves as a backup-system when the ubiquitin proteasome system is overwhelmed or incapable of dealing with aggregated protein species. In agreement, alpha-synuclein is degraded by both the proteasome and autophagy (Webb *et al.*, 2003), and aggregated Huntington is cleared by autophagy (Iwata *et al.*, 2005). Moreover, autophagy is involved in the removal of aggresomes (Olzmann and Chin, 2008; Fortun *et al.*, 2003). Evidence for the importance of autophagy even under physiological conditions derived from experiments with deletion of Atg (autophagy-related) genes, which are essential for functional autophagy, but do not affect proteasomal degradation. Atg5 and Atg7 deficiency in mice causes neurodegeneration via accumulation of poly-ubiquitylated proteins in inclusion bodies, which increased in size and number with aging. Clearance of diffuse cytosolic

proteins through basal autophagy is thus important for preventing the accumulation of abnormal proteins, indicating an interconnection of autophagy and the ubiquitin proteasome system (Hara *et al.*, 2006; Komatsu *et al.*, 2006). This is further supported by the demonstration that proteasome impairment induces compensatory autophagy (Pandey *et al.*, 2007; Iwata *et al.*, 2005) and autophagy suppression compromises proteasome-mediated protein degradation (Korolchuk *et al.*, 2009). Recent data suggest that the topology of ubiquitin linkages and acetylation influence the route of substrate degradation. K63-linked ubiquitylation promotes targeting of cargo to the autophagic system (Tan *et al.*, 2008; Wooten *et al.*, 2008) and acetylation destines mutant huntingtin for degradation via the autophagic route (Jeong *et al.*, 2009). p62 protein could be the adaptor that couples ubiquitylated proteins to autophagy because it contains a UBA (ubiquitin-associated) domain that interacts with ubiquitylated proteins and a LIR (LC3-interacting region) domain that binds ATG8, a component of autophagic vesicles (Pankiv *et al.*, 2007; Bjorkoy *et al.*, 2005). Nbr1 protein serves a similar function to p62, also binding poly-ubiquitin and Atg8 on autophagic vesicles, thereby targeting misfolded proteins to the autophagic machinery. Interestingly, recruitment of ubiquitin-positive cargo to the lysosome requires both p62 and Nbr1 (Kirkin *et al.*, 2009b). The identification of receptors for selective autophagosomal degradation of ubiquitylated proteins points to a selective mechanism of macroautophagy rather than unspecifically digesting cytoplasmic components (Kirkin *et al.*, 2009a; Iwata *et al.*, 2005).

## ***1.5 Asymmetric inheritance of damaged proteins***

Sequestering misfolded proteins into larger aggregates lowers their toxicity. Still, protein aggregates are harmful to the cell by directly exerting a toxic effect or indirectly through trapping of essential proteins (Muchowski and Wacker, 2005). Recent data suggest that asymmetric distribution of protein inclusions between two dividing cells is employed to generate offspring free of aggregate load. This seems to be an evolutionary ancient principle, because all organisms use it as a protective mechanism.

### **1.5.1 Unequal aggregate inheritance in bacteria**

Protein aggregates have recently been demonstrated to lead to bacterial aging and cell death (Maisonneuve *et al.*, 2008). In *E. coli*, accumulation of protein damage and aggregation causes reduced cellular growth rates (Winkler *et al.*, 2010; Lindner *et al.*, 2008). However, the diminished growth rate can be reverted by positioning protein inclusions at the cell poles. Subsequent division dilutes the protein aggregates out, generating offspring not containing

inclusions. Thus, a bypass mechanism is created that allows eradicating protein aggregates under conditions continuously overwhelming the proteostasis network. If a single inclusion was positioned on the old cell pole, a single division would generate offspring devoid of parental aggregates. In contrast, the cell inheriting the old pole suffers from a reduced growth rate and slower division kinetics when compared to the inclusion-free sibling. Thus, the dividing cell partitions damaged proteins in a biased fashion, leading to differential growth potential distinguishing the old-pole aging cell and its young-pole counterpart. (Winkler *et al.*, 2010; Lindner *et al.*, 2008). Recent experimental data generated in our laboratory demonstrates that abolishing the asymmetric distribution of protein aggregates diminishes growth rate and division speed differences between *E. coli* cells emerging from a cell division (Winkler *et al.*, 2010).

Bacteria entering stationary phase increase their expression of chaperone genes (Saint-Ruf *et al.*, 2004). This suggests that bacteria could potentially invest more energy in protein maintenance under physiological growth conditions. Since evolution has selected against higher chaperone levels in logarithmic growth, it could be argued that this would not be as cost efficient as simply rejuvenating offspring by unequal aggregate partitioning (Lindner *et al.*, 2008). Notably, under stress conditions a different picture emerges, because expression of chaperone genes is highly upregulated to counteract misfolding proteins. Taken together, asymmetric inheritance of protein inclusions plays a central role in improving the fitness of an entire *E. coli* population at the expense of aging individuals.

### **1.5.2 Biased aggregate segregation in yeast**

Yeast cells can undergo only a limited number of replicative cycles before they die, which is known as their replicative life span. Mother yeast cells of advanced replicative age become enlarged and have wrinkled surfaces, and the time between cell divisions becomes greatly extended during their last few mitotic rounds (Mortimer and Johnston, 1959). Daughter cells possess in turn the full replicative potential. Thus, an age asymmetry exists between parent and offspring in *S. cerevisiae*. The closer a mother cell is to the end of her life, the shorter the life span of the daughter cells she produces. At the extreme, daughter cells produced by very old mother cells have life spans only 25 % the length of the mother cell's life span (Kennedy *et al.*, 1994). These findings led to the hypothesis that aging factors exist that invoke cellular senescence once accumulating beyond a certain concentration limit. Protein aggregates, and in particular carbonylated protein species, have been suggested to constitute such a senescence factor (Aguilaniu *et al.*, 2003). The amount of carbonylated protein increases over time in

yeast and also in higher eukaryotes (Henderson and Gottschling, 2008; Nystrom, 2005). Furthermore, carbonylated proteins are preferentially retained in the mother cell during cytokinesis. This asymmetric distribution between mother and daughter is likely to have important implications in cellular deterioration and senescence (Erjavec and Nystrom, 2007; Aguilaniu *et al.*, 2003). How damaged proteins are retained in the mother cell is not well understood. Hsp104, the conserved NAD-dependent histone deacetylase Sir2, the actin cytoskeleton, the polarisome, and myosin motor proteins seem to be major players in this process, as their distraction results in breakdown of damage asymmetry, preventing rejuvenation of daughter cells (Liu *et al.*, 2010; Tessarz *et al.*, 2009; Erjavec *et al.*, 2007; Aguilaniu *et al.*, 2003). It has furthermore been suggested that daughter cells can clear themselves of damaged proteins by a polarisome- and tropomyosin-dependent flow of aggregates into mother cells (Liu *et al.*, 2010). As observed in prokaryotes, evolution has selected also in yeast for an asymmetric distribution of damage, which ‘wins’ over unbiased dilution of damage. It can thus be concluded that rejuvenation of progeny is not achieved by gain-of-function, but rather a loss of dysfunction (Lindner *et al.*, 2008).

### **1.5.3 Unequal partitioning of protein inclusions in mammalian cells**

Mammalian cells, like bacteria and yeast, inherit damaged proteins asymmetrically. Interestingly, the aggregate load is always segregated into the shorter-lived cell, indicative of a mechanism to preserve the long-lived progeny (Funtealba *et al.*, 2008; Rujano *et al.*, 2006). In humans with a polyglutamine disease called ‘spinocerebellar ataxia type 3’, aggregated mutant ataxin-3 is absent in the long-lived stem cells of intestinal crypts, but present in the differentiated daughter cells that have a shorter life expectancy. Also in drosophila embryonic neuroblasts expressing heterologous polyglutamin-huntingtin fragment, which forms aggresomes, the aggregated protein was inherited by the short-lived neuroblast progenitor rather than the long-lived ganglion mother cell. As aggresomes colocalize with centrosomes, the unequal partitioning of damaged proteins could be inherent to the intrinsic differences between replicated centrosomes (Piel *et al.*, 2000). Before division the centrosome consists of a centriole and the peri-centriolar matrix (Stearns, 2001). During mitosis the centriole duplicates and asymmetry is achieved by inheritance of the peri-centriolar material by the mother centriole. The daughter centriole that separates and migrates to the opposite cell pole lacks the matrix until it has reached its destination (Rebollo *et al.*, 2007; Rusan and Peifer, 2007; Yamashita *et al.*, 2007). Since microaggregates in mammalian cells are actively transported to the centrosome, this spatial coupling could provide a mechanism by which cells

specifically retain aggregated proteins in one of the dividing cells. Indeed, poly-ubiquitylated proteins targeted for degradation were localized to centrosomes and shown to be inherited only by one mitotic daughter during somatic cell division (Funtealba *et al.*, 2008). The generality of aggregate localization to the centrosome is still in question, because the JUNQ and IPOD compartments in *S. cerevisiae* do not co-localize with the spindle pole body, the yeast counterpart to the mammalian centrosome (Kaganovich *et al.*, 2008). Interestingly, some cells divide to produce a daughter that dies. In *C. elegans*, for example, the hermaphrodite produces 1090 cells and loses 131 to apoptosis. The dying cells might function as a repository for any misfolded protein aggregates (Singhvi and Garriga, 2009). Therefore, asymmetric inheritance of aggregated proteins might not simply ensure the generation of fit offspring, but also might provide a physiological mechanism to dispose of aberrant protein species. If this were the case, non-dividing cells such as neurons would be at a disadvantage and more susceptible to protein misfolding diseases (Funtealba *et al.*, 2008).

## 2. Aims of the Thesis

In *S. cerevisiae* two distinct compartments for accumulating misfolded proteins upon proteasomal inhibition have been described, a juxtannuclear compartment termed JUNQ (juxtannuclear quality control) and a perivacuolar compartment termed IPOD (insoluble protein deposit) (Kaganovich *et al.*, 2008). The JUNQ accumulates more mobile misfolded proteins that are ubiquitylated and likely represent substrates for proteasomal degradation. In contrast, the IPOD compartment is suggested to harbor terminally aggregated, insoluble proteins, including amyloidogenic proteins such as yeast prions (Kaganovich *et al.*, 2008).

To get further insight into the spatio-temporal organization of misfolded proteins in *S. cerevisiae*, I utilized three different fluorescent reporter proteins (mCherry-VHL, mCitrine-luciferase, and Hsp104-mCFP). Both mCherry-VHL and mCitrine-luciferase aggregate upon stress application. Measuring the enzymatic activity of luciferase allowed monitoring its folding status. Hsp104-mCFP in turn binds to protein aggregates and thus enabled me to follow the localization of yeast endogenous aggregated proteins. I used two different experimental setups to induce protein misfolding: (i) prolonged mild thermal stress (37°C) in cells with blocked proteasomal degradation and (ii) sublethal heat shock (45°C) followed by a recovery phase (30°C) in cells with intact proteasomal degradation.

Little is known about cellular factors that control the deposition of protein aggregates at specific sites within *S. cerevisiae* cells. Frydman and colleagues could demonstrate that components of the quality control system (Sti1, Ubc4/5) affect the distribution of misfolded proteins between JUNQ and IPOD compartments (Kaganovich *et al.*, 2008). Small heat shock proteins (sHsps) co-aggregate efficiently with misfolded proteins, thereby changing the properties of protein aggregates and facilitating protein disaggregation upon return to physiological growth conditions. In a candidate approach I therefore analyzed the impact of the *S. cerevisiae* sHsps, namely Hsp26 and Hsp42, on the refolding and localization of protein aggregates.

The formation of both the JUNQ and IPOD compartments is suggested to rely on a functional microtubule cytoskeleton (Kaganovich *et al.*, 2008). The microtubule-depolymerizing drug benomyl has been shown to reversibly inhibit the formation of JUNQ and IPOD compartments. To exclude microtubule-independent effects of the drug, I used a benomyl-resistant yeast strain containing a mutation in tubulin-2, which prevents benomyl from depolymerizing microtubules. To further understand the role of the *S. cerevisiae* cytoskeleton, I also analyzed whether refolding and sorting of protein aggregates requires an intact actin cytoskeleton.

### 3. Materials

#### 3.1 *General equipment*

Agarose gel chambers and trays	ZMBH workshop
Äkta FPLC system	Amersham Pharmacia Biotech
Äkta Purifier system	Amersham Pharmacia Biotech
Analytical balance, AE100	Mettler
Balances	Mettler
Centrifuges	Sorvall, Eppendorf, Heraeus
Columns	Amersham Pharmacia Biotech
French Press	SLM Amin.co
Glass ware	Schott
Incubators	Heraeus
Lumat, LB9501	Berthold
PCR machine, T-Gradient	Biometra
Photometer, Specord 205	Analytik Jena
Power supply	Perkin-Elmer
SDS gel chambers    midi/maxi gels	ZMBH workshop
mini gels	BioRad
Sonifier 450	Branson
Thermocycler, T-Personal	Biometra
Ultracentrifuges	Beckman
Vortex mixer	Neolab
Western blot apparatus, semi-dry or wet,	ZMBH workshop
Yeast dissection microscope	Nikon Eclipse E400 equipped with a micromanipulator

#### 3.2 *Microscopic equipment*

##### 3.2.1 *Confocal microscopy*

405 nm, 440 nm, 640 nm diode lasers	Zeiss
488 nm, 514 nm Argon laser	Zeiss
568 nm Krypton laser	Zeiss
Camera EMCCD, C9100-50	Hamamatsu

Confocal scanner unit, CSU 22	Yokogawa
Laser scanning confocal microscope, A1R	Nikon
Inverted microscope, Axiovert 200M	Zeiss
Objective Plan-APOCHROMAT 100x/1,4 Oil	Zeiss
Spinning disc microscope, UltraVIEW ERS	PerkinElmer

### 3.2.2 Peltier element

Aluminium objective slide	ZMBH workshop
Aluminium spacer	ZMBH workshop
Bench controller	Ovenindustries
Insulation gasket, GSK-universal	Melcor
Liquid heat exchanger, LI-201	Melcor
Peltier element, CP1.4-127-045L, expoy sealed	Melcor
PVC body	ZMBH workshop

### 3.3 Software

Acrobat 7.0	Adobe
Clone Manager 5	Scientific & Educational Software
DNA Strider	(Marck, 1988)
EndNote X1	ISI ResearchSoft
Illustrator 10.0	Adobe
ImageJ	NIH
Image Gauge	Fujifilm
Image Reader	Fujifilm
IrfanView	Irfan Skiljan
KaleidaGraph 4.0	Synergy Software
Office XP	Microsoft Corp.
Openlab	Improvisation
Photoshop 8.0.1	Adobe
PyMol	Delano Scientific
UltraVIEW ERS Imaging Suite	PerkinElmer

### 3.4 Expendable items

Cell culture plasticware	Greiner/Sarstedt
Cellulose acetate filters, pore size 0.2 µm	Sartorius
Cuvettes	Sarstedt
Dialysis tubing, SpectraPor	Spectrum
Filter papers	Schleicher & Schuell
Glass bottom culture dishes	MatTek
Microcentrifuge tubes	Eppendorf
PVDF membrane, Roti-PVDF	Roth
Plastic tubes 1.5, 2 ml	Sarstedt
15, 50 ml	Greiner
Scintillation vials	Zinsser
Sterile filters	Millipore
Vivaspin concentrator columns	Vivascience
Whatman paper, 3 mm	Schleicher & Schuell

### 3.5 Primers, plasmids, and strains

#### 3.5.1 Primers

**Table 1. Primers used in this study.**

Primer name and sequence in 5'-3' orientation are given. Restriction sites are denoted in lower case letters.

Primer name	Sequence (5'-3')/source
F5-Abp140	AAAATGTACCGCTGCTGGGTACAAGCTGTGTTTGACGTTCTCAAGGTGACGGTGCTGGTT A
F5-Hsp104	GATGACGATAATGAGGACAGTATGGAAATTGATGATGACCTAGATGGTGACGGTGCTGGTT TA
Forw bamHI GSGG-linker eCFP,eYFP	GGCCggateccGGAGGTGGAATGGTGAGCAAGGGCGAGGA
Forw BamHI yEmCFP,Citrine	GCGCggatccATGTCTAAAGGTGAAGAATTATCACT
Forw fus oh htb1-mCher	TCTTCTCTACTCAAGCAggatccATGGTGAGCAAGGGCGAGGAGGATAACATGGCCATC
Forw Gpd xhoI	CCGGctcgagGAGCTCAGTTTATCATTATCAATACTCG
Forw hsp26 up400bp	GAACATCCACAACCAACG
Forw hsp42 up 400bp	GGTAATGCTTGGCTCTCG
Forw hsp42 up500bp speI	GGCCactagtGGTAACAAGTGAGCAAGGG
Forw htb1 xmaI	GCGCcccgggATGTCTGCTAAAGCCGAAAAG
Forw o.h. pdr5-nat1	AGACCCTTTTAAGTTTTTCGTATCCGCTCGTTTCGAAAAGACTTTAGACAAAAAGCTTGCCTTGT CC

Primer name	Sequence (5'-3')/source
Forw pACT1 xhoI	CCGGctcgagCCTACATTCTTCCTTATCG
Forw P-adh1 xhoI	CCGGctcgagGACTACACCAATTACTACTGC
Forw up500 of pdr5	CTCTTTCCGCGGAATCG
Forw ver end yEmGFPs	CTGCTGCTGGTATTACCC
Forw ver his3 300bp down	GCAGAGGCTAGCAGAATTAC
Forw ver nat1 300bp down	CGAGCAGGCGCTCTAC
Forw ver 30up nat1 stop	CTGGTCGCTATACTGCTGTC
Forw veri Abp140	CAAGCCATGGATAACCTTCAC
Forw veri Hsp104	GATGATATGGGTGCACGTC
Forw XmaI Cerulean	CGCGcccgggATGAGTAAAGGAGAAGAAGAACTTTTC
Forw XmaI QP25,103	CGCGcccgggATGGCGACCCTGGAAAAGC
Forw XmaI yEmCFP,Citrine	CGCGcccgggATGTCTAAAGGTGAAGAATTATCACT
Fw BamHI Term_hsp42	GCAGggatccATATCGTATCTGTTTATACACACATAC
Fw EcoRI HSP42	GCAGgaattcATGAGTTTTTATCAACCATCCC
Fw EcoRI HSP42deltaN (+ATG)	GCAGgaattcATGTCACCAGAAGTGAATGTC
Fw_Hsp26_EcoRI	GCAGgaattcATGTCATTTAACAGTCCATTT
Fw_OH_hsp26crys_hsp42 Cext	GTTCCAAAATTGAAGCCTCAGAAGCCGAAGCCAAAAAAGAGGAT
Fw_OH_26deltaC_42deltaN	TTCCCATCTGGTTTCGGTTTCCCTTCACCAGAAGTGAATGTCTATGAT
Fw_OH42deltaC_26deltaN_new	AACGAGAATGGACTTACCATTTAGAAGTGTGCGCAGTTCAGTT
Fw veri Hsp42(741up)	CGGTTACTGTTTCTACGATTGATA
R3-Abp140	GTTTTATGATGAGAGAGGAGGTGGTACTTGTCTCAGAACTTCTATCGATGAATTCGAGCTC G
R3-Hsp104	TGATTCTTGTTTCGAAAGTTTTTAAAAATCACACTATATTAATTATCGATGAATTCGAGCTC G
Hsp26_A	CCGGggtctcAGGTGGTATGTCATTTAACAGTCCATTTTTTG
Hsp26_B	CCGGctcgagTTAGTTACCCACGATTCTTGAGA
Hsp42_A	CCGGcgtctcAGGTGGTATGAGTTTTTATCAACCATCCCTA
Hsp42_B	CCGGaagcttTCAATTTTCTACCGTAGGGTTGGG
Rev 5'yEmGFPs	GAATAATTCTTCACCTTAGACAT
Rev BamHI Cerulean	CGCGggatccTTTGTATAGTTCATCCATGCCTAG
Rev C-tag Cerulean Hsp42	TAAGAATAATATAATAGCATGACGCTGACGTGTGATTCTAATCGATGAATTCGAGCTCG
Rev down500 of pdr5	CGTTGTACTTCCAGTCGTGATC
Rev eYFP,eCFP until BsrGI	GGCCtgtacaGCTCGTCCATGCC
Rev fus oh mche-htb1	CTCGCCCTTGCTCACCATggatccTGCTTGAGTAGAGGAAGAGTACTTGGTAACAGCTCT

Primer name	Sequence (5'-3')/source
Rev Gpd xmaI	CGCGccccgggCGTCGAAACTAAGTTCTGGTG
Rev hsp26 down450bp	CGCTTATTACCGCCATTC
Rev hsp42 down 350bp	GAGCAAGGTAAGAAGTGACAA
Rev hsp42down500bp ClaI	GGCCatcgatCCGAGCAAGTCGATGAAG
Rev hsp42down500bp hindIII	GGCCaagcttCCGAGCAAGTCGATGAAG
Rev mcherry BamHI	GCGCggatccCTTGTACAGCTCGTCCATGCC
Rev mcherry SacII	CGCGccccgggTACTTGTACAGCTCGTCCAT
Rev nat1-o.h. pdr5	AAAAAGTCCATCTTGGTAAGTTTCTTTTCTTAACCAAATTCAAATTTCTATCGACACTGGAT GGC
Rev pACT1 xmaI ohne ATG	GCCGccccgggTGTAAATTCAGTAAATTTTCGATC
Rev P-adh1 xmaI	CCGccccgggTGTATATGAGATAGTTGATTGTATGC
Rev SacII Cerulean	CCGccccgggTTTGTATAGTTCATCCATGCCTAG
Rev SacII QP25,103	CCGccccgggTACTTGTACAGCTCGTCCATGCC
Rev Tef-Promoter 100 bp	GGATGTATGGGCTAAATGTACG
Rev veri yEmGFPs bp90	GCATCACCTTCACCTCAC
Rev yEmCFP,Citrine SacII	GCCGccccgggTTATTTGTACAATTCATCCATACCATG
Rv_Hsp26FLAG_BamHI	GCACggatccTACTTGTTCATCGTCGTCCTTGTAAATCGTTACCCACGATTCTTGAGA
Rv HSP42 BamHI	GCACggatccTCAATTTTCTACCGTAGGGTTG
Rv_hsp42crystallineFLAG	GCACggatccTCACTTGTTCATCGTCGTCCTTGTAAATCCTTTTTCAGTGTATTGACAATTTTAGG
Rv HSP42FLAG BamHI	GCACggatccTCACTTGTTCATCGTCGTCCTTGTAAATCCTTTTCTACCGTAGGGTTGGGA
Rv_OH26deltaN_42deltaC_new	TCAACTGGAAGTGCAGACTTCTAAATGGTAAGTCCATTCTCGTT
Rv_OH_hsp42Cext_hsp26_crys	ATCCTCTTTTTTGGCTTCGGCTTCTGAGGCTTCAATTTTGGAAAC
Rv Prom_hsp42 EcoRI	GCACgaatcTGCTTCGGCTTGGTATGATC
Rv veri hsp26	CGTTGTTGATGTTGTCAAAGA
Rv veri Hsp42deltaN	ACGTAAGTGTCTCGGTATCAT
Rv veri Hsp42fulllength	TTCAAAACGTCATAAAGAGATAGG
Seq forw end of Padh1	GTTTCTTTTTCTGCACAATATTC

## 3.5.2 Plasmids

### 3.5.2.1 Bacterial plasmids / Expression plasmids

**Table 2. Bacterial plasmids for protein expression.**

Plasmid name and source are given. Features of the plasmid can be found under “Description”.

Plasmid	Source	Description
pDS56-cHis	lab collection	ColE1-based; <i>lac</i> promoter; Amp <sup>R</sup> ; encodes for His <sub>6</sub> tag downstream of poly-linker
pDS56-cHis-CFP-luciferase	this study	pDS56-cHis; CFP-luciferase
pDS56-cHis-YFP-luciferase	this study	pDS56-cHis; YFP-luciferase
pMDH-NHis	Axel Mogk	pDS56-nHis; MDH
pSUMO	Claes Andreasson	T7-promoter; N-terminal His <sub>6</sub> -SUMO tag; Kan <sup>R</sup>
pSUMO-Hsp26	this study	pSUMO; Hsp26
pSUMO-Hsp42	this study	pSUMO; Hsp42

### 3.5.2.2 Yeast shuttle vectors

**Table 3. Yeast shuttle vectors used in this study.**

Features of the vector are given under „Description“. CEN = centromeric; YIP = yeast integration vector; 2 $\mu$  = 2 $\mu$  origin of replication

Plasmid	Source	Description
p414-GPD-QP103	(Dehay & Bertolotti, 2006)	P414; GPD promoter; N-terminal region of Huntingtin and a poly(Q) stretch with 103 glutamines fused to GFP
pESC-mCherry-VHL	(Kaganovich et al. 2008)	GAL1 promoter; mCherry-VHL; Amp <sup>R</sup> ; URA3; 2 $\mu$
pRS303	(Sikorski & Hieter, 1989)	pBluescript based; Amp <sup>R</sup> ; His3; YIP
pRS303-ACT-Cerulean-luciferase	this study	pRS303; ACT1 promoter; Cerulean-luciferase
pRS303-ACT-yEmCitrine-luciferase	this study	pRS303; ACT1 promoter; yEmCitrine-luciferase
pRS303-ADH-HTB-Cerulean	this study	pRS305; ADH1 promoter; HTB1-Cerulean
pRS303-PHsp42	this study	pRS303; HSP42 including promoter and terminator (500bp up- and downstream of HSP42)
pRS305	(Sikorski & Hieter, 1989)	pBluescript based; Amp <sup>R</sup> ; LEU2; YIP
pRS305-ADH-HTB-Cerulean	this study	pRS305; ADH1 promoter; HTB1-Cerulean
pRS305-ADH-HTB-mCherry	this study	pRS305; ADH1 promoter; HTB1-mCherry
pRS305-GAL-RNQ1-YFP	lab collection	pRS305; Gal1, 10 promoter; RNQ1-YFP
pRS306	(Sikorski & Hieter, 1989)	pBluescript based; Amp <sup>R</sup> ; URA3; YIP

Plasmid	Source	Description
pRS306-ACT-yEmCitrine-luciferase	this study	pRS306; ACT1 promoter; yEmCitrine-luciferase
pRS313	(Sikorski & Hieter, 1989)	pBluescript based; Amp <sup>R</sup> ; HIS3; CEN
pRS315	(Sikorski & Hieter, 1989)	pBluescript based; Amp <sup>R</sup> ; LEU2; CEN
pRS315-PHsp42	this study	pRS315; HSP42 including promoter and terminator (500bp up- and downstream of HSP42)
pSM006	this study	pRS303; HSP42 promoter and terminator (500bp up- and downstream of HSP42); Hsp42
pSM012	this study	pRS303; HSP42 promoter and terminator (500bp up- and downstream of HSP42); N42-Hsp26
pSM013	this study	pRS303; HSP42 promoter and terminator (500bp up- and downstream of HSP42); Hsp42-FLAG
pSM014	this study	pRS303; HSP42 promoter and terminator (500bp up- and downstream of HSP42); Hsp42ΔN
pSM015	this study	pRS303; HSP42 promoter and terminator (500bp up- and downstream of HSP42); Hsp42ΔC
pSM016	this study	pRS303; HSP42 promoter and terminator (500bp up- and downstream of HSP42); N26-Hsp42
pSM017	this study	pRS303; HSP42 promoter and terminator (500bp up- and downstream of HSP42); Hsp26-C42
pSM018	this study	pRS303; HSP42 promoter and terminator (500bp up- and downstream of HSP42); NC42-Hsp26
pSM019	this study	pRS303; HSP42 promoter and terminator (500bp up- and downstream of HSP42); Hsp26-FLAG

### 3.5.2.3 Yeast integration / knock-out vectors

**Table 4. Yeast integration / knock-out vectors used in this study.**

Original name and source are given, if generated during this study.

Plasmid	Source	Integrated Cassette (Resistance/Auxotrophy)
pBS10	NCRR Yeast Resource Center	pFA6a-link-Cerulean-hphMX4
pFA6-kanMX4	(Wach et al., 1994)	kanMX4 (G418/Geneticin)
pGA25	(Goldstein & McCusker, 1999)	natMX4 (CloNat)
pGA32	(Goldstein & McCusker, 1999)	hphMX4 (Hygromycin B)
pKT211	(Sheff & Thorn, 2004)	pFA6a-link-yEmCFP-SpHIS5
pKT212	(Sheff & Thorn, 2004)	pFA6a-link-yEmCitrine-SpHIS5

### 3.5.3 Bacterial strains

**Table 5. Bacterial strains used in this study.**

Strain nomenclature, source, and the genotype of the strains are given.

Strain	Source	Genotype
BL21*	Novagen	F- ompT hsdSB (rB-mB-) gal dcm rne131 (DE3) F- ompT hsdSB (rB-mB-) gal dcm rne131 (DE3) pLysS (CamR)
<i>E. coli</i> DH5 $\alpha$ pir	(Hanahan, 1983)	<i>supE44, lacU169</i> ( $\Phi$ 80 <i>lacZ</i> M15), <i>hsdR17, recA1, endA1, gyrA96, thi-1, relA1</i>

MC4100	lab collection	araD139 D(argF-lac)205 flb-5301 pstF25 rpsL150 deoC1 relA1
XL1 Blue	lab collection	recA1 endA1 gyrA96 thi-1 hsdR17 supE44 relA1 lac [F proAB lacI. q. ΔAM15 Tn10]

### 3.5.4 *S. cerevisiae* strains

**Table 6. Yeast strains used in this study.**

It is indicated under “source“ if strain was received from a different lab.

Name	Genotype	Source
BY4741	<i>MATa his3Δ1 leu2Δ0 met15Δ0 ura3Δ0</i>	EUROSCARF
hsp26Δ	<i>BY4741 hsp42Δ::kanMX4</i>	EUROSCARF
hsp42Δ	<i>BY4741 hsp42Δ::kanMX4</i>	EUROSCARF
hsp104Δ	<i>BY4741 hsp104Δ::kanMX4</i>	EUROSCARF
pdr5Δ	<i>BY4741 pdr5Δ::natMX4</i>	this study
hsp26Δ pdr5Δ	<i>BY4741 hsp26Δ::kanMX4 pdr5Δ::natMX4</i>	this study
hsp42Δ pdr5Δ	<i>BY4741 hsp42Δ::kanMX4 pdr5Δ::natMX4</i>	this study
hsp104Δ pdr5Δ	<i>BY4741 hsp104Δ::kanMX4 pdr5Δ::natMX4</i>	this study
KAY0173 (LatA-Resistant)	<i>ura3-52 his3Δ200 leu2-3,112 ade4 can1-1 tub2-201 Act1-117</i>	Ayscough lab
KAY0173 (LatA-Resistant) hsp42Δ	<i>KAY0173 hsp42Δ::kanMX4</i>	this study
KAY0159 (Benomyl-Resistant)	<i>ura3-52 his3Δ200 leu2-3,112 cry1 tub2-201 Act1::His3</i>	Ayscough lab
WT (HSP104-mCFP)	<i>BY4741 HSP104-yEmCFP-spHIS5</i>	this study
hsp26Δ (HSP104-mCFP)	<i>BY4741 hsp26Δ::kanMX4 HSP104-yEmCFP-spHIS5</i>	this study
hsp42Δ (HSP104-mCFP)	<i>BY4741 hsp42Δ::kanMX4 HSP104-yEmCFP-spHIS5</i>	this study
WT pdr5Δ (HSP104-mCFP)	<i>BY4741 pdr5Δ::natMX4 HSP104-yEmCFP-spHIS5</i>	this study
hsp26Δ pdr5Δ (HSP104-mCFP)	<i>BY4741 hsp26Δ::kanMX4 pdr5Δ::natMX4 HSP104-yEmCFP-spHIS5</i>	this study
hsp42Δ pdr5Δ (HSP104-mCFP)	<i>BY4741 hsp42Δ::kanMX4 pdr5Δ::natMX4 HSP104-yEmCFP-spHIS5</i>	this study
WT pdr5Δ (HSP26-mCitrine)	<i>BY4741 pdr5Δ::natMX4 HSP26-yEmCitrine-spHis5</i>	this study
WT pdr5Δ (HSP42-mCitrine)	<i>BY4741 pdr5Δ::natMX4 HSP42-yEmCitrine-spHis5</i>	this study
WT pdr5Δ (HSP42-Cerulean)	<i>BY4741 pdr5Δ::natMX4 HSP42-Cerulean-hphMX4</i>	this study
W303	<i>Mata; can1-100; his3-11,15; leu2-3,112; trp1-1; ura3-1; ade2-1</i>	Lindquist lab
W303 hsp42Δ	<i>W303 hsp42Δ::hphMX4</i>	this study
WT (ABP140-yEmCitrine)	<i>BY4741 Abp140-yEmCitrine-URA3</i>	this study
WT pdr5Δ (ABP140-yEmCitrine)	<i>BY4741 pdr5Δ::natMX4 Abp140-yEmCitrine-URA3</i>	this study
hsp42Δ pdr5Δ (ABP140-yEmCitrine)	<i>BY4741 hsp42Δ::kanMX4 pdr5Δ::natMX4 Abp140-yEmCitrine-URA3</i>	this study

Gene replacements were carried out using primers described in (3.5.1) by standard methods described in (4.1).

### 3.6 Chemicals

#### 3.6.1 General chemicals

All used chemicals were analytical grad and purchased from Roth, Sigma, or Fluka.

Luciferin (sodium salt)	AppliChem
-------------------------	-----------

#### 3.6.2 Column materials

Ni-NT agarose	Qiagen
Protino Ni-IDA	Machery-Nagel
Sephacryl S-300 HR 16/60 column	GE Healthcare Life Sciences

#### 3.6.3 Inhibitors

Benomyl	Sigma-Aldrich
Latrunculin A	Biomol
MG132 (Z-Leu-Leu-Leu-CHO)	Peptide Institute Inc.

#### 3.6.4 Media

Amino acids (for drop out medium)	Sigma
Bacto agar	Roth/Difco
Bacto peptone	Roth/Difco
Complete supplementary medium (CSM, for drop out medium)	QBiogene
Glucose, monohydrate	Roth
Nutrient broth	Difco
Yeast extract	Roth/Difco
Yeast nitrogen base (YNB)	Difco

#### 3.6.5 DNA and protein size standards

Gene ruler	Fermentas
Kb-ladder	Roche

Prestained protein weight marker #441	Fermentas
Prestained protein weight marker #671	Fermentas
Protein weight marker #431	Fermentas

### 3.7 *Kits*

Gel extraction	Amersham Pharmacia
MiniElute PCR Purification Kit	Qiagen
QIAprep Spin Miniprep Kit	Qiagen
QIAquick Gel Extraction Kit	Qiagen
YeaStar Genomic DNA Kit	Zymoresearch
YeaStar RNA kit	Zymoresearch
Zyppy Plasmid Miniprep Kit	Zymoresearch

### 3.8 *Antibodies*

Goat $\alpha$ -luciferase	Abcam
Goat $\alpha$ -mouse IgG (alkaline phosphatase)	Vector
Goat $\alpha$ -rabbit, Alexa Fluor 488 F(ab') <sub>2</sub> of IgG	Molecular Probes
Goat $\alpha$ -rabbit IgG (alkaline phosphatase)	Vector
Mouse $\alpha$ -actin	Sigma
Mouse $\alpha$ -goat IgG (alkaline phosphatase)	Vector
Rabbit $\alpha$ -glucose-6-phosphate-dehydrogenase	Sigma
Rabbit $\alpha$ -Hsp104	lab collection
Rabbit $\alpha$ -Hsp26	Buchner lab
Rabbit $\alpha$ -Hsp42	Buchner lab
Rabbit $\alpha$ -YFP	lab collection

### 3.9 *Enzymes and miscellaneous proteins*

Bovine serum albumin (BSA) fraction V	Roth
Concanavalin A	Sigma-Aldrich
L-malate dehydrogenase (L-MDH)	Roche
Opti Taq polymerase	Roboklon
Phusion™ High Fidelity polymerase	NEB, lab collection

---

RNase A	Sigma
Restriction enzymes	NEB, Fermentas
T4-DNA ligase	Roche, lab collection
T4-DNA polymerase	Roche
Taq polymerase	lab collection

### ***3.10 Growth media and antibiotics***

#### **3.10.1 Bacterial media**

LB-medium	1 % Bacto-peptone 0.5 % yeast extract 1 % NaCl (1.5 % Bacto-agar)
2xYT-medium	1.6 % Bacto-peptone 1 % yeast extract 0.5 % NaCl
TB-medium	1.2 % tryptone 2.4 % yeast extract 0.4 % (w/v) glycerol 0.23 % KH <sub>2</sub> PO <sub>4</sub> 1.25 % K <sub>2</sub> HPO <sub>4</sub>

#### **3.10.2 Yeast media**

Rich medium (YPD)	2 % Bacto-peptone 1 % yeast extract (2 % Bacto-agar) 2 % glucose
Synthetic complete yeast medium	0.67 % Bacto-yeast nitrogen base 0.78 % CSM amino acids/bases

---

(2 % Bacto-agar)

2 % glucose

### 3.11 Antibiotics

Final concentrations are listed.

Ampicillin (Na-salt)	100 µg/ml
Chloramphenicol	25 µg/ml (in ethanol)
CloNAT	100 µg/ml
Cycloheximide	10-15 µg/ml
G418 (Geneticin disulfate)	300 µg/ml
Hygromycin B	200 µg/ml
Kanamycin	20 µg/ml
Tetracycline	10 µg/ml

## 4. Methods

### 4.1 Molecular biology methods

#### 4.1.1 Molecular cloning

All molecular biology standard methods were carried out as described previously (Maniatis *et al.*, 1989). Plasmid preparations and DNA extractions from agarose gel electrophoresis were performed using the aforementioned kits (3.7).

#### 4.1.2 Agarose gel electrophoresis

Agarose flat-bed gels in various concentrations (0.6 – 2 % agarose in 0.5x TBE buffer) and sizes were run to separate DNA-fragments in an electrical field (10 – 20 V/cm) for analytical or preparative use. The desired amount of agarose was boiled in 0.5x TBE buffer until completely molten. After cooling down to ca. 60°C, ethidium bromide solution (2-3 µl per 100 ml agarose) was mixed into the liquid agar, and then poured in a flat-bed tray with combs. As soon as the agarose solidified, the DNA in DNA-loading buffer was loaded into the slots and separated electrophoretically. The DNA was detected on a UV-light tray (265 nm). For

preparative gels, a less strong UV-light source was used (365 nm) to avoid irradiation damage to the DNA.

5x TBE (1l)	54 g Tris base 27.5 g Boric acid 4.7 g Na <sub>4</sub> EDTA
6x DNA loading buffer	40 % sucrose 0.25 % bromophenol blue

### 4.1.3 Preparation of chemically competent cells and transformation

Cells were made competent via the CaCl<sub>2</sub> method by growing 50 ml of XL1 blue cells to mid-logarithmic phase. Cells were subsequently chilled on ice and washed 1x with 20 ml 0.1 M MgCl<sub>2</sub>, 1x with 20 ml CaCl<sub>2</sub>, and finally cells were resuspended in 4 ml 0.1 M CaCl<sub>2</sub> and incubated on ice for another 2 hr. 1 ml 50 % glycerol was added, cells were aliquoted and snap-frozen in liquid nitrogen for storage at -80°C.

Cells were thawed on ice and transformed by addition of 1 µl plasmid DNA or 10 µl ligation reaction to 90 µl of cells, followed by an incubation of 10 min on ice. Cells were subsequently heat shocked for 75 sec at 42°C in a water bath and chilled for 2 min on ice. Finally, 500 µl LB were added and growth was allowed for 30 min to 1 hr for phenotypic expression before plating.

### 4.1.4 Polymerase chain reaction (PCR)

The polymerase chain reaction (PCR) was used to clone genes from plasmids or genomic templates as well as to verify the correct insertion of C-terminal tagging and gene deletion cassettes. Generally, the reaction was performed in 50 µl total volume containing 50 pmol of each primer and 250 µM of a dNTP mix. Depending on the purpose, different DNA polymerases and their recommended buffer systems were used. The New England Biolab Phusion™ High Fidelity polymerase was utilized for cloning because of its high productivity and proof-reading capabilities, the Taq polymerase for analytical PCRs due to its robust amplification properties, and the Roboklon Opti Taq (Taq and Pfu polymerase mixture) for genomic DNA due to its combination of robust amplification and proofreading activity. The PCR reaction was performed in a cycler with the basic amplification protocols outlined

below. Annealing was performed at the primer melting temperature ( $T_m$ ) – 5°C. The final 5-10 min incubation period at 72°C was conducted to allow filling up of incomplete PCR fragments. The PCR products were analyzed by agarose gel electrophoresis and, if necessary, purified with the Qiagen MiniElute PCR purification kit.

**Table 7. Basic PCR amplification protocols**

	<b>Phusion</b>	<b>(Opti) Taq</b>
Initial denaturation	98°C, 30’’	94°C, 4’
Denaturation	98°C, 15’’	94°C, 1’
Annealing	$T_m - 5^\circ\text{C}$ , 20’’	$T_m - 5^\circ\text{C}$ , 1’
Elongation	72°C, 15’’/ kb	72°C, 1’ / kb
Cycle number	28 – 30	28 – 30
Final elongation	72°C, 2’	72°C, 10’

#### 4.1.4.1 Colony PCR

In order to verify the correct integration of fluorescent C-terminal tagging or gene deletion cassettes, colony PCR was performed. Fluorescent tagging was confirmed by utilizing primers that annealed ca. 300 bp upstream of the stop codon of the gene of interest and 90 bp downstream of the start codon of the fluorescent protein. For verification of gene deletions, primers were used that annealed in the 5’ flanking region (ca. 300 bp upstream of the start codon) and 90 bp downstream of the start codon of the TEV-promoter, which is contained within the deletion cassette. Cells lysis was achieved by adding one pipette tip of cells from plate to the PCR mix and incubation at 98°C for 10 min. Subsequently, Taq polymerase was added and a normal PCR reaction (Table 7) was performed.

## 4.2 Protein purification

Protein expression was carried out in *E. coli*. All purification protocols yielded high amounts of pure protein of interest.

### 4.2.1 Purification of Hsp26

- transform BL21 STAR [DE3] / pCodon Plus cm<sup>R</sup> with pSUMO-Hsp26
- inoculate an overnight culture in 8 l of 2 xYT medium supplemented with 50 µg/ml kanamycin and 20 µg/ml chloramphenicol
- grow cells at 30°C to an OD<sub>600</sub> of 0.7 - 1.0 and induce expression with 0.5 mM IPTG
- harvest cells after 3 hr
- resuspend pellet in lysis buffer
- French press 2 x at 1200 psi
- centrifuge at 17000 rpm, rotor F21S, at 4°C for 30 min
- remove supernatant, resolubilize pellet with denaturing buffer, and stir for 2 hr at 4°C
- centrifuge at 17000 rpm, rotor F21S, at 4°C for 30 min to remove insoluble compounds
- rotate supernatant with Protino matrix for 1 hr at 4°C
- wash Protino matrix in batch 5 x with denaturing buffer (4°C)
- wash 1 x with 2 M urea buffer to achieve partial refolding
- elute with elution buffer (4°C)
- add SUMO protease and dialyze overnight with dialysis buffer at 4°C
- deplete His-tagged material by incubation with Protino matrix in a column
- concentrate protein to a volume of approx. 800 µl
- apply on a Sephacryl S-300 HR 16/60 column equilibrated with dialysis buffer to purify Hsp26 oligomer
- analyze fractions and pool
- aliquot, snap freeze, and store at -80°C

Lysis buffer	40 mM Hepes/KOH (pH 7.5) 150 mM KCl 5 % glycerol (v/v) 30 mM 2-mercaptoethanol 1 mM PMSF DNase
--------------	---

Denaturing buffer	40 mM Hepes/KOH (pH 7.5) 150 mM KCl
-------------------	--

---

	30 mM 2-mercaptoethanol
	1 mM PMSF
	8 M urea
2 M urea buffer	40 mM Hepes/KOH (pH 7.5)
	150 mM KCl
	30 mM 2-mercaptoethanol
	1 mM PMSF
	2 M urea
Elution buffer	40 mM Hepes/KOH (pH 7.5)
	150 mM KCl
	30 mM 2-mercaptoethanol
	1 mM PMSF
	250 mM imidazole
	2 M urea
Dialysis buffer	40 mM Hepes/KOH (pH 7.5)
	150 mM KCl
	30 mM 2-mercaptoethanol

#### 4.2.2 Purification of Hsp42

- transform BL21 STAR [DE3] / pCodon Plus cm<sup>R</sup> with pSUMO-Hsp42
- inoculate overnight culture in 2 xYT medium supplemented with 50 µg/ml kanamycin and 20 µg/ml chloramphenicol
- grow cells at 30°C to an OD<sub>600</sub> of 0.7 - 1.0 and induce expression with 0.5 mM IPTG
- harvest cells after 3 hr
- resuspend pellet in buffer A
- stir at room temperature for 1 hr; lysis is complete when the suspension is translucent
- ultrasonicate to destroy slimy DNA
- remove insoluble compounds by centrifugation at 17000 rpm, rotor F21S, at 4°C for 30 min
- rotate supernatant with Protino matrix for 1 hr at room temperature

- wash Protino matrix in batch 4 x with denaturing buffer (4°C) and subsequently 1 x with buffer B
- elute with buffer C (4°C)
- collect 10 x 2 ml
- pool and determine protein concentration
- add 4 mM EDTA to inhibit metalloproteases
- incubate for 5-10 min with SUMO protease
- latest after 10 min start overnight dialysis in buffer B
- deplete His-tagged material by incubation with Protino matrix in a column
- dialyze overnight with dialysis buffer at 4°C to induce refolding
- concentrate protein to a volume of approx. 800 µl
- apply on a Sephacryl S-300 HR 16/60 column equilibrated with buffer E to purify Hsp42 oligomer
- analyze fractions and pool
- aliquot, snap freeze, and store at -80°C

Buffer A

- 40 mM Hepes/KOH (pH 8.0)
- 150 mM KCl
- 30 mM 2-mercaptoethanol
- 1 mM PMSF
- DNase
- 6 M guanidine hydrochloride

Denaturing buffer

- 40 mM Hepes/KOH (pH 7.5)
- 150 mM KCl
- 30 mM 2-mercaptoethanol
- 1 mM PMSF
- 8 M urea

Buffer B

- 40 mM Hepes/KOH (pH 7.5)
- 150 mM KCl
- 30 mM 2-mercaptoethanol
- 1 mM PMSF
- 4 M urea

---

Buffer C	40 mM Hepes/KOH (pH 7.5) 150 mM KCl 30 mM 2-mercaptoethanol 1 mM PMSF 250 mM imidazole 4 M urea
Buffer D	40 mM Hepes/KOH (pH 7.5) 150 mM KCl 30 mM 2-mercaptoethanol 1 mM PMSF 4 M urea
Dialysis buffer	40 mM Hepes/KOH (pH 7.5) 150 mM KCl 30 mM 2-mercaptoethanol
Buffer E	40 mM Hepes/KOH (pH 7.5) 150 mM KCl 2 mM DTT

#### 4.2.3 Purification of CFP- and YFP-luciferase

- transform *E. coli* MC4100 cells with pDS56-nHis-CFP-luciferase or pDS56-nHis-YFP-luciferase, respectively.
- inoculate an overnight culture in 2 xYT medium supplemented with 100 µg/ml ampicillin
- grow cells at 30°C to an OD<sub>600</sub> of 0.7 and add benzyl alcohol (1:1000, v/v)
- grow cells at 20°C for 30 min
- induce expression with 100 µM IPTG
- grow cells overnight
- harvest cells by centrifugation at 4000 rpm, F7 rotor, for 30 min at 4°C
- resuspend cells in lysis buffer

- French press 2 x at 1200 psi
- centrifuge at 17000 rpm, rotor F21S, at 4°C for 30 min
- incubate supernatant with Ni-NTA material for 1 hr at 4°C on a shaker (use less than 3 ml Qiagen Ni-NT agarose slurry per 50 ml of lysate)
- apply on a self-pack plastic column
- collect flow-through and reload it
- wash Ni-NTA agarose 2 x with 50 ml wash buffer
- elute protein from the column in 6 fractions by applying 500 µl elution buffer per fraction
- analyze fractions and pool
- dialyze overnight in order to remove the imidazole
- determine protein concentration
- aliquot and snap freeze in liquid nitrogen

Lysis buffer	50 mM NaH <sub>2</sub> PO <sub>4</sub> 300 mM NaCl 15 mM imidazole 3 mM 2-mercaptoethanol 1 mM PMSF protease inhibitor cocktail trace amounts of DNase adjust pH to 8.0 using NaOH
Wash buffer	50 mM NaH <sub>2</sub> PO <sub>4</sub> 300 mM NaCl 30 mM imidazole 3 mM 2-mercaptoethanol adjust pH to 8.0 using NaOH
Elution buffer	50 mM NaH <sub>2</sub> PO <sub>4</sub> 300 mM NaCl 250 mM imidazole 3 mM 2-mercaptoethanol adjust pH to 8.0 using NaOH

Dialysis buffer	50 mM NaH <sub>2</sub> PO <sub>4</sub>
	300 mM NaCl
	10 % glycerol
	3 mM 2-mercaptoethanol
	adjust pH to 8.0 using NaOH

### 4.3 Protein analysis

#### 4.3.1 Bradford colorimetric protein quantification method

The Bradford method for protein quantification is a colorimetric assay based on the shift of the coomassie brilliant blue absorption maximum from 465 to 595 nm upon interaction with basic or aromatic amino acid residues. By comparison to a BSA standard calibration curve (0, 1, 2, 4 and 6 mg/ml BSA), the precise concentration of a protein in solution can be determined. The Bradford reagent was diluted 1:5 with water and 1 ml mixed with 1 – 5 µl of the protein solution. The absorption was measured at 595 nm in a photospectrometer.

#### 4.3.2 Gel-electrophoresis with SDS-PAGE

Proteins of different sizes can be separated by discontinuous SDS-polyacrylamide gel electrophoresis (SDS-PAGE) under denaturing conditions. The gels used for this are bipartite: a lower separation gel, with polyacrylamide concentrations from 8 to 15 % depending on the size of the proteins to be separated, and a stacking gel with 4 % polyacrylamide to focus all proteins before they enter the lower part (Table 8, Table 9).

**Table 8. Composition of the separating SDS-gel.**

Amounts for 4 mini gels / one maxi gel are given.

	8 %	10 %	12 %	14 %	15 %
Acrylamide (30 %) in ml	8	10	12	14	15
4x SDS separation buffer in ml	7.5	7.5	7.5	7.5	7.5
Water in ml	14.5	12.5	10.5	8.5	7.5
10 % APS in µl	240	240	240	240	240
TEMED in µl	40	40	40	40	40

**Table 9. Composition of the stacking SDS-gel.**

Acrylamide (30 %) in ml	3
4x SDS stacking buffer in ml	5
Water in ml	12
10 % APS in $\mu$ l	90
TEMED in $\mu$ l	40

The samples were prepared by mixing with Laemmli protein loading buffer (Laemmli, 1970) and boiling for 5 min at 95°C. The samples were then loaded into the rinsed slots of the gel with a Hamilton syringe. All gels were run with 120 V in 1x SDS gel running buffer until the samples entered the separating gel. The current was then raised to 200-230 V, depending on the gel size. The gel run was continued until the bromophenol blue marker had reached the bottom of the gel to guarantee optimal partitioning of the proteins.

1 x SDS gel running buffer	25 mM Tris, pH 8.0 200 mM Glycine 0.1 % (w/v) SDS
4 x Laemmli buffer (SDS gel loading buffer)	500 mM Tris/HCl, pH 6.8 8 % (w/v) SDS 40 % (v/v) glycerol 20 % (v/v) $\beta$ -mercaptoethanol 0.6 % (w/v) bromophenol blue

#### 4.3.2.1 Coomassie Blue staining of gels

Proteins can be visualized in SDS gels by Coomassie Blue staining. The dye complexes with basic and aromatic side chains, resulting in a blue color of the protein bands. Before staining, the gel was fixed with destaining solution for 15 to 30 min to wash out the SDS, which results in less background staining. The gel was then incubated on a shaker in staining solution for at least 1 hr or at maximum overnight. Finally, the Coomassie solution was removed and the stained gel was again incubated in destaining solution until the background signal was low and the protein bands were clearly visible.

Staining solution	0.2 % (w/v) Coomassie Brilliant Blue R250 50 % (v/v) methanol 5 % (v/v) acetic acid -> filter before use
Fixing/Destaining solution	50 % (v/v) methanol 5 % (v/v) acetic acid

#### 4.3.2.2 Silver stain of protein bands in SDS-polyacrylamide gels

The silver stain method is a sensitive staining method to visualize protein bands that cannot be detected with Coomassie staining. All steps are carried out at room temperature on a shaker. The SDS was washed out of the gel by incubation in an excess of fixing solution for at least 2 hr, or optimally, overnight. The gel should always be covered by the solutions added. After a wash step of 2x 25 min in washing solution, the prestaining solution was applied for 1 min, followed by 20 min incubation in the silver nitrate staining solution. To wash away the remains of the staining solution, the gel was rinsed with deionized water 3 x. Immediately afterwards, the gel was incubated in developing solution until the bands became clearly visible. Depending on the amount of the protein, this step took from 10 to 30 min. The complete reaction was stopped with stop solution.

Fixing solution	50 % (v/v) ethanol 10 % acetic acid 0.05 % formaldehyde (37 %)
Washing solution	50 % ethanol
Prestaining solution	0.02 % (w/v) $\text{Na}_2\text{S}_2\text{O}_3/5\text{H}_2\text{O}$
Staining solution	0.2 % (w/v) $\text{AgNO}_3$ 0.075 % (v/v) formaldehyde (37 %)
Developing solution	6 % (w/v) $\text{Na}_2\text{CO}_3$ 0.0004 % (w/v) $\text{Na}_2\text{S}_2\text{O}_3/5\text{H}_2\text{O}$

	0.05 % (v/v) formaldehyde (37 %)
Stop solution	44 % (v/v) ethanol 12 % acetic acid

### 4.3.3 Western blotting of SDS-PAGE gels

The Western blotting technique is used to transfer proteins from a SDS-polyacrylamide gel and immobilize them on a PVDF membrane. Both methods described here utilize the negative net charge of proteins in a SDS-polyacrylamide gel to transfer them onto a PVDF membrane by applying an electrical field.

Ponceau S solution	0.1 % acetic acid 0.2 % (w/v) Ponceau S
Blocking solutions for Western blots	3 % (w/v) BSA in TBST 5 % milk powder in TBST
1x TBST buffer	10 mM Tris/HCl, pH 8.0 150 mM NaCl 0.05 % (v/v) Tween 20
1x TBS buffer	10 mM Tris/HCl, pH 8.0 150 mM NaCl

#### 4.3.3.1 Wet blotting technique

The proteins are transferred to the PVDF membrane in a chamber completely filled with 1x blotting buffer. This method was used for blotting of maxi gels. The setup was assembled in the following order in a tray filled with blotting buffer to keep all components wet:

- anode side (bottom)
- plexiglass frame
- foamed plastic (5 mm thick)
- 3 layers Whatman 3 mm paper (wet with 1x blotting buffer before)
- PVDF membrane (activated by incubation in methanol for 20 sec)
- SDS-polyacrylamide gel

- 3 layers Whatman 3 mm paper (wet with 1x blotting buffer before)
- foamed plastic (5 mm thick)
- plexiglass frame
- cathode side (top)

All layers must be free of air bubbles to allow an even transfer. The complete stack was placed in the blotting tank, completely filled with 1 x blotting buffer, and blotted overnight with 15 V.

1x Blotting buffer	25 mM Tris, pH 8.0
	200 mM glycine
	10 % (v/v) methanol

#### 4.3.3.2 Semi-dry blotting technique

This technique requires only moistured membranes and papers between two graphite plates. Semi dry blotting was used to transfer proteins from mini or midi gels. The setup was assembled from bottom to top in the following order:

- anode (bottom)
- 6 layers Whatman 3 mm paper (wet with blotting buffer before)
- PVDF membrane (activated by incubation in methanol for 20 sec)
- SDS polyacrylamide gel
- 6 layers Whatman 3 mm paper (wet with blotting buffer before)
- cathode (top)

All layers must be flattened to avoid air bubbles. The gels were blotted for 45 min with 15 V.

1x Blotting buffer	25 mM Tris, pH 8.0
	200 mM glycine
	0.01 % (w/v) SDS
	20 % (v/v) methanol

#### 4.3.3.3 Immunodetection of immobilized proteins

The proteins on the blotted membranes were detected with immunological methods. First, the membrane was stained with Ponceau S solution to visualize the size marker. The dye was washed away with water and the membrane was blocked with 3 % BSA in 1x TBST for at least 1 hr at room temperature or overnight at 4°C. Then, the blot was washed 4x for 5 min with an excess of 1x TBST. Next, the PVDF membrane was incubated with the first antibody, which was diluted 1:500 to 1:100'000 in 1x TBST for 1 hr at room temperature. After washing with 1x TBST, the secondary antibody (diluted 1:1000 to 1:10'000) was applied in 1x TBST for 1 hr at room temperature. The secondary antibody was conjugated with either alkaline phosphatase, which releases a fluorophore from the synthetic ECF substrate in an enzymatic reaction, or horseradish peroxidase, which produces optically active hydroxyl peroxide. A final wash with 1x TBST for 5x 5 min was followed by incubation with the substrate. The ECF stock solution was diluted 1:10 in 1x TBST and evenly distributed onto the PVDF membrane. The membrane was placed on a clean glass surface and covered with an acetate sheet after applying the ECF substrate, avoiding air bubbles. Incubation time was 10 to 15 min at room temperature. The signals were detected with a Fuji fluoroimage reader. The same procedure was followed using ECL developing, but for detection, a film was put onto the membrane for several time points (15 s – 30 min), depending on the signal, and subsequently developed.

#### 4.3.3.4 Quantification of Western blot signals

The Image J software was used for quantification. To compare the expression and degradation levels of yEmCitrine-luciferase in wild-type, hsp26Δ, hsp42Δ, and hsp104Δ strains, luciferase protein amounts were determined by quantification of the Western blot bands after preconditioning (37°C, 45 min) and 120 min recovery (30°C) (see paragraph 4.5.9). Subsequently, the values were normalized to the loading control.

#### 4.3.4 Solubility assay of luciferase aggregates

To compare the solubility of total protein aggregates induced by heat shock in wild-type and hsp42Δ cells, we conducted a protein solubility assay according to published protocols (Kaganovich *et al.*, 2008) with minor modifications. Cells expressing yEmCitrine-luciferase were heat-shocked and recovered as described in paragraph 4.5.9.

- wash 1x with sterile double-distilled water
- resuspend in native yeast lysis buffer
  - where indicated, lysis buffer also contained 0.5 % Triton
- add 1 volume glass beads and lyse 6x 30 sec with 1 min breaks in ice slurry or use bead beater
- remove beads by centrifugation for 5 min at 2000 rpm at 4°C
- clarify by centrifugation for 3x 5 min at 4500 rpm at 4°C
- set aside 50 µl of the supernatant as “total protein”
- spin at full speed for 30 min at 4°C
- remove supernatant as “soluble fraction”
- resolubilize pellet by heating in 50 µl 1x SDS sample buffer
- add 50 µl of 4x SDS sample buffer to the “total protein” and “soluble fraction” samples
- resolve equal amounts of each fraction by SDS–PAGE followed by immunoblot analysis with anti-luciferase antisera.

Native yeast lysis buffer	30 mM HEPES (pH 8.0)
	150 mM NaCl
	1 % glycerol
	1 mM DTT
	1 mM PMSF
	1 mg/ml pepstatin-A

#### **4.4 *In vitro work***

##### **4.4.1 Malate dehydrogenase (MDH) prevention of aggregation assay**

Heat-induced aggregation of MDH leads to the formation of inclusions that scatter light. The light scattering can be prevented by the addition of molecular chaperones.

Preparation of MDH:

- gently swirl ammonium sulfate stock of MDH and take out 500 µl
- centrifuge at 13 000 rpm for 30 min at 4°C
- discard supernatant
- resuspend pellet in 1 ml MDH buffer

- centrifuge at 13 000 rpm for 15 min at 4°C
- filter supernatant with 0.22  $\mu\text{m}$  pore size

Testing of MDH aggregation in a fluorimeter:

- heat water bath of the fluorimeter to 47°C
- centrifuge MDH buffer for 1 min at 13 000 rpm to remove air bubbles
- incubate 400  $\mu\text{l}$  MDH buffer at 47°C for 10 min
- add 0.5  $\mu\text{M}$  MDH final concentration and mix carefully
- pipette 30  $\mu\text{l}$  of the mix to a pre-warmed glass cuvette
- measure aggregation at 600 nm excitation and emission wavelength for 30 min

Prevention of aggregation by small heat shock proteins (sHsps):

- follow the above protocol except pre-warming MDH buffer for 15 min at 47°C with the appropriate amount of sHsps (0.5 – 2  $\mu\text{M}$  final concentration)

MDH buffer: 50 mM Tris HCl pH 7.5  
150 mM KCl  
20 mM MgCl<sub>2</sub>  
2 mM DTT

#### **4.4.2 CFP-luciferase and YFP-luciferase prevention of aggregation assay**

The assay was performed as the MDH prevention of aggregation assay (4.4.1). 0.5  $\mu\text{M}$  CFP-luciferase and YFP-luciferase final concentration were used.

#### **4.4.3 Monitoring the aggregation rate of CFP-luciferase and YFP-luciferase by measuring the FRET signal**

The Fluorescence Resonance Energy Transfer (FRET) signal generated by co-aggregation of CFP-luciferase and YFP-luciferase was measured in a fluorimeter with an excitation wavelength of 435 nm and an emission wavelength of 530 nm. Measuring solely the CFP or YFP signal was performed at 435 nm or 515 nm excitation and 475 nm or 530 nm emission wavelength, respectively.

- heat water bath of the fluorimeter to 47°C



- allow phenotypic expression of strains supplemented with antibiotic resistance cassettes overnight on YPD plates before replication on selective plates

#### **4.5.2 Deletion of genes in the *S. cerevisiae* genome**

Since *S. cerevisiae* cells possess a very efficient DNA recombination system, about 50 base pairs of homologous sequence, flanking large non-homologous DNA stretches, are sufficient for targeted insertion into the yeast genome. Thus, genes can be deleted by replacing their coding sequence with selection markers. The knock-out cassettes were amplified by PCR, using specific primers with 50 - 75 bp homology to the genomic sequence flanking the target gene. The linear PCR product (at least 10 µg DNA) was transformed into the strain background of interest, and cells were kept on selective agar plates for multiple replica rounds to isolate single clones. Potential positive clones were tested for correct insertion of the gene deletion cassette by colony PCR (4.1.4.1).

#### **4.5.3 Isolation of genomic DNA from *S. cerevisiae***

Genomic DNA was prepared from yeast using the YeaStar DNA prep kits (3.7) according to the manufacturer's protocols.

#### **4.5.4 Chromosomal fluorescent protein tagging**

Chromosomal mCFP and mCitrine tagging was carried out using the optimized cassettes for fluorescent protein tagging in *Saccharomyces cerevisiae* (Sheff and Thorn, 2004). Chromosomal Cerulean tagging of Hsp42 was performed as described elsewhere (Rizzo *et al.*, 2004).

#### **4.5.5 MG132, latrunculin A, benomyl, and cycloheximide treatment**

Cells were grown until mid-log phase ( $OD_{600} = 0.5$ ) at 30°C. For experiments using MG132, BY4741 strains lacking the Pdr5 transporter were used as wild type. Deletion of Pdr5 sensitizes cells to the proteasome inhibitor. Before temperature shift to 37°C, MG132, dissolved in DMSO, was added to a final concentration of 80 µM. Where indicated, latrunculin A or benomyl, dissolved in DMSO, was added before temperature shift to 37°C or sublethal heat shock to a final concentration of 200 µM or 20 µg/ml, respectively. The same amount of DMSO was added to the control. In order to monitor the stability of JUNQ and

IPOD compartments, cells were incubated at 37°C for 180 min (+ MG132). Subsequently, cells were washed and the translation inhibitor cycloheximide, dissolved in ethanol, was added to final concentration 10 µg/ml before starting the recovery at 30°C. The same amount of ethanol was added to the control. For all experiments, VHL expression was shut off before temperature shift and microscopy by addition of 2 % glucose.

#### **4.5.6 Thermotolerance analysis**

Overnight cultures of yeast cells were diluted into fresh YPD medium and grown to mid-log phase. Cells were first shifted to 37°C for 60 min, and then incubated at 50°C for the indicated period of time. Samples were taken, serially diluted, spotted onto YPD plates, and survival of cells was determined by calculating the plating efficiency after two days growth at 30°C.

#### **4.5.7 Serial dilution spot tests**

Growth behavior under various conditions was tested by spotting dilution series on agar plates. The optical density of an overnight culture was measured at 600 nm and the cells were diluted to a final OD<sub>600</sub> of 0.5, which is equivalent to approximately 10<sup>7</sup> yeast cells per ml. The cells were 5-fold diluted, spotted on the respective plates, and grown for two to three days, until the positive (wild type) control spots were clearly visible at the lowest dilution.

#### **4.5.8 Preparation of *S. cerevisiae* cell extracts for Western blotting**

Cells were grown to mid-log phase and ca. 1 OD<sub>600</sub> unit was transferred to an Eppendorf tube. The yeast cells were pelleted, resuspended in 240 µl of 1.85 M NaOH and incubated on ice for 10 min. After the addition of an equal volume of 50 % TCA, the cells were placed on ice for an additional 10 min and pelleted by centrifugation (13 000 rpm, 4°C, 10 min in a table top centrifuge). The resulting pellet was washed with 1 M Tris base. 50 µl of sample buffer was added and 10 - 20 µl of this solution were loaded on a SDS-polyacrylamide gel.

#### **4.5.9 *In vivo* luciferase assay with *S. cerevisiae***

The standard luciferase assay was similarly performed as described previously (Schroder *et al.*, 1993). Luciferase activities were measured from 100  $\mu$ l cell suspensions in a luminometer.

- grow cells to mid-log phase
- shift cells to 37°C for 45 min
- add cycloheximide (10  $\mu$ g/ml) to stop translation
- heat shock cells at 45°C for 20 min
- allow recovery at 30°C for 120 min

#### **4.6 *Microscopy***

Confocal micrographs were obtained from living yeast cells on a spinning disc microscope with a 100x oil lens (NA 1.4). Digital (12-bit) images were acquired with a cooled CCD camera and processed by using Image J and Adobe Photoshop software.

##### **4.6.1 Image acquisition**

For snapshot imaging, cells were recovered by centrifugation, washed in phosphate-buffered saline (PBS), and immobilized on agarose pads. To avoid dehydration, the agarose pads were sealed with Apiezon grease and covered with cover slips. For time-lapse imaging, cells were immobilized on concanavalin A coated cover slips, immersed in medium, and sealed in a custom-made aluminum slide using cover slips on each side. The slide was subsequently placed into a custom made metal holder that was connected to a peltier element, which allowed accurate temperature control.

##### **4.6.2 Image processing and data analysis**

Image processing was carried out using Image J and Adobe Photoshop software. Statistics of aggregation foci number and localization, and plotting of the data were performed with Excel and KaleidaGraph. At least 100 individual cells were analyzed.

### 4.6.3 Fluorescence Loss in Photobleaching (FLIP)

In order to examine the diffusion properties of misfolded proteins in the distinct compartments, Fluorescence Loss in Photobleaching (FLIP) was performed. In brief, a small area of cytosol apart from the mCherry-VHL inclusions is repeatedly bleached with a laser pulse. The resulting fluorescence loss in the region of interest (ROI), as a function of time, provides a measure of the relative exchange rate with the bleached cytoplasmic fraction of molecules. Cells were grown to mid-log phase, immobilized on concanavalin A coated glass bottom culture dishes, and incubated at 37°C for 180 min (+MG132) before FLIP measurements were started. 25 individual cells for the wild-type and hsp42 $\Delta$  strains were measured. A small section of cytosolic fluorescence outside of the inclusions was bleached in 30 cycles of acquisition (0.5 sec, 1-2 % laser intensity) and bleach (0.49 sec, 100 % laser intensity). Measurements were performed at 37°C on a laser scanning confocal microscope (A1R; Nikon).

### 4.6.4 Immunofluorescence

Cells were fixed and stained as described previously (Gavin, 2009). Incubation with anti-Hsp42 (1:400 dilution) and anti-Hsp26 (1:100 dilution) was carried out for 2 hr at room temperature. Secondary antibody (Alexa Fluor 488 F(ab')<sub>2</sub> fragment of goat anti-rabbit IgG) was diluted 1:1000 and incubation was carried out for 1 hr at room temperature.

## 5. Results

### 5.1 Monitoring the fate of protein aggregates in yeast cells using fluorescent reporters

In order to analyze the spatio-temporal organization of protein aggregates in yeast cells, I employed various fluorescent reporter proteins. First, I used a previously characterized fusion construct of mCherry and von Hippel-Lindau (VHL) tumor suppressor. Unassembled VHL, when expressed at 37°C in absence of its cofactor elongin BC, cannot fold properly and is degraded rapidly (McClellan *et al.*, 2005). Upon inhibition of proteasomal degradation, mCherry-VHL aggregates have been described to partition between two different intracellular sites, the juxtannuclear quality control (JUNQ) and insoluble protein deposit (IPOD) compartments (Kaganovich *et al.*, 2008). As alternative fluorescent aggregation reporters, I generated a fully functional C-terminal fusion of monomeric CFP to the disaggregase Hsp104 (Figure 5.1), which was expressed from the authentic promoter and served as an indirect marker by binding to aggregated proteins.

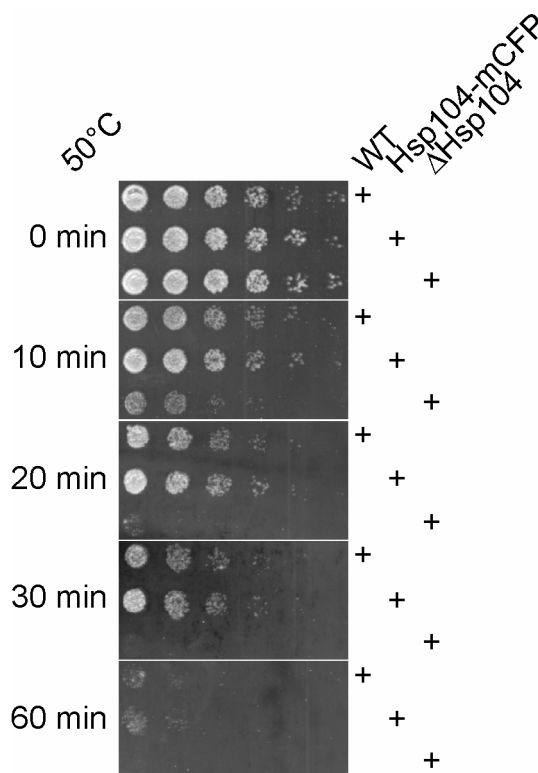


**Figure 5.1 Hsp104-mCFP provides wild-type like thermotolerance.**

*S. cerevisiae* wild-type (WT), Hsp104-mCFP expressing, and *hsp104*Δ cells were grown at 30°C and shifted to 37°C for 60 min. Subsequently, the cells were incubated at 50°C for the indicated time period and spotted in a serial dilution onto YPD plates. Images were acquired after two days growth at 30°C.

In addition, I constructed an N-terminal fusion of monomeric Citrine with the thermolabile model protein *Photinus pyralis* luciferase. The construct was integrated into the yeast chromosome under control of the constitutive *ACT1* promoter, yielding moderate production levels of mCitrine-luciferase (data not shown). Immunoblot analysis revealed only single protein bands corresponding to the proper size of the individual full-length fusion proteins (data not shown), allowing me to monitor protein aggregation by tracking the fluorescent signal of mCherry-VHL, Hsp104-mCFP and mCitrine-luciferase. In *S. cerevisiae* cells with blocked proteasomal activity I analyzed the localization of all fusion proteins at 30°C and various time points after shift to 37°C (Figure 5.2). At 30°C mCherry-VHL and mCitrine-luciferase displayed a homogenous cytosolic distribution, whereas Hsp104-mCFP was enriched in the nucleus (Figure 5.3 A).

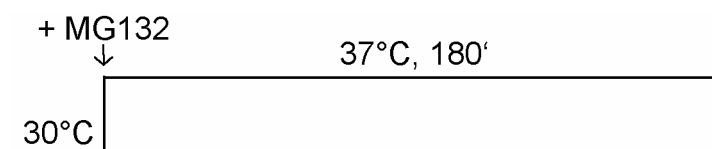


**Figure 5.2 Outline of the experimental setup.**

The localization of all fluorescent reporters was monitored at 30°C and various time points after shift to 37°C. The proteasome inhibitor MG132 was added before the temperature shift.

Incubation at 37°C for 30 min induced the formation of more than three cytosolic mCherry-VHL and Hsp104-mCFP punctae in most cells (60 %) in accordance with published data, while slightly less mCitrine-luciferase foci were detectable (Figure 5.3 A/B). After prolonged incubation at 37°C for 180 min, the number of inclusions was reduced and mCherry-VHL accumulated in one juxtannuclear and one peripheral inclusion in approx. 50 % of the cells. The remaining cells stored misfolded VHL in single or multiple juxtannuclear or peripheral inclusions, or a combination of both. Longer incubation at 37°C (up to 6 hours) did not result in a higher percentage of cells carrying one juxtannuclear and one peripheral aggregate (data not shown). Similar to mCherry-VHL, 180 min incubation at 37°C resulted in accumulation of Hsp104-mCFP and mCitrine-luciferase in one juxtannuclear and one peripheral inclusion in 40-45 % of the cells. The remaining cells mainly possessed a single juxtannuclear inclusion. In conclusion, comparable numbers of inclusions were detectable at similar cellular locations, irrespective of the investigated aggregation reporter (VHL, Hsp104, luciferase). The overall reduced number of mCitrine-luciferase inclusions could be accounted to lower expression levels and only partial misfolding of the thermolabile reporter at 37°C. Simultaneous expression of mCherry-VHL and mCitrine-luciferase revealed perfect co-localization upon

stress treatment (37°C, + MG132) (Figure 5.4), underscoring that different substrates share the same fate and are recruited to the same compartments. Taken together, my observations are similar, but also distinct in parts, from the described partition of misfolded proteins between two distinct compartments, as half of the cells contained only one or more than two foci. Hereafter, I will adopt the terminology of Kaganovich *et al.*, 2008, considering inclusions with juxtannuclear localization as JUNQ and those with peripheral localization as IPOD-like compartments.

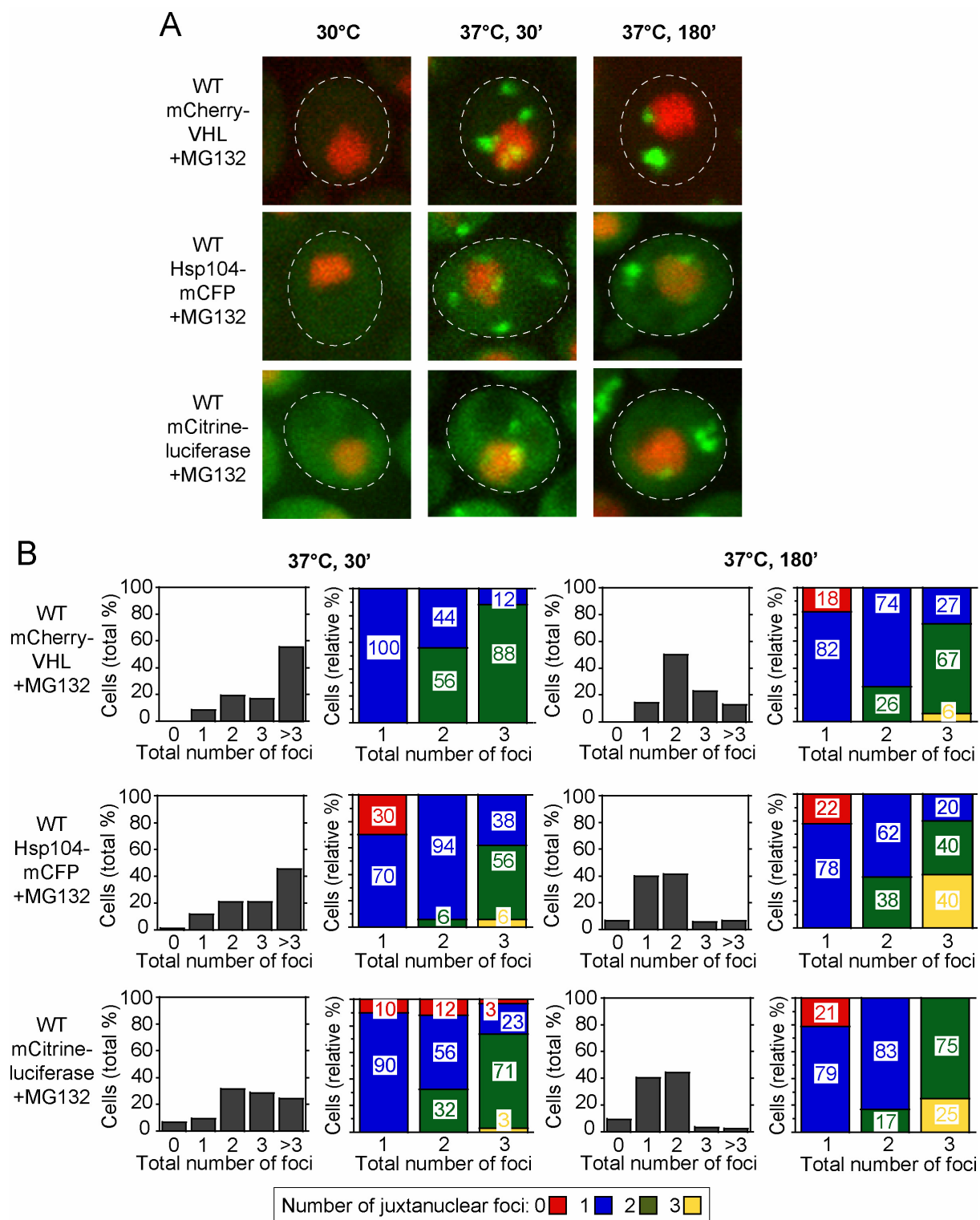


**Figure 5.3 Spatio temporal organization of protein aggregates.**

Time-dependent changes in the localization of mCherry-VHL, endogenous yeast aggregates stained by Hsp104-mCFP, and mCitricine-luciferase (all green) at 30°C and after shift to 37°C for 30 and 180 min in wild-type (WT) cells. The proteasome inhibitor MG132 was added before the temperature shift. Nuclei were visualized by co-expressing HTB1-Cerulean or HTB1-mCherry (red). (B) Number and localization (colored columns) of mCherry-VHL, Hsp104-mCFP, and mCitricine-luciferase inclusions in WT cells after incubation at 37°C for 30 and 180 min. The proteasome inhibitor MG132 was added before the temperature shift. The color code deciphers the foci localization. Red corresponds to zero juxtannuclear inclusions, blue to one, green to two, and yellow to three. The total number of foci per cell is depicted in all diagrams on the x-axis. Quantifications are based on the analysis of  $n = 100$  cells.

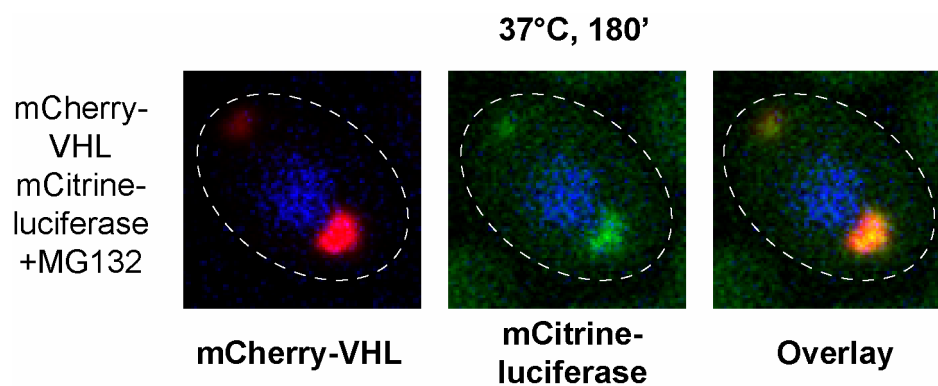


**Figure 5.4 Different substrates are sorted to the same compartments.**

mCherry-VHL (red) and mCitrine-luciferase (green) were co-expressed in *S. cerevisiae* cells. Protein localizations were determined after temperature shift to 37°C for 180 min, revealing co-localization of mCherry-VHL and mCitrine-luciferase. The proteasome inhibitor MG132 was added before the temperature shift. Nuclei were visualized by co-expressing HTB1-Cerulean (blue).

## ***5.2 The small heat shock protein Hsp42 affects the organization of protein aggregates***

Little is known about cellular factors that control the deposition of aggregates at specific sites within yeast cells. Frydman and colleagues could demonstrate that components of the quality control system (Sti1, Ubc4/5) affect the distribution of misfolded proteins between JUNQ and IPOD compartments (Kaganovich *et al.*, 2008). Small heat shock proteins (sHsps) co-aggregate efficiently with misfolded proteins, thereby changing the properties of protein aggregates and facilitating protein disaggregation upon return to physiological growth conditions (Ratajczak *et al.*, 2009; Cashikar *et al.*, 2005; Haslbeck *et al.*, 2005b; Friedrich *et al.*, 2004; Mogk *et al.*, 2003). In a candidate approach I tested for a role of the *S. cerevisiae* sHsps, Hsp26 and Hsp42, in the cellular sorting of misfolded proteins by comparing the localization of mCherry-VHL and Hsp104-mCFP in *hsp26Δ* and *hsp42Δ* mutant cells (Figure 5.5). The lack of Hsp26 had only a minor influence on stress-induced formation of mCherry-VHL and Hsp104-mCFP inclusions. Numbers and localization of respective foci were largely similar to those observed for wild-type (WT) cells after incubation at 37°C for 30 min and 180 min (Figure 5.6). On the contrary, in the vast majority of *hsp42Δ* cells only one juxtannuclear mCherry-VHL inclusion was detected, whereas peripheral inclusions were virtually absent 30 min and 180 min after stress application (Figure 5.5 and Figure 5.6).

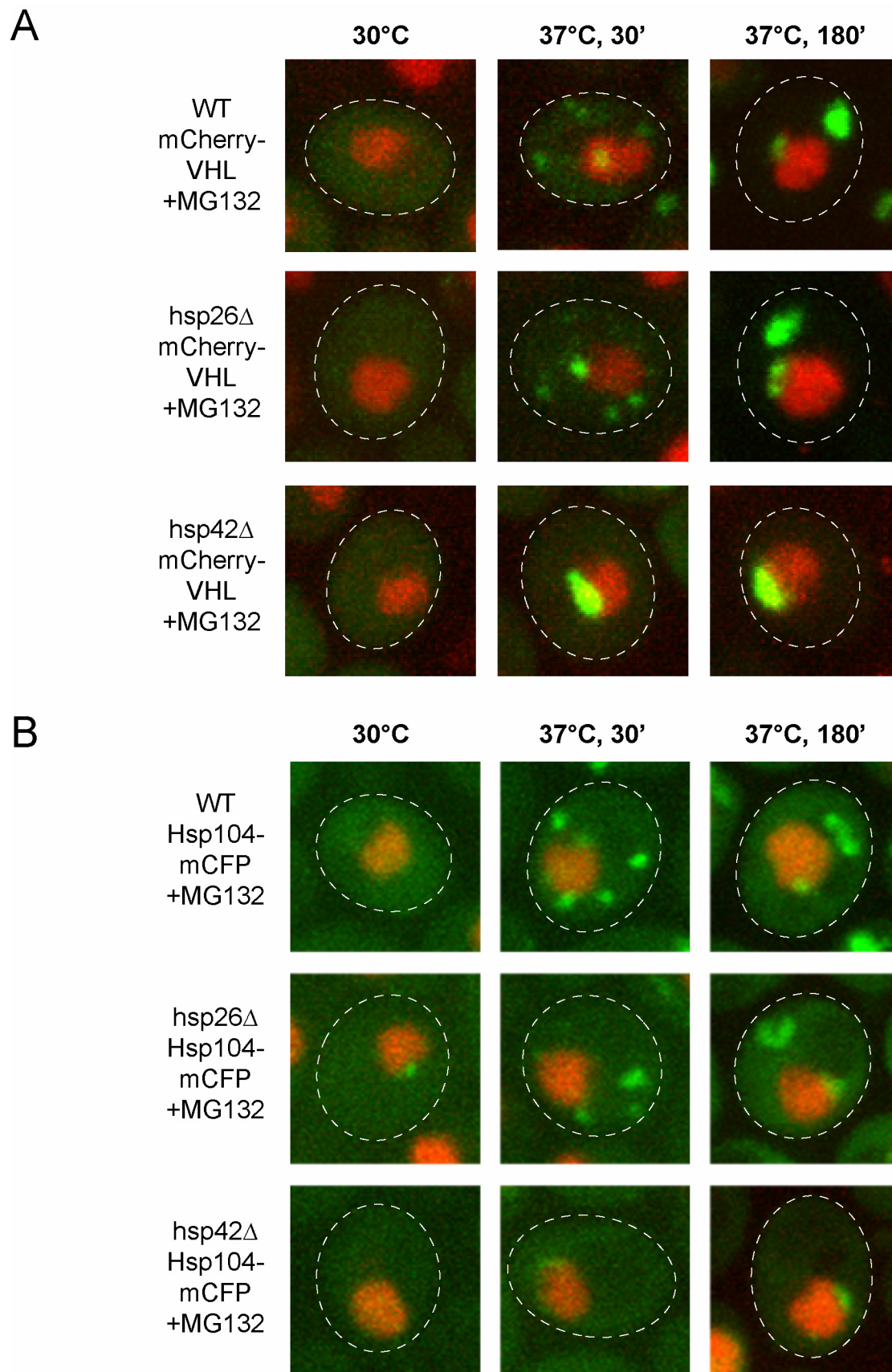


**Figure 5.5 Hsp42 is essential for the targeting of misfolded proteins to peripheral compartments.**

Time-dependent changes in the localization of mCherry-VHL (A) and Hsp104-mCFP (B) (both green) at 30°C and after shift to 37°C for 30 and 180 min in the isogenic wild-type (WT), hsp26Δ, and hsp42Δ strains. The proteasome inhibitor MG132 was added before the temperature shift. Nuclei were visualized by co-expressing HTB1-Cerulean or HTB1-mCherry (red).

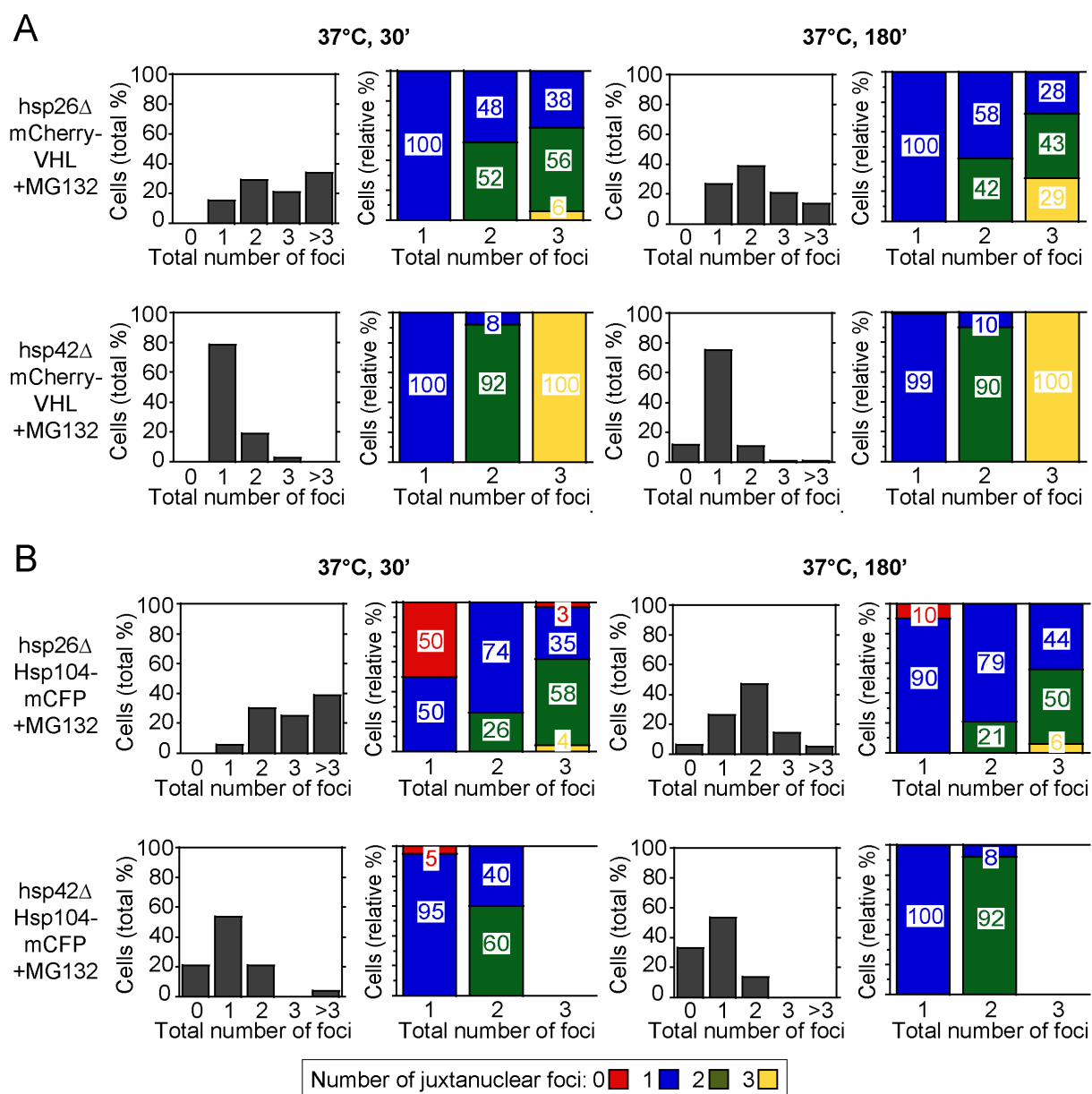


**Figure 5.6 Hsp42 is essential for the targeting of misfolded proteins to peripheral compartments.**

Number (dark grey columns) and localization (colored columns) of mCherry-VHL (A) and Hsp104-mCFP (B) inclusions in hsp26Δ and hsp42Δ cells after incubation at 37°C for 30 and 180 min. The proteasome inhibitor MG132 was added before the temperature shift. The color code deciphers the foci localization. Red corresponds to zero juxtannuclear inclusions, blue to one, green to two, and yellow to three. The total number of foci per cell is depicted in all diagrams on the x-axis. Quantifications are based on the analysis of n = 100 cells.

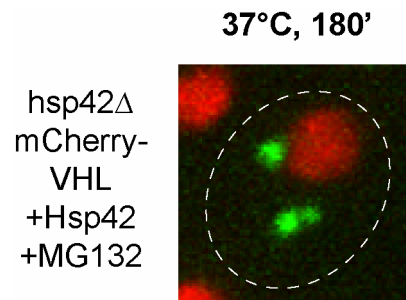


**Figure 5.7 The lack of peripheral inclusions in hsp42Δ cells is directly caused by missing Hsp42.**

Complementing the hsp42Δ strain with Hsp42 expressed from its native promoter induces reappearance of peripheral aggregation foci. Image of an hsp42Δ cell expressing both mCherry-VHL (green) and Hsp42 is shown after incubation at 37°C for 180 min in the presence of the proteasome inhibitor MG132. Nuclei were visualized by co-expressing HTB1-mCherry (red).

The remaining juxtannuclear foci exhibited an increased fluorescent intensity, suggesting that the pool of misfolded mCherry-VHL is entirely directed to the JUNQ compartment. Also endogenous yeast aggregates stained by Hsp104-mCFP localized mostly at the nucleus in hsp42Δ cells (Figure 5.5 and Figure 5.6). Complementing the hsp42Δ cells with Hsp42 expressed from its native promoter restored the occurrence of peripheral aggregation foci (Figure 5.7). Performing single cell time-lapse microscopy, I observed in WT cells that visible inclusions of mCherry-VHL appeared at the nucleus and in the periphery after 15 min at 37°C (Figure 5.8). On the contrary, in the hsp42Δ strain aggregation foci became apparent exclusively at the nucleus, indicating that visible peripheral inclusions are not formed at all. In conclusion, the sorting of misfolded proteins to peripheral deposition sites seems to rely on Hsp42.

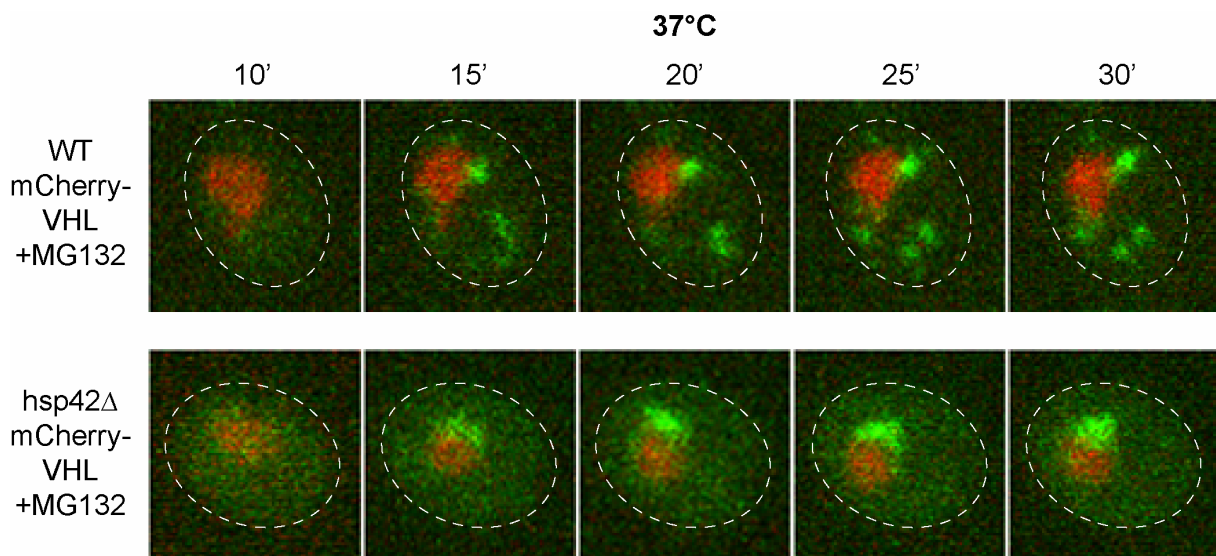


**Figure 5.8 In hsp42Δ cells mCherry-VHL foci form exclusively at the nucleus.**

Time-lapse microscopy pictures are shown of single wild-type (WT) and hsp42Δ cells expressing mCherry-VHL (green) after shift to 37°C for the indicated time period. The proteasome inhibitor MG132 was added before the temperature shift. Nuclei were visualized by co-expressing HTB1-Cerulean (red).

### ***5.3 Hsp42 localizes exclusively in IPOD-like compartments***

To determine whether the absence of peripheral aggregation foci is a direct effect of lacking Hsp42, I constructed chromosomal Hsp26 and Hsp42 C-terminal fusions with mCitrine to monitor their cellular localization (Figure 5.9). The Hsp26-mCitrine fusion exhibits WT-like luciferase reactivation after heat shock, unlike *hsp26Δ* cells, which display a delay in reactivation (Figure 5.10, also see paragraph 5.11). Complementation of *hsp42Δ* cells with Hsp42-mCitrine led to reappearance of peripheral aggregation foci, demonstrating that both fusion proteins possess WT-like activity at least partly. At 30°C both sHsp fusion proteins showed a homogenous cytosolic staining. Incubation at 37°C (+MG132) for 30 min resulted in co-localization of Hsp26-mCitrine with all mCherry-VHL inclusions (Figure 5.9 A). At the same time point Hsp42-mCitrine stained peripheral mCherry-VHL punctae uniformly, while displaying strongly diminished co-localization with one juxtannuclear focus (Figure 5.9 A). Thus, Hsp26 seems to be present in all compartments of misfolded proteins, while Hsp42 is almost absent from the JUNQ. To corroborate these findings I performed immunofluorescence analysis. Here, only analysis of Hsp42 localization was possible, since the utilized Hsp26 antibody proved not suitable for immunofluorescence (data not shown). 30 min after stress application Hsp42 co-localized perfectly with all mCherry-VHL inclusions except for one juxtannuclear focus, which completely lacked staining by the sHsp (Figure 5.9 B). Prolonged incubation (180 min) at 37°C resulted in Hsp42 staining of peripheral mCherry-VHL foci, while the juxtannuclear inclusion still displayed no co-localization (Figure 5.9 B). Taken together, Hsp26 is uniformly distributed among the distinct aggregate compartments, while Hsp42 localizes exclusively to IPOD-like compartments. This observation suggests a direct role of Hsp42 in controlling the flux of misfolded proteins to IPOD-like compartments.

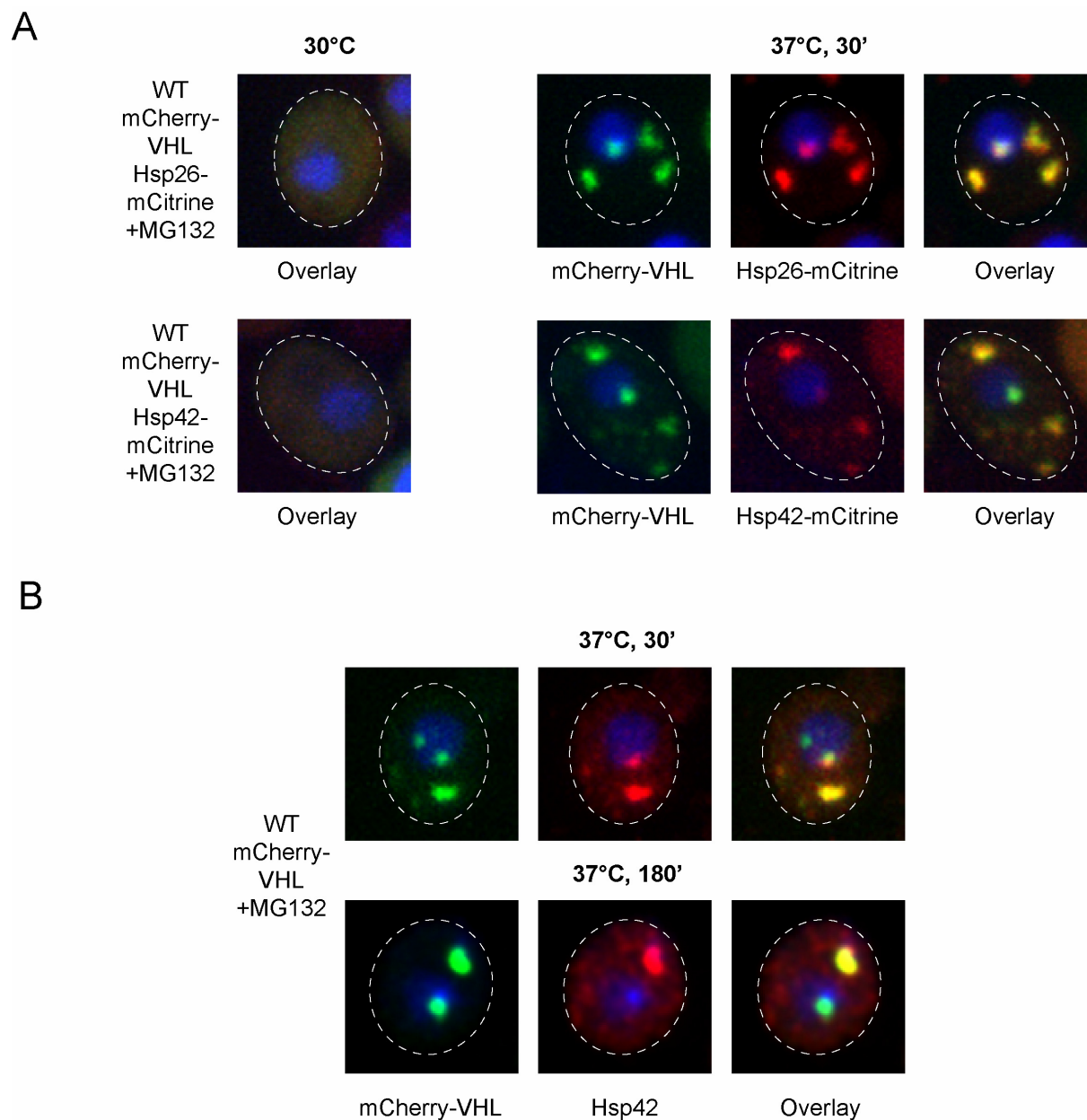


**Figure 5.9 Hsp42 localizes exclusively to IPOD-like compartments.**

(A) *S. cerevisiae* cells co-expressing mCherry-VHL and Hsp26-mCitrine (top) or Hsp42-mCitrine (bottom) were grown at 30°C and shifted to 37°C (+ MG132) for 30 min. mCherry-VHL is depicted in green and sHsp-mCitrine fusions are shown in red. Nuclei were visualized by co-expressing HTB1-Cerulean (blue). Hsp26-mCitrine is uniformly distributed among the different mCherry-VHL compartments, whereas Hsp42-mCitrine is almost absent from one juxtannuclear inclusion. (B) *S. cerevisiae* cells expressing mCherry-VHL were grown at 30°C and shifted to 37°C (+ MG132). The cellular localizations of mCherry-VHL (green) and Hsp42 (red) were determined at the indicated time points. Hsp42 localization was determined by immunofluorescence using specific Hsp42 antibodies. Nuclei were visualized by co-expressing HTB1-Cerulean (blue).

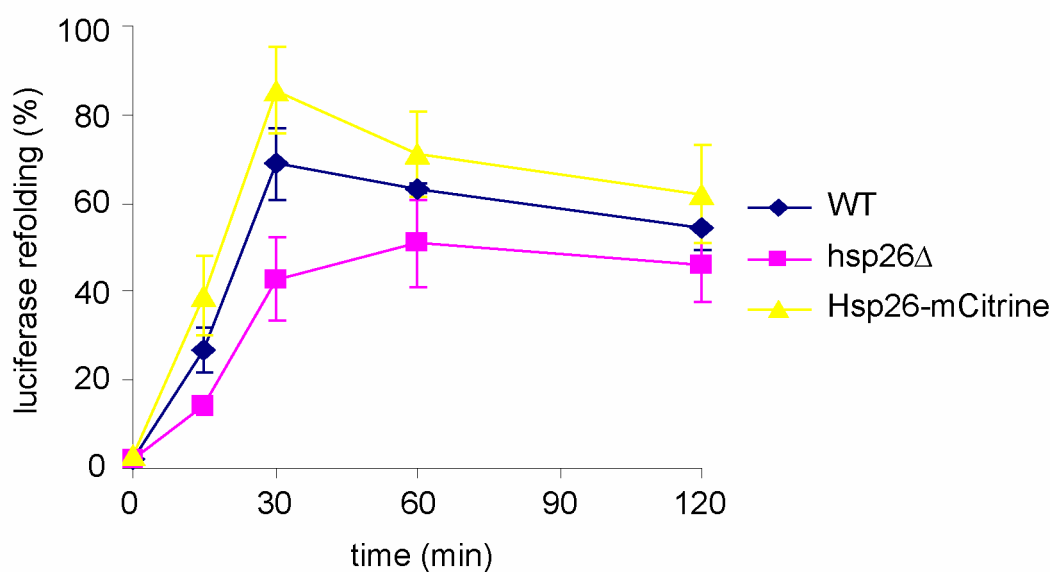


**Figure 5.10 Hsp26-mCitrine exhibits WT-like luciferase refolding after heat shock.**

Cells expressing mCFP-luciferase were preconditioned at 37°C for 45 min, subjected to sublethal heat shock at 45°C for 20 min, and allowed to recover at 30°C. Luciferase activity during recovery at 30°C is depicted in the isogenic wild-type (WT) (blue) and hsp26Δ (pink) strains, and cells expressing a genomic C-terminal fusion of Hsp26 with mCitrine (yellow). The luciferase activity before heat shock was set as 100%. *De novo* synthesis of mCitrine-luciferase was inhibited by addition of 10 μg/ml cycloheximide before heat shock.

#### ***5.4 The N-terminal domain of Hsp42 is crucial for aggregate sorting***

What is the molecular basis for the specific role of Hsp42 in controlling the sorting of misfolded proteins to IPOD-like compartments? sHsps are composed of a conserved  $\alpha$ -crystallin domain and N- and C-terminal flanking regions. N-terminal domains (NTDs) are highly variable in both sequence and length with *S. cerevisiae* Hsp42 possessing a remarkably elongated NTD (243 residues). The large NTD of Hsp42 is therefore a prime candidate for mediating functional specificity. To investigate the role of the different Hsp42 domains, I generated Hsp42 domain deletion and Hsp26 - Hsp42 domain swap constructs as follows (Figure 5.11). I deleted Hsp42 of its NTD (Hsp42 $\Delta$ N) or C-terminal extension (CTE) (Hsp42 $\Delta$ C). I furthermore replaced the NTD, CTE, or both domains of Hsp26 with the corresponding domain of Hsp42 (N42-Hsp26, Hsp26-C42, or NC42-Hsp26, respectively). Moreover, I substituted the NTD of Hsp42 with the respective domain of Hsp26 (N26-Hsp42). All constructs harbored in addition a C-terminal Flag-tag to control construct expression and were genomically integrated at the *hsp42* locus in *hsp42* $\Delta$  cells. Hsp42-Flag and Hsp26-Flag that were expressed from the same site served as controls. The various sHsps constructs were expressed to similar levels (data not shown) and tested for their activity to restore the formation of peripheral mCherry-VHL foci. An inclusion pattern similar to WT cells was observed upon expression of Hsp42-Flag (Figure 5.12 and Figure 5.13). In cells expressing Hsp26-Flag, Hsp42 $\Delta$ N, Hsp26-C42, or N26-Hsp42 very few or no IPOD-like mCherry-VHL inclusions were observed (Figure 5.12, Figure 5.13, and Figure 5.14). Remarkably, Hsp42 $\Delta$ C and N42-Hsp26 restored the occurrence of peripheral fluorescent foci. Here, the number of cells carrying more than two inclusions after 30 min incubation at 37°C (+ MG132) was reduced compared to WT cells, suggesting that both variants exhibit partial activity. Expression of NC42-Hsp26 also restored occurrence of IPOD-like foci. However, the number of cells carrying more than three inclusions was increased, implying slightly enhanced aggregate formation. Taken together, these findings indicate that the Hsp42 NTD directly mediates the sorting of misfolded proteins to peripheral deposition sites.

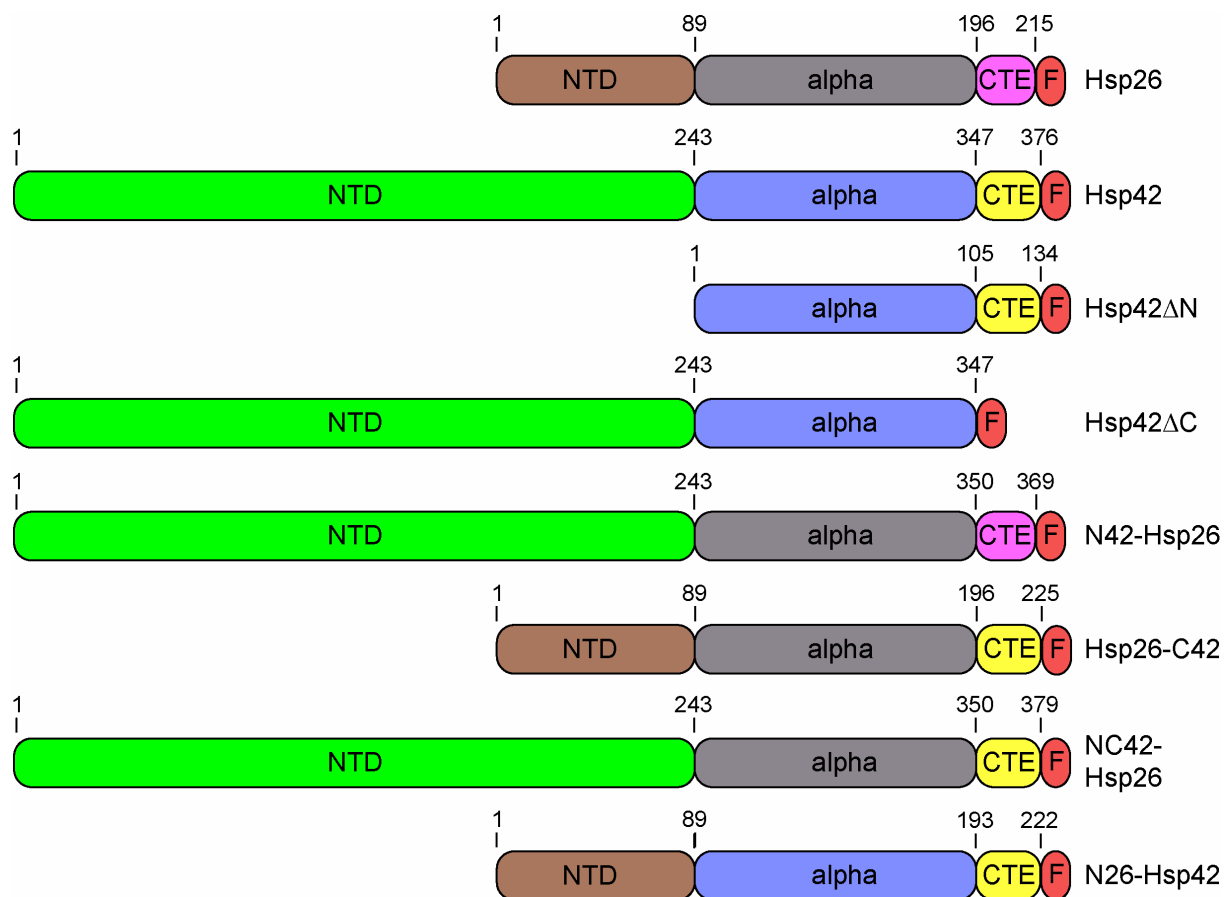


**Figure 5.11 Hsp42 domain deletion and Hsp26 – Hsp42 domain swap constructs.**

Domain organization of Hsp26, Hsp42, and their variants. Both sHsps consist of an N-terminal domain (NTD), a conserved  $\alpha$ -crystallin domain (alpha), and a C-terminal extension (CTE). All constructs were C-terminally fused to a FLAG-tag (F). Domain boundaries are indicated by residue numbers. All constructs were under control of the native *HSP42* promoter and integrated at the Hsp42 locus in hsp42Δ cells.

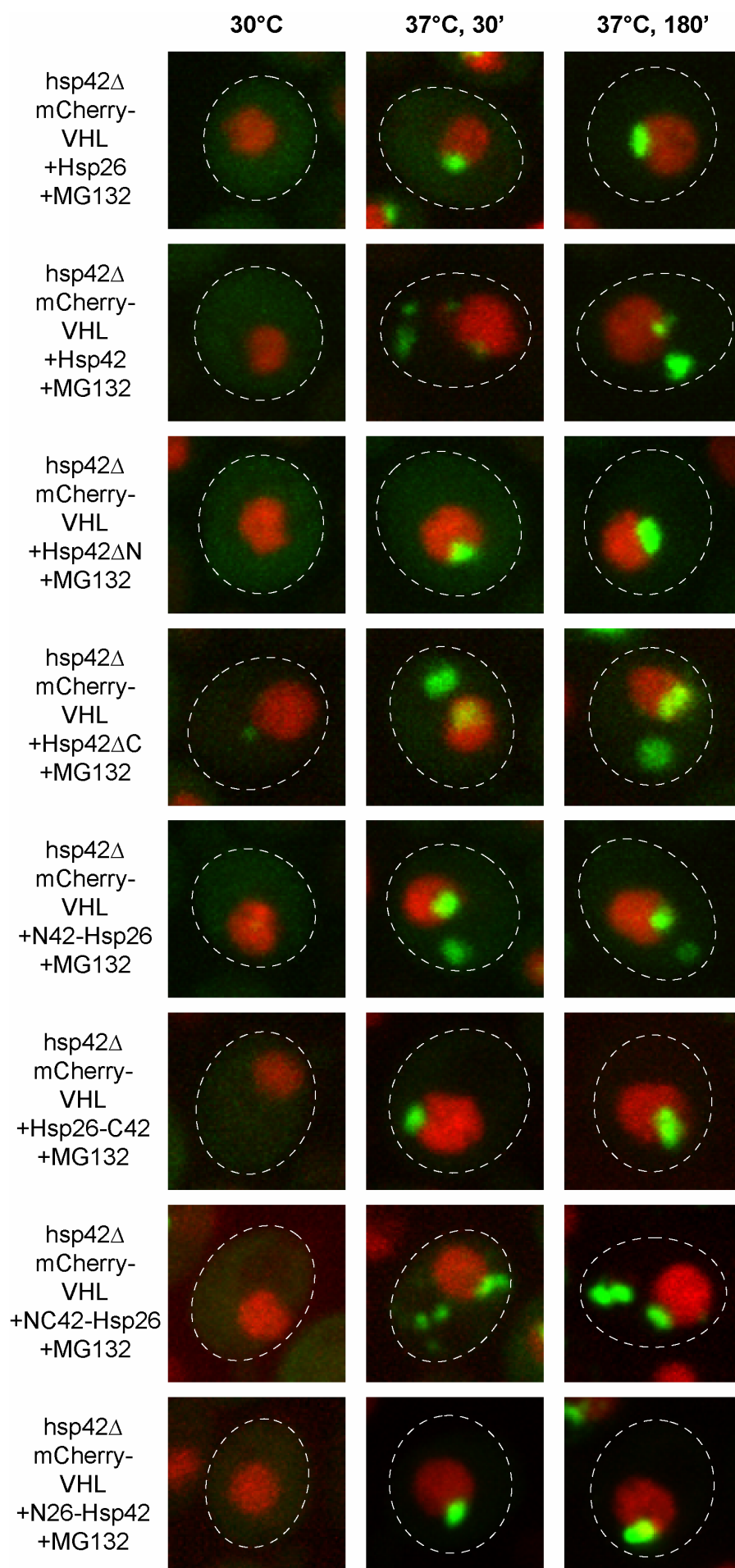


**Figure 5.12 The N-terminal domain of Hsp42 mediates sorting of misfolded proteins to peripheral inclusions.**

*S. cerevisiae* hsp42Δ cells expressing mCherry-VHL and the indicated sHsp constructs (see Figure 5.11) were grown at 30°C and shifted to 37°C (+ MG132). mCherry-VHL localization (green) was determined at the indicated time points. Nuclei were visualized by co-expressing HTB1-Cerulean (red).

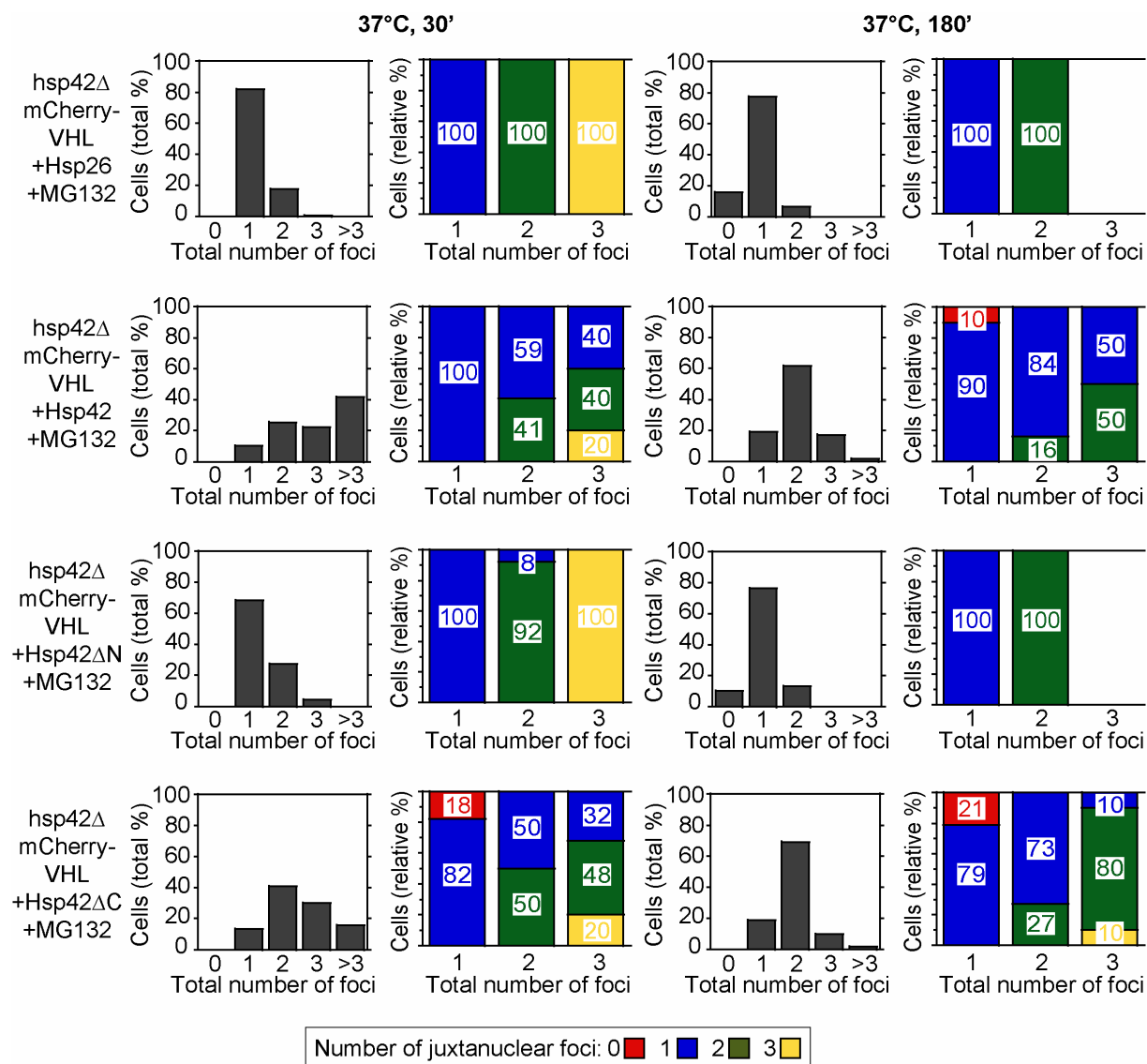


**Figure 5.13 The N-terminal domain of Hsp42 mediates sorting of misfolded proteins to peripheral inclusions.**

Number (dark grey columns) and localization (colored columns) of mCherry-VHL inclusions in hsp42Δ cells expressing the indicated sHsp construct after incubation at 37°C for 30 and 180 min. The proteasome inhibitor MG132 was added before the temperature shift. The color code deciphers the foci localization. Red corresponds to zero juxtannuclear inclusions, blue to one, green to two, and yellow to three. The total number of foci per cell is depicted in all diagrams on the x-axis. Quantifications are based on the analysis of n = 100 cells.

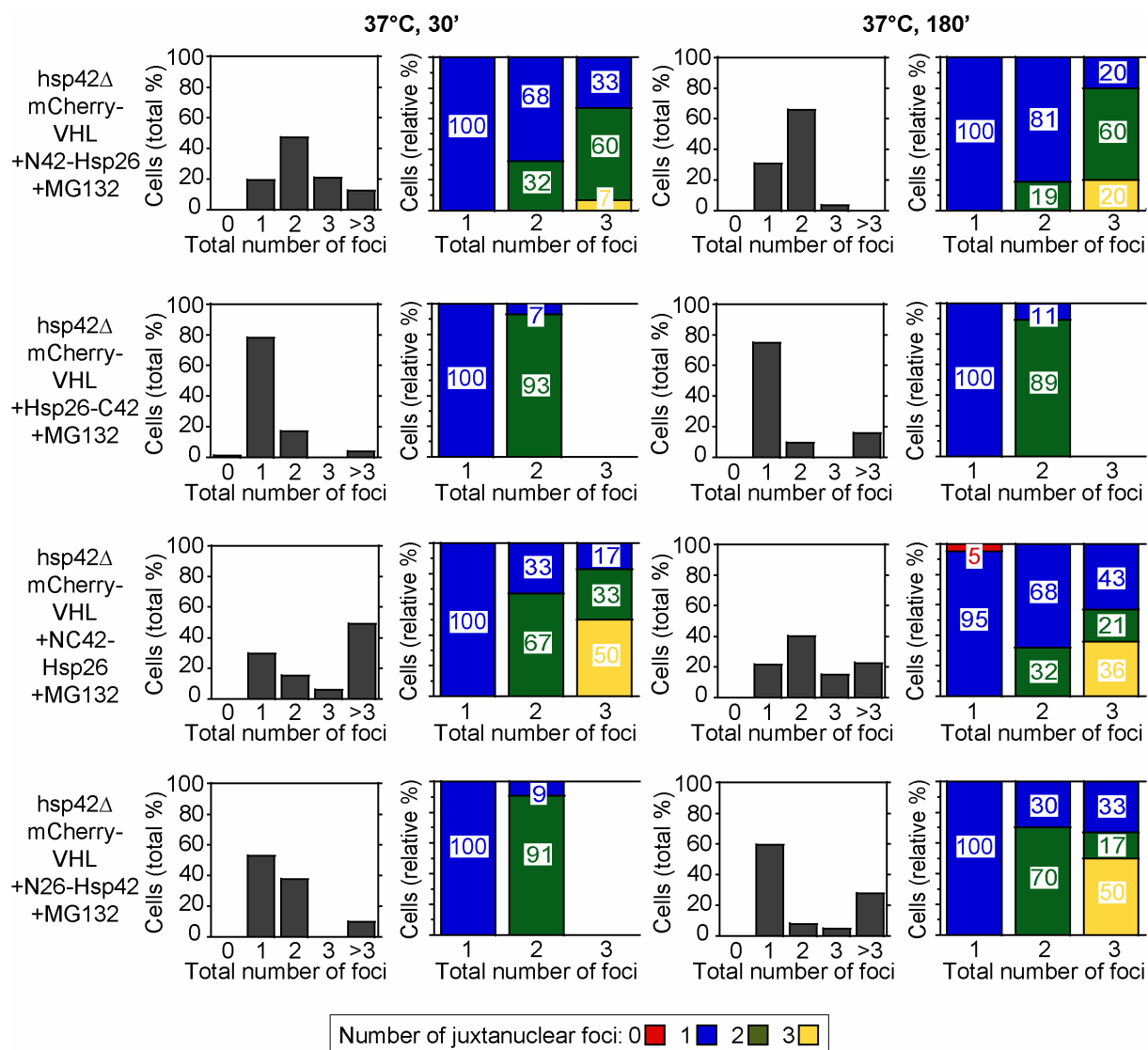


**Figure 5.14 The N-terminal domain of Hsp42 mediates sorting of misfolded proteins to peripheral inclusions.**

Number (dark grey columns) and localization (colored columns) of mCherry-VHL inclusions in hsp42Δ cells expressing the indicated sHsp construct after incubation at 37°C for 30 and 180 min. The proteasome inhibitor MG132 was added before the temperature shift. The color code deciphers the foci localization. Red corresponds to zero juxtannuclear inclusions, blue to one, green to two, and yellow to three. The total number of foci per cell is depicted in all diagrams on the x-axis. Quantifications are based on the analysis of n = 100 cells.

### ***5.5 Localization of amorphous but not of amyloidogenic aggregates to the IPOD depends on Hsp42***

The IPOD has been shown to be composed of both amyloidogenic as well as misfolded proteins (Kaganovich *et al.*, 2008). I therefore analyzed whether amyloidogenic aggregates are still present at the IPOD in *hsp42Δ* cells. For that purpose I expressed in *S. cerevisiae* WT and *hsp42Δ* mutant cells the yeast prion protein RNQ1, which had been C-terminally fused to YFP. In both strains peripheral RNQ1-YFP foci were detectable, demonstrating that RNQ1-YFP deposition at IPOD-like compartments is not affected in *hsp42Δ* cells (Figure 5.15 A). Next, I compared the relative spatial localization of Hsp42-mCitrine and RNQ1-YFP. After incubation for 30 min at 37°C one of the Hsp42-stained inclusions was in close proximity to RNQ1-YFP, however, no overlapping fluorescence was detected (Figure 5.15 B). Since Hsp42-mCitrine acts as a marker for rather amorphous aggregates, misfolded and amyloidogenic proteins might be targeted to the same cellular sites, but no mixing of the distinct aggregate types occurs. In conclusion, Hsp42 is essential for the localization of thermally induced amorphous, but not amyloidogenic aggregates to IPOD-like compartments.

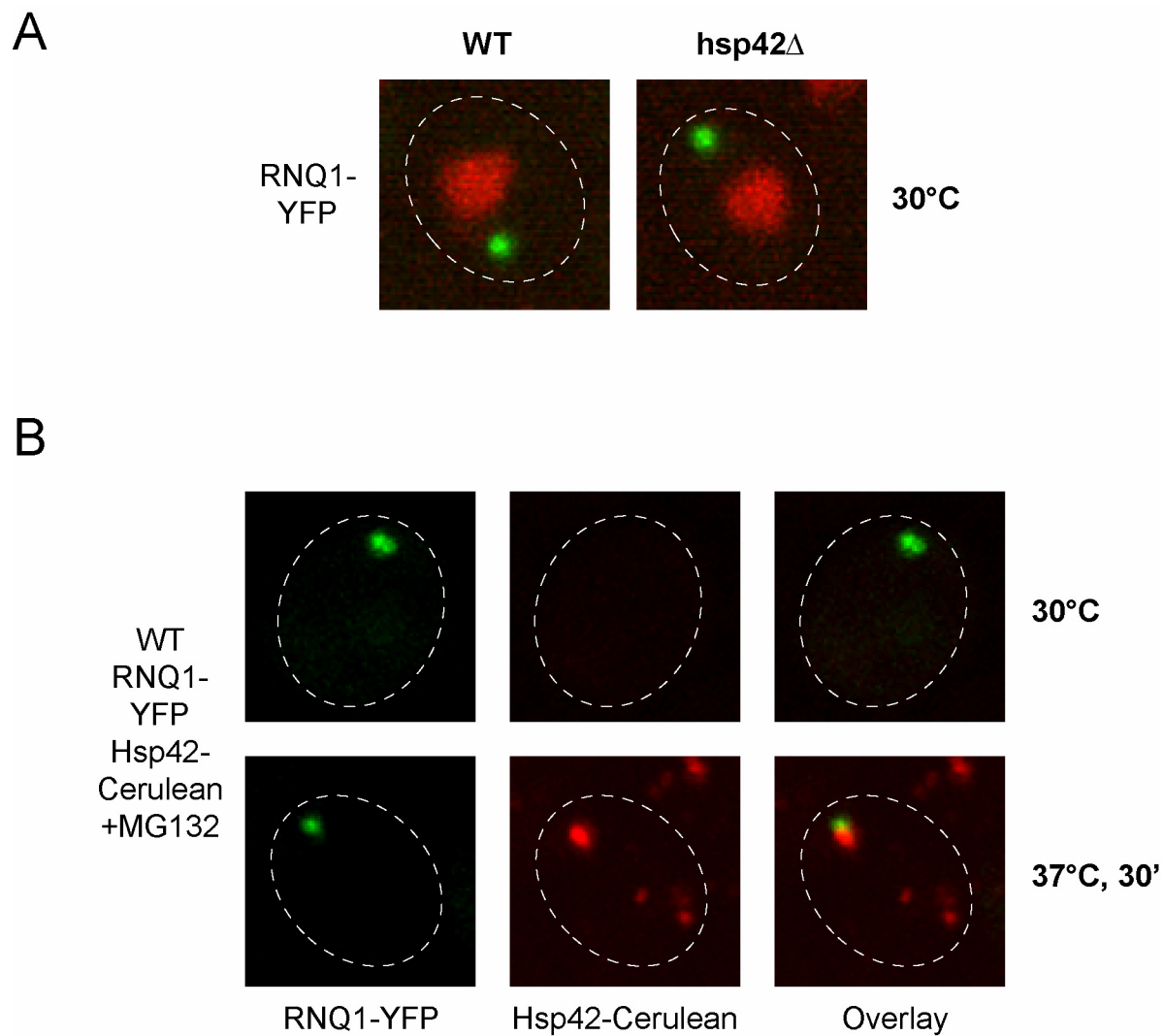


**Figure 5.15 Hsp42 does not affect the localization of amyloidogenic aggregates.**

(A) RNQ1-YFP (green) was expressed in *S. cerevisiae* wild-type (WT) and hsp42 $\Delta$  cells. Nuclei were visualized by co-expressing HTB1-mCherry (red). (B) *S. cerevisiae* cells co-expressing RNQ1-YFP and Hsp42-Cerulean were incubated at 30°C and shifted to 37°C for 30 min (+ MG132). RNQ1-YFP (green) is localizing in close proximity to one Hsp42-Cerulean foci (red) after temperature shift, however, no overlapping fluorescence is detectable.

## 5.6 The JUNQ compartment of *hsp42Δ* cells exhibits moderate changes in dynamics and stability

What are the consequences of directing the pool of misfolded proteins exclusively to the JUNQ compartment in *hsp42Δ* cells? I compared the mobility and stability of mCherry-VHL deposited at the JUNQ in WT and *hsp42Δ* cells. First, I examined the diffusion properties of misfolded proteins in the distinct compartments utilizing Fluorescence Loss in Photobleaching (FLIP). Briefly, a small area of cytosol apart from the mCherry-VHL inclusions is repeatedly bleached with a laser pulse. The resulting fluorescence loss in the inclusions, as a function of time, provides a measure of their relative exchange rate with bleached cytoplasmic mCherry-VHL molecules. Cytosolic fluorescence, which corresponds to soluble mCherry-VHL, vanished rapidly upon laser bleaching (data not shown). In *S. cerevisiae* WT cells the JUNQ displayed a more rapid and pronounced loss of fluorescence in comparison to the IPOD compartment in agreement with previous findings (Kaganovich *et al.*, 2008) (Figure 5.16). Consequently, misfolded mCherry-VHL in the JUNQ exchanges more frequently with the cytosolic pool and is thus more soluble, in accordance with published data (Kaganovich *et al.*, 2008). In *hsp42Δ* cells bleaching caused, in comparison to WT cells, a more rapid fluorescent loss in juxtannuclear inclusions. The JUNQ therefore displays an overall increased exchange rate with the cytosolic mCherry-VHL pool in *hsp42Δ* cells.

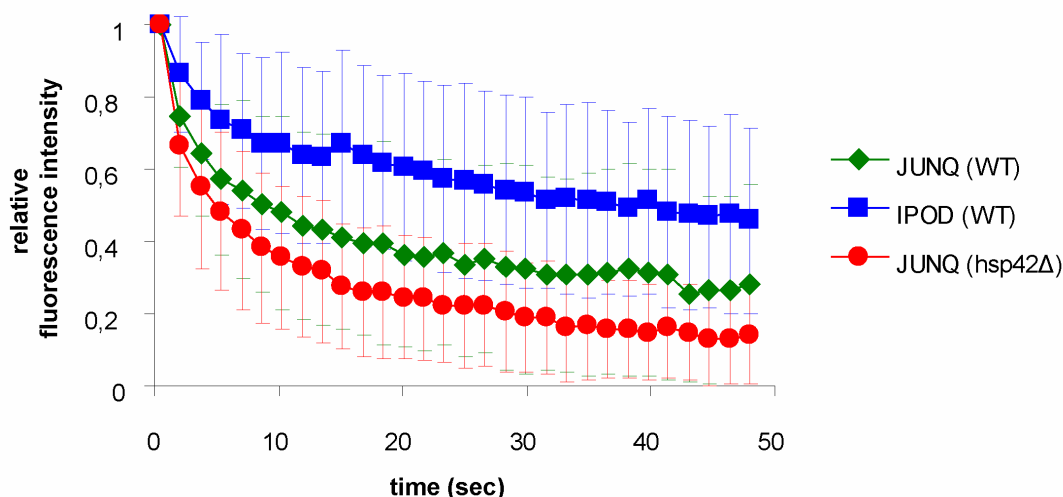


**Figure 5.16 The JUNQ compartment of *hsp42Δ* cells exhibits an increased exchange rate with the cytosolic mCherry-VHL pool.**

FLIP measurements of mCherry-VHL were carried out in wild-type (WT) and *hsp42Δ* cells after incubation at 37°C for 180 min (+ MG132). Bleaching curves were calculated based on the analysis of 25 cells.

I next studied the stability of the individual compartments by monitoring their fate upon return to physiological conditions (30°C, - MG132). After one hour recovery 1-2 mCherry-VHL inclusions were still detectable in WT cells (80 %), whereas the majority (60 %) of hsp42Δ cells were free of aggregates (Figure 5.17 and Figure 5.18 A/B). After two hours 50 % of WT cells still harbored one focus, which predominantly (63 %) exhibited a peripheral localization (Figure 5.17 and Figure 5.18 A). While this finding implies that IPOD compartments are more stable compared to the JUNQ, I observed that peripheral foci were significantly reduced in size, indicating that misfolded proteins in IPOD-like compartments are also subject to protein disaggregation. At the same time point hsp42Δ cells were almost completely devoid of mCherry-VHL foci, suggesting more rapid disaggregation (Figure 5.17 and Figure 5.18 B). Similar findings were obtained when Hsp104-mCFP foci were followed in *S. cerevisiae* WT and hsp42Δ cells upon return to physiological growth conditions, indicating that a more rapid disintegration of endogenous yeast aggregates occurs in hsp42Δ cells (data not shown). Foci disintegration could be linked to Hsp104-mediated protein disaggregation since clearance of juxtannuclear and peripheral mCherry-VHL foci was no longer observed in hsp104Δ cells (Figure 5.19).

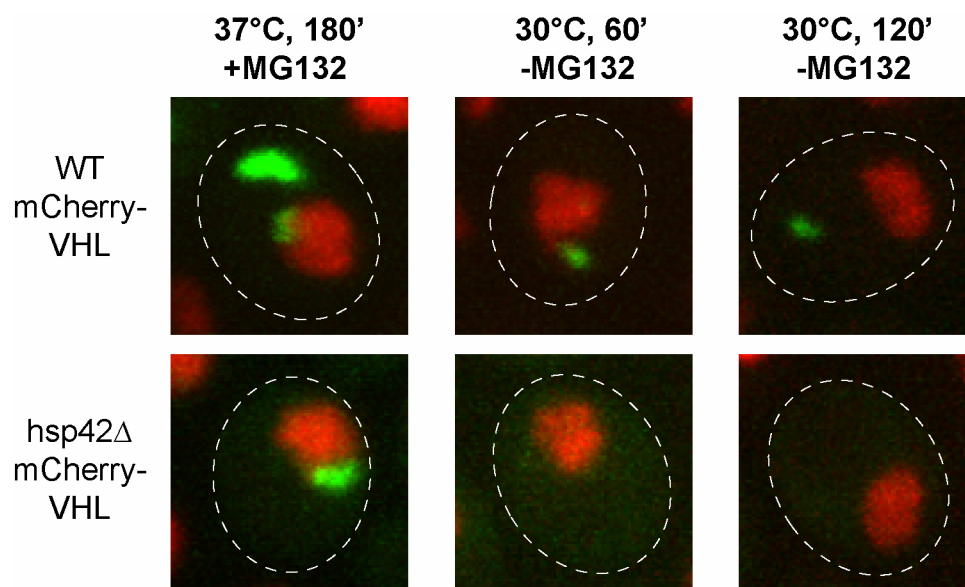


**Figure 5.17 mCherry-VHL aggregation foci are more rapidly resolved in the hsp42Δ strain.**

Wild-type (WT) and hsp42Δ cells expressing mCherry-VHL (green) were grown at 30°C and shifted to 37°C for 180 min (+ MG132). MG132 was washed out and cells were shifted to 30°C for 120 min. *De novo* synthesis of mCherry-VHL was inhibited by addition of 10 μg/ml cycloheximide. Nuclei were visualized by co-expressing HTB1-Cerulean (red).

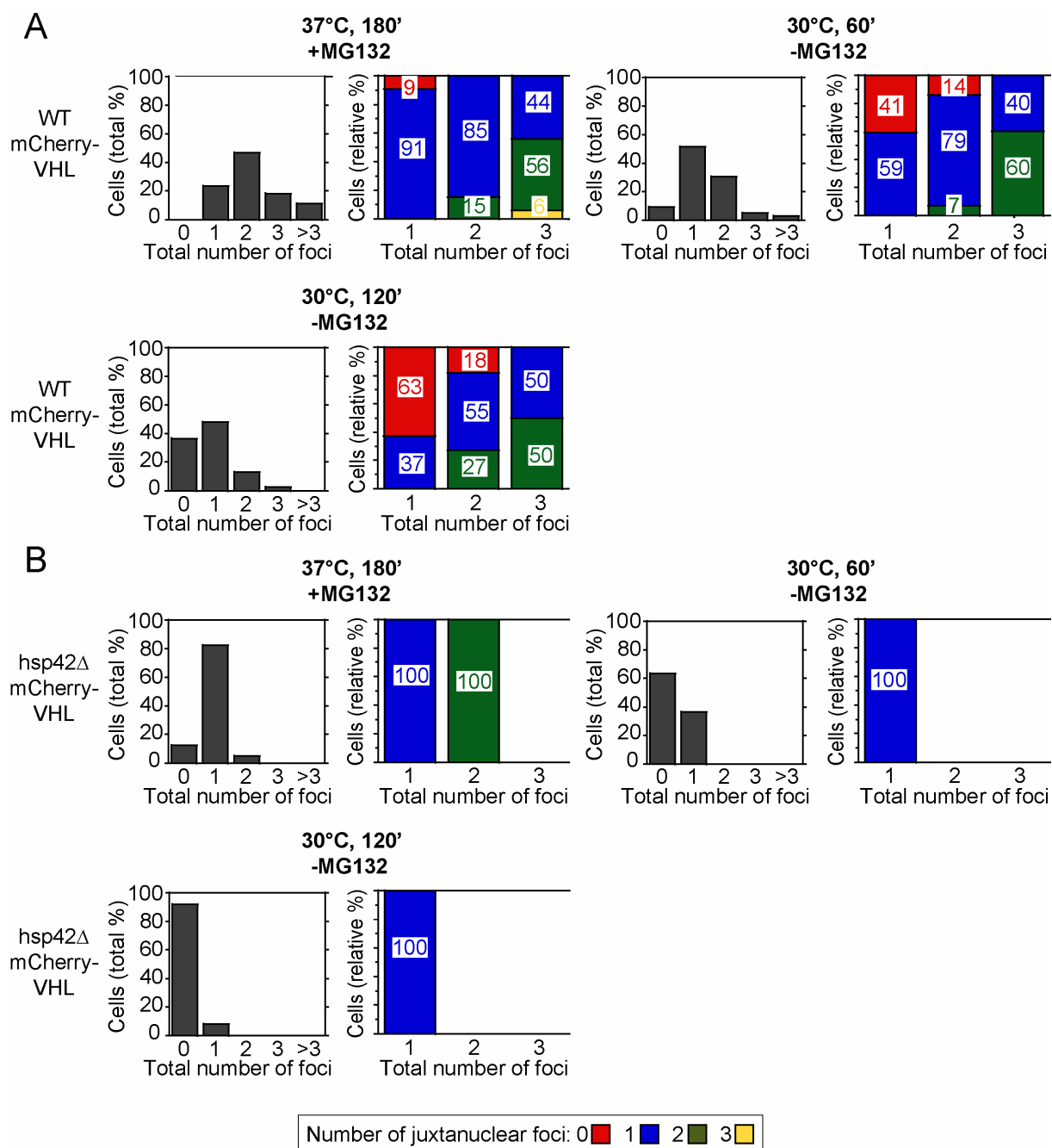


**Figure 5.18 mCherry-VHL aggregation foci are more rapidly resolved in the hsp42Δ strain.**

Wild type (WT) and hsp42Δ cells expressing mCherry-VHL were grown at 30°C and shifted to 37°C for 180 min (+ MG132). MG132 was washed out and cells were shifted to 30°C for 120 min. *De novo* synthesis of mCherry-VHL was inhibited by addition of 10 μg/ml cycloheximide. Number (dark grey columns) and localization (colored columns) of mCherry-VHL inclusions are shown in the respective strain at the indicated time point. The color code deciphers the foci localization. Red corresponds to zero juxtannuclear inclusions, blue to one, green to two, and yellow to three. The total number of foci per cell is depicted in all diagrams on the x-axis. Quantifications are based on the analysis of n = 100 cells.

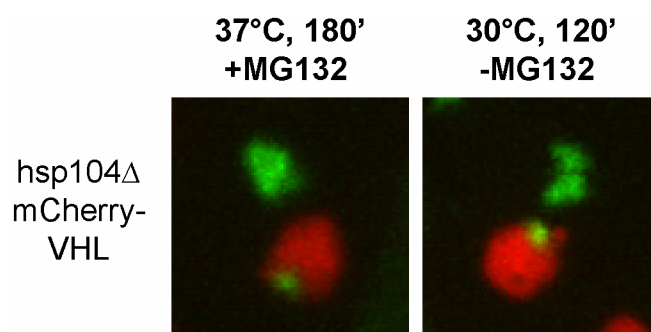


**Figure 5.19 Disintegration of protein inclusions requires Hsp104-mediated protein disaggregation.**

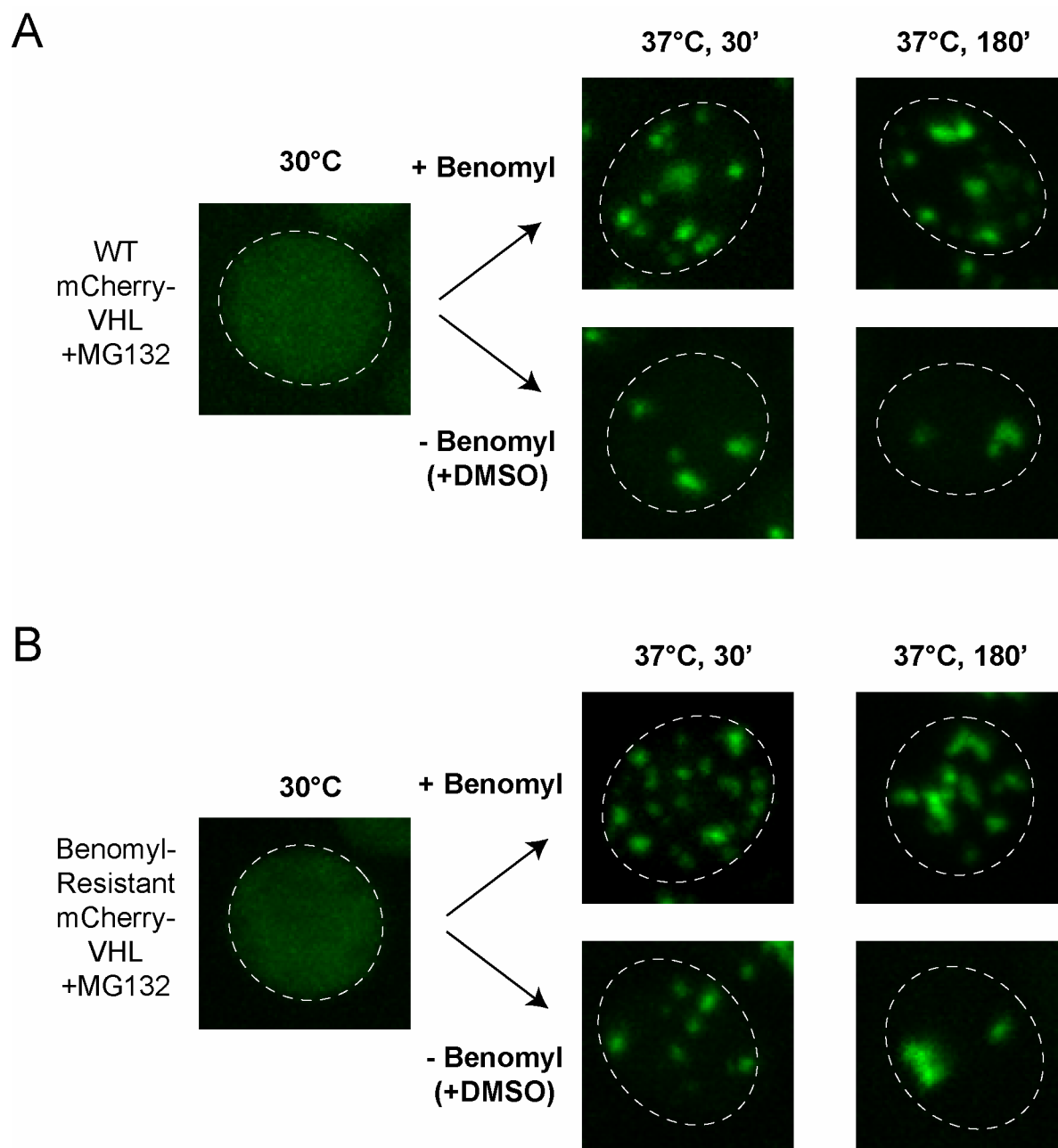
*hsp104*Δ cells expressing mCherry-VHL (green) were grown at 30°C and shifted to 37°C for 180 min (+MG132) (left image). MG132 was washed out and cells were shifted to 30°C for 120 min. *De novo* synthesis of mCherry-VHL was inhibited by addition of 10 μg/ml cycloheximide. After 120 min (right images) incubation at 30°C, the inclusions were not cleared. Nuclei were visualized by co-expressing HTB1-Cerulean (red)

### 5.7 Aggregate sequestration depends on the actin cytoskeleton

I next sought to determine whether the *S. cerevisiae* cytoskeleton is required for distributing misfolded mCherry-VHL to the JUNQ and IPOD-like compartments. The microtubule-depolymerizing drug benomyl has been shown to reversibly inhibit the formation of JUNQ and IPOD compartments, implying a crucial role of the microtubule cytoskeleton in aggregate sorting (Kaganovich *et al.*, 2008). I here confirmed this observation, but used in addition a benomyl-resistant yeast strain containing a mutation in tubulin-2, which prevents benomyl from depolymerizing microtubules, to exclude secondary effects of the drug (Figure 5.20 A/B). Similar to WT cells, the benomyl-resistant cells did not exhibit JUNQ and IPOD-like compartments. Instead, they contained multiple dispersed mCherry-VHL foci in the presence of benomyl after 30 and 180 min incubation at 37°C, demonstrating that the inhibitory effect of benomyl is microtubule-independent, thereby questioning the role of microtubules in aggregate sorting.

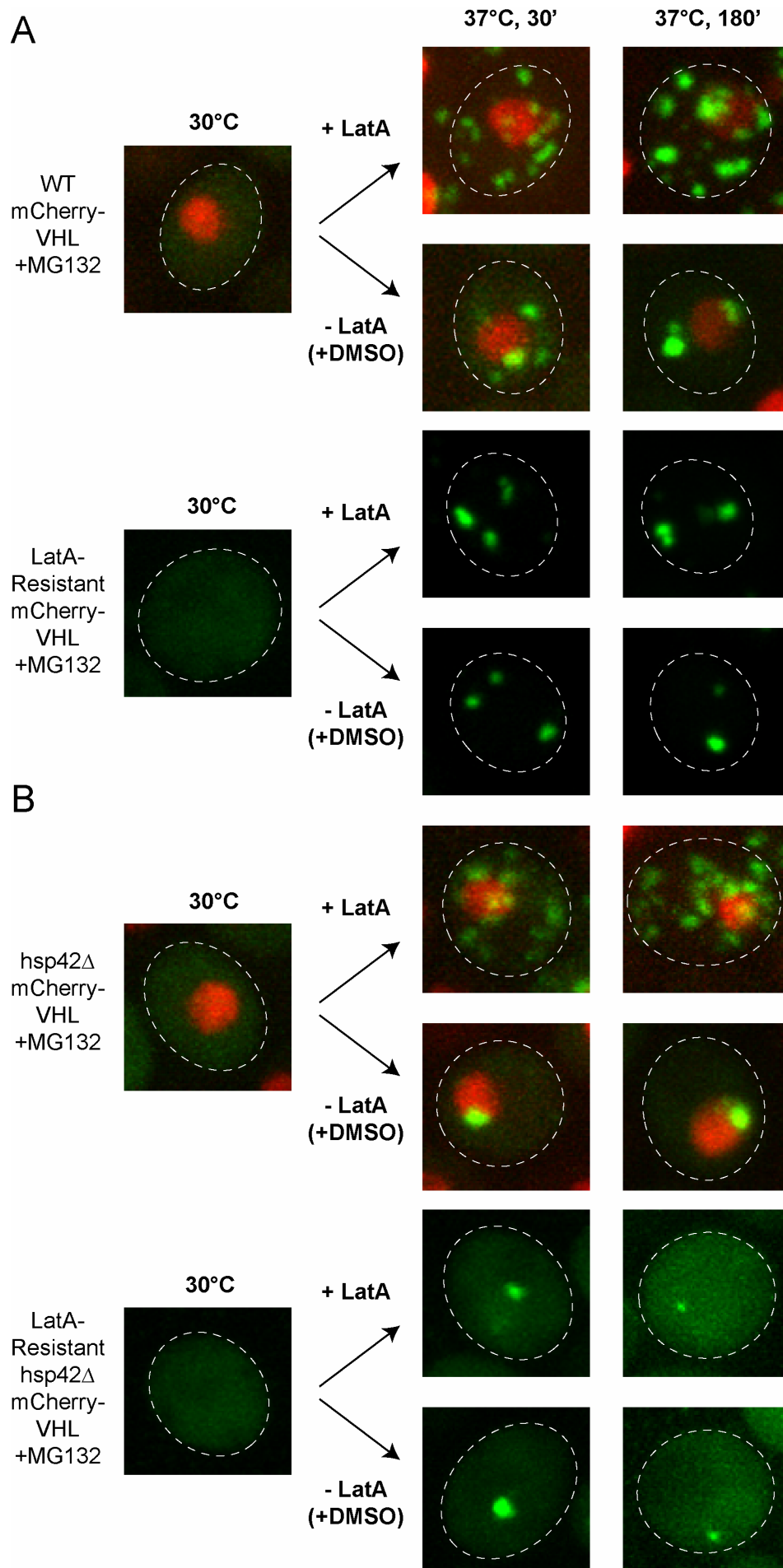
I therefore determined whether partitioning of misfolded mCherry-VHL into distinct compartments requires an intact actin cytoskeleton. For this purpose I monitored mCherry-VHL misfolding in the presence of the actin-depolymerizing drug latrunculin A (LatA), which causes complete disruption of the yeast actin cytoskeleton (Ayscough *et al.*, 1997). After 30 min incubation at 37°C the LatA-treated cells displayed a vastly increased number of inclusions in comparison to the DMSO-treated control cells (Figure 5.21 A). Prolonged incubation (180 min) at 37°C did not result in a reduction of foci number as LatA-treated cells still displayed multiple punctae dispersed throughout the cytosol, in contrast to DMSO-treated control cells. Since LatA could possibly have actin-independent secondary effects, I employed

a yeast strain containing a mutation in *actin-1*, which prevents LatA-mediated disassembly of the actin cytoskeleton (Ayscough *et al.*, 1997). The LatA-resistant strain partitioned misfolded mCherry-VHL efficiently into JUNQ and IPOD-like compartments in the presence of LatA, reminiscent of untreated WT cells. Since LatA treatment did not reduce cell viability (Figure 5.22), the inhibitory effect of LatA can be directly linked to a non-functional actin cytoskeleton. The exclusive formation of juxtannuclear inclusions in *hsp42Δ* cells also strictly depended on an intact actin cytoskeleton, since addition of LatA prevented juxtannuclear accumulation of mCherry-VHL inclusions, whereas LatA-resistant *hsp42Δ* cells displayed a single focus in the presence of LatA (Figure 5.21 B). Notably, the deletion of *HSP42* did not affect the organization of the actin cytoskeleton at both physiological and folding stress conditions (Figure 5.23), thus ruling out the possibility that the *hsp42Δ* phenotype is directly caused by an alteration of the actin cytoskeleton. Taken together, the actin cytoskeleton is of crucial importance for aggregate partitioning to both JUNQ and IPOD-like compartments.



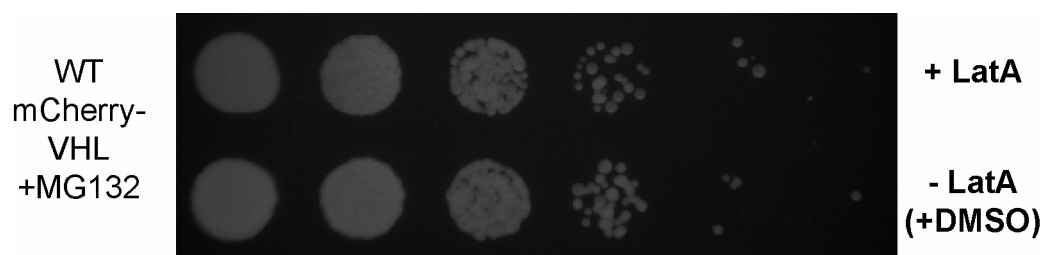
**Figure 5.20 Microtubule-independent effects of benomyl prevent aggregate sorting of misfolded mCherry-VHL into JUNQ and IPOD-like compartments.**

mCherry-VHL (green) localization was analyzed after stress application in the presence of the microtubule-depolymerizing drug benomyl in wild-type (WT) cells (A) and a yeast strain containing a mutation in tubulin-2, which renders the microtubule cytoskeleton resistant to benomyl (B). After 30 and 180 min incubation at 37°C (+ MG132) in the presence of benomyl, both WT and benomyl-resistant cells contained multiple dispersed mCherry-VHL foci and did not exhibit JUNQ and IPOD-like compartments. Instead of benomyl, control cells were treated with the same amount of DMSO.



**Figure 5.21 The actin cytoskeleton is required for aggregate compartmentalization.**

Reduction of mCherry-VHL (green) foci numbers during prolonged folding stress requires actin polymerization. *S. cerevisiae* cells expressing mCherry-VHL were grown at 30°C and shifted to 37°C (+ MG132). The actin-depolymerizing drug latrunculin A (LatA) was added prior to temperature shift. Instead of LatA, control cells were treated with the same volume of DMSO. (A) mCherry-VHL localization was monitored in wild-type (WT) cells and a yeast strain containing a mutation in actin-1, rendering the actin cytoskeleton resistant to LatA. LatA treatment prevented reduction of mCherry-VHL foci numbers in WT but not in LatA-resistant cells during 180 min incubation at 37°C. Nuclei were visualized by co-expressing HTB1-Cerulean (red) (B) hsp42Δ cells expressing VHL-mCherry were treated as described above. The juxtannuclear accumulation of mCherry-VHL foci in hsp42Δ cells also requires a functional actin cytoskeleton.

**Figure 5.22 Latrunculin A treatment does not reduce cell viability**

Wild-type (WT) cells were incubated for 180 min at 37°C in the presence of the actin-depolymerizing drug LatA and proteasome inhibitor MG132. Instead of LatA, control cells were treated with same amount of DMSO. Subsequently, the cells were washed and spotted in a serial dilution onto an agar plate. The image was acquired after two days growth at 30°.

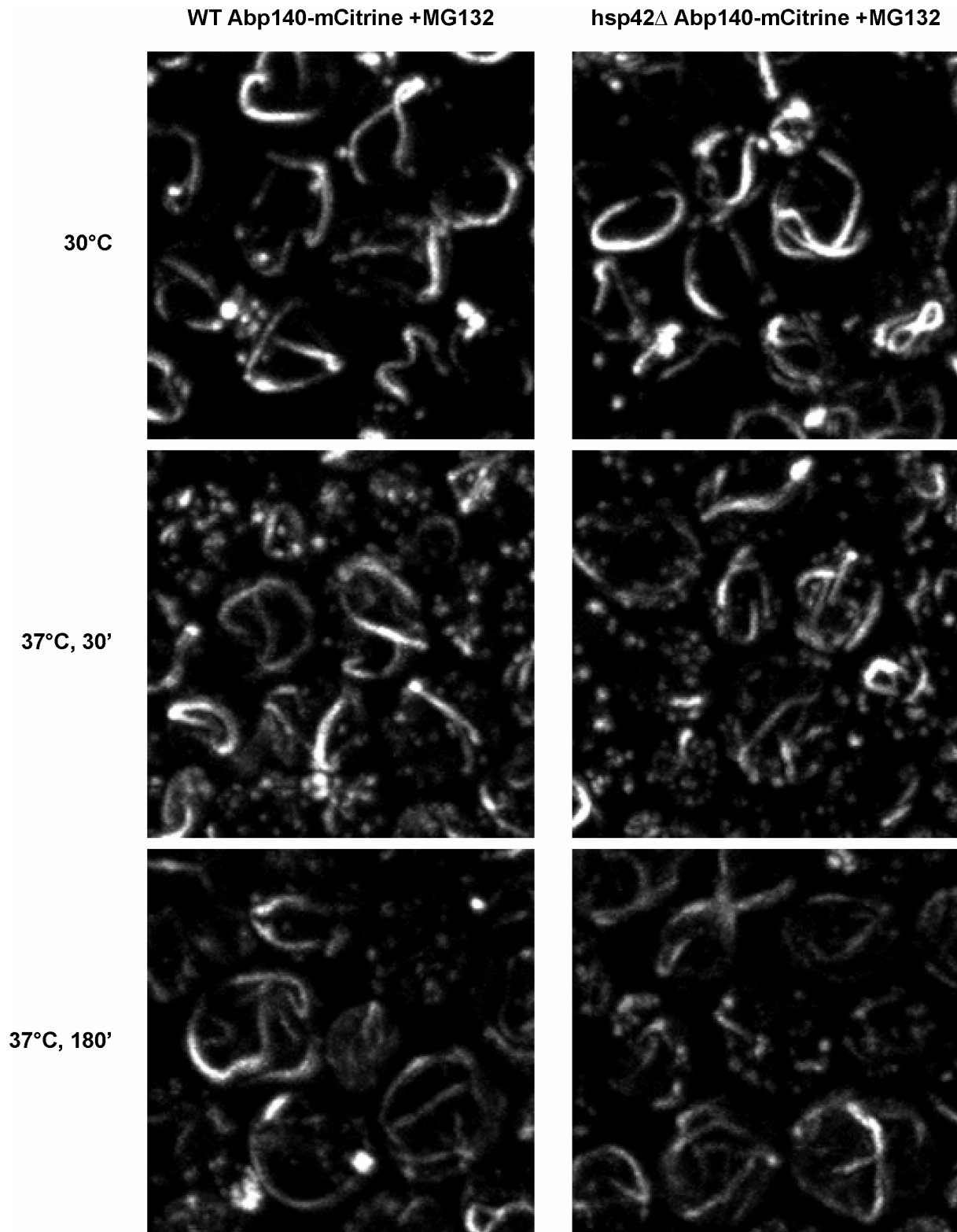


**Figure 5.23 Actin cytoskeleton is not altered in hsp42 $\Delta$  cells at both physiological and folding stress conditions.**

*S. cerevisiae* wild-type (WT) and hsp42 $\Delta$  cells were incubated at 30°C (top) and shifted to 37°C (+ MG132) for 30 min (middle) and 180 min (bottom). The actin cytoskeleton was visualized via a genomic C-terminal fusion of mCitrine to the actin binding protein 140 (Abp140).

### 5.8 Monitoring organization of misfolded proteins upon severe heat stress using fluorescent reporters

Misfolded proteins, which are generated in yeast cells during mild thermal stress (37°C) and inhibited proteasomal degradation, are partitioning between specific deposition sites, namely the JUNQ and IPOD-like compartments. In order to address the question whether the spatio-temporal organization of misfolded proteins is altered in cells subjected to sublethal heat shock, I analyzed the localization of mCitrine-luciferase and endogenous yeast aggregates stained by Hsp104-mCFP in cells with intact proteasomal degradation at physiological temperature (30°C), after a preconditioning period (37°C, 45 min) that was followed by sublethal heat shock (45°C, 20 min), and various time points of recovery (30°C) (Figure 5.24).

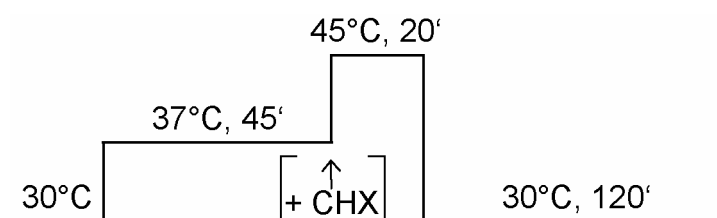


**Figure 5.24 Outline of the experimental setup for heat shock treatment followed by a recovery period.**

The localization of the fluorescent reporters was monitored in cells with intact proteasomal degradation at 30°C, after a preconditioning period (37°C, 45 min), sublethal heat shock (45°C, 20 min), and various time points of recovery at 30°C. When the reactivation of aggregated luciferase was assessed by measuring its enzymatic activity, *de novo* synthesis of mCitrine-luciferase was inhibited by addition of 10 µg/ml cycloheximide before heat shock.

Concomitantly, the folding status of mCitrine-luciferase was monitored by measuring its enzymatic activity. The preconditioning period is required for efficient reactivation of luciferase during the recovery phase (data not shown). At physiological temperature (30°C) mCitrine-luciferase displayed a homogenous cytosolic distribution, whereas Hsp104-mCFP was enriched in the nucleus (Figure 5.25). Preconditioning at 37°C resulted in the formation of heterogeneous numbers of fluorescent foci, mainly zero to three for mCitrine-luciferase, while Hsp104-mCFP displayed even higher inclusion numbers (Figure 5.25 and Figure 5.26 A/B). Cells harboring such foci localized one inclusion preferentially in close proximity to the nucleus. It should be noted that foci formation of mCitrine-luciferase was neither accompanied by a significant loss of cytosolic mCitrine-luciferase fluorescence nor by a decrease of luciferase activity, indicating that only a minor fraction of mCitrine-luciferase aggregates at 37°C. Heat shock at 45°C caused the loss of a homogenous cytosolic staining and induced the formation of numerous inclusions that were distributed throughout the cytosol (Figure 5.25). mCitrine or mCFP alone did not form inclusions in response to heat

shock, demonstrating that foci formation is driven either by aggregation of the fusion partner luciferase or the binding of Hsp104 to generated aggregates (data not shown). After recovery at 30°C for 60 min, cytosolic mCitrine-luciferase and Hsp104-mCFP fluorescence was regained and most inclusions were cleared, leaving cells with zero to three mCitrine-luciferase and even more Hsp104-mCFP aggregation foci. Concordant with mild thermal stress during preconditioning, cells preferred to localize one aggregate juxtannuclear (Figure 5.25 and Figure 5.26). 120 min recovery were sufficient for most cells to eliminate mCitrine-luciferase inclusions, while half of the Hsp104-mCFP expressing cells still possessed mainly one or two inclusions, of which one was often found close to the nucleus (Figure 5.25 and Figure 5.26).

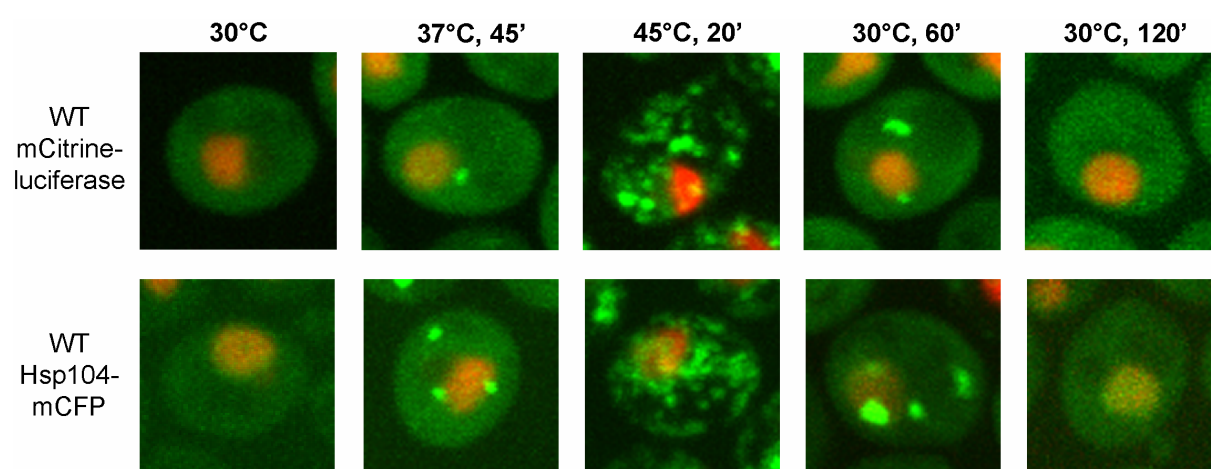


**Figure 5.25 Spatio-temporal organization of heat shock-induced protein aggregates.**

Time-dependent changes in the localization of mCitrine-luciferase and endogenous yeast aggregates stained by Hsp104-mCFP (bottom) (both green) in wild-type (WT) cells at 30°C, after preconditioning at 37°C for 45 min, heat shock at 45°C for 20 min, and recovery at 30°C for 60 min and 120 min. Nuclei were visualized by co-expressing HTB1-mCherry (red).

Summarized, I observed similar numbers and localization of fluorescent foci of mCitrine-luciferase and Hsp104-mCFP at the various time points. Hsp104-mCFP stained more inclusions than visualized with mCitrine-luciferase, demonstrating that the use of the thermolabile luciferase reporter does not lead to artificial results, and indicating the existence of highly heat-labile proteins in *S. cerevisiae*. Simultaneous expression of Hsp104-mCFP and mCitrine-luciferase revealed perfect co-localization upon heat stress, underscoring the recruitment of Hsp104 to heat-induced aggregates and demonstrating that both fluorescent fusion proteins are valuable tools to study protein aggregation (Figure 5.27). The aggregation pattern of mCitrine-luciferase was also analyzed in the presence of the translation inhibitor cycloheximide that was added after preconditioning. Cycloheximide treatment did not reduce cell viability (data not shown) and resulted in the same numbers and localizations of fluorescent foci as compared to non-treated cells (Figure 5.28). Consequently, the observed

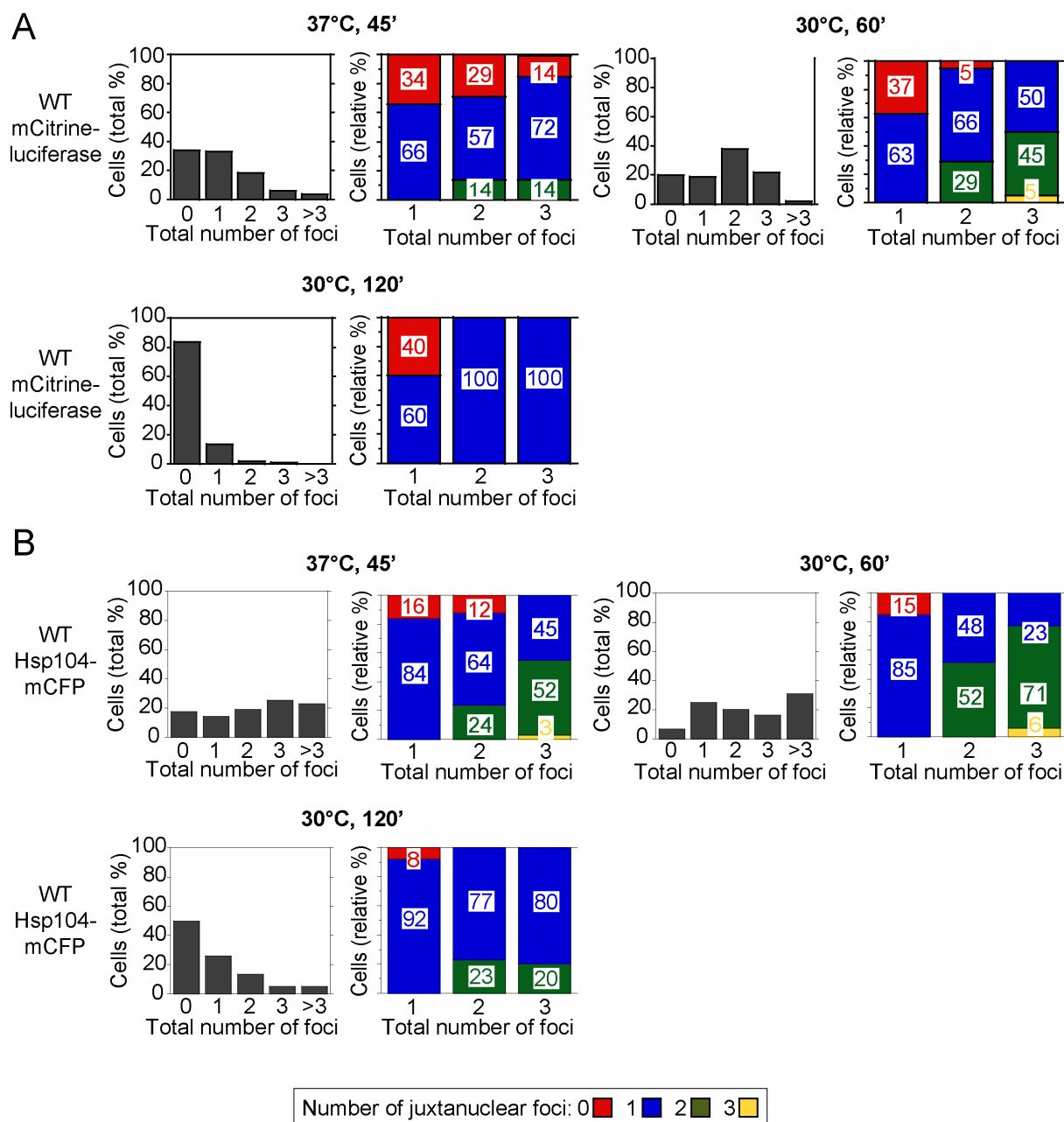


**Figure 5.26 Spatio-temporal organization of heat shock-induced protein aggregates.**

Number (dark grey columns) and localization (colored columns) of mCitrine-luciferase (A) and Hsp104-mCFP (B) inclusions after the preconditioning period (37°C, 45 min) and recovery at 30°C for 60 min and 120 min in wild-type (WT) cells. The color code deciphers foci localization. Red corresponds to zero juxtannuclear inclusions, blue to one, green to two, and yellow to three. The total number of foci per cell is depicted in all diagrams on the x-axis. Quantifications are based on the analysis of  $n = 100$  cells.

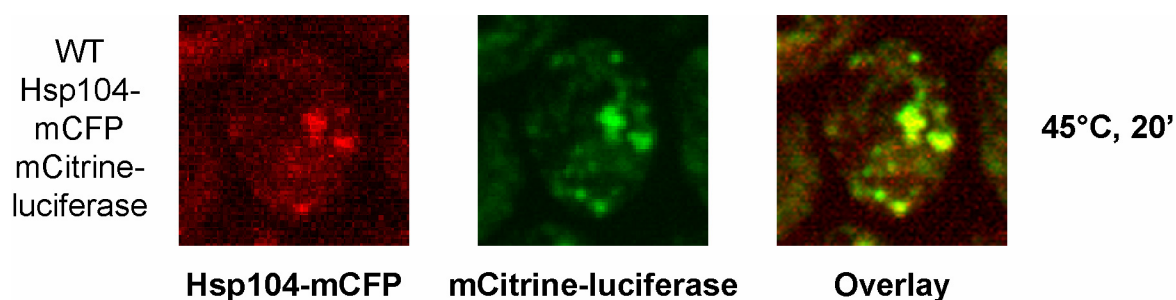


**Figure 5.27 Hsp104-mCFP co-localizes with mCitrine-luciferase.**

Hsp104-mCFP (red) and mCitrine-luciferase (green) were co-expressed in wild-type (WT) cells. Protein localizations were determined after heat shock (45°C, 20 min), revealing co-localization of Hsp104-mCFP and mCitrine-luciferase inclusions.

differences in cellular localization reflect an active redistribution of the preexisting fusion protein. Cycloheximide treatment also allowed clarifying to which extent mCitrine-luciferase is refolded during the recovery phase. The majority (60-70 %) of mCitrine-luciferase was reactivated upon solubilization within 30 min recovery at 30°C (Figure 5.29). To assess the dependence of mCitrine-luciferase solubilization and reactivation on Hsp104, I monitored localization of mCitrine-luciferase in the isogenic *hsp104Δ* strain. Preconditioning at 37°C resulted in the formation of higher numbers of fluorescent foci in approx. 20 % of cells in comparison to WT, implying a minor role for Hsp104 during mild thermal stress (Figure 5.30 A/B). Heat shock induced numerous aggregates that were dispersed throughout the cytosol, reminiscent of WT cells. During the recovery phase the *hsp104Δ* strain did not clear the fluorescent inclusions, which remained distributed throughout the cytosol. In agreement with the persistence of aggregation foci, mCitrine-luciferase enzymatic activity was barely reactivated (Figure 5.29). Notably, Hsp104-mCFP expressing cells provided WT-like mCitrine-luciferase reactivation, indicating full functionality of the fusion construct (Figure 5.29).

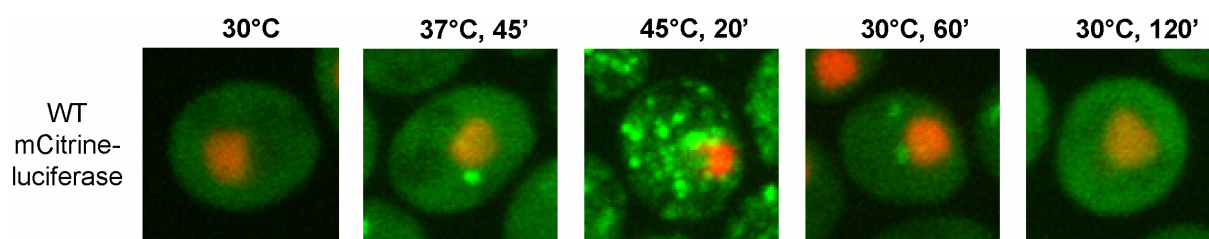


**Figure 5.28 A translation inhibitor does not change the spatio-temporal organization of mCitrine-luciferase aggregates.**

Time-dependent changes in the localization of mCitrine-luciferase (green) in wild-type (WT) cells at 30°C, after preconditioning at 37°C for 45 min, heat shock at 45°C for 20 min, and recovery at 30°C for 60 and 120 min. *De novo* synthesis of mCitrine-luciferase was inhibited by addition of 10 µg/ml cycloheximide (CHX) before the heat shock. Nuclei were visualized by co-expressing HTB1-mCherry (red).

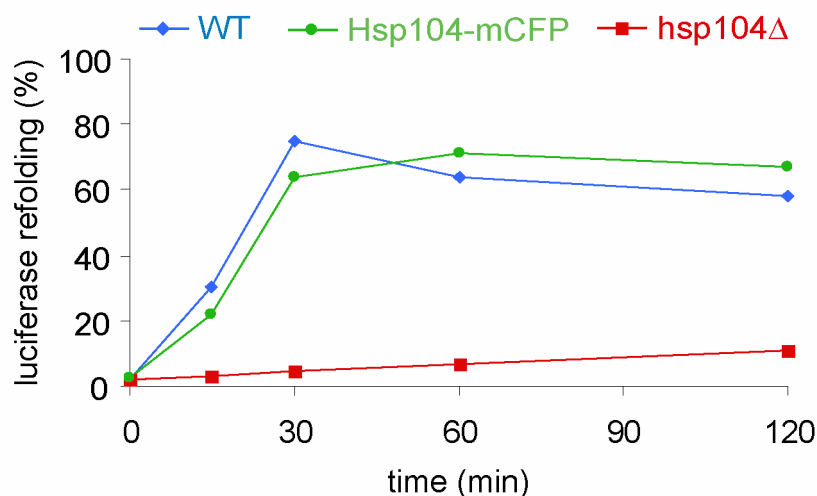


**Figure 5.29 Reactivation of aggregated mCitrine-luciferase is completed within 30 min and dependent on the presence of Hsp104.**

Reactivation of aggregated mCitrine-luciferase is shown in the isogenic wild-type (WT) (blue) and hsp104Δ (red) strains, and cells expressing Hsp104 C-terminally tagged in the genome with mCFP (green). Luciferase activity during the recovery phase at 30°C is displayed. The luciferase activity before heat shock was set as 100%. *De novo* synthesis of mCitrine-luciferase was inhibited by addition of 10 μg/ml cycloheximide before heat shock. Within 30 min recovery at 30°C, luciferase reactivation is completed in the WT strain. Hsp104-mCFP exhibits WT-like luciferase refolding after heat shock

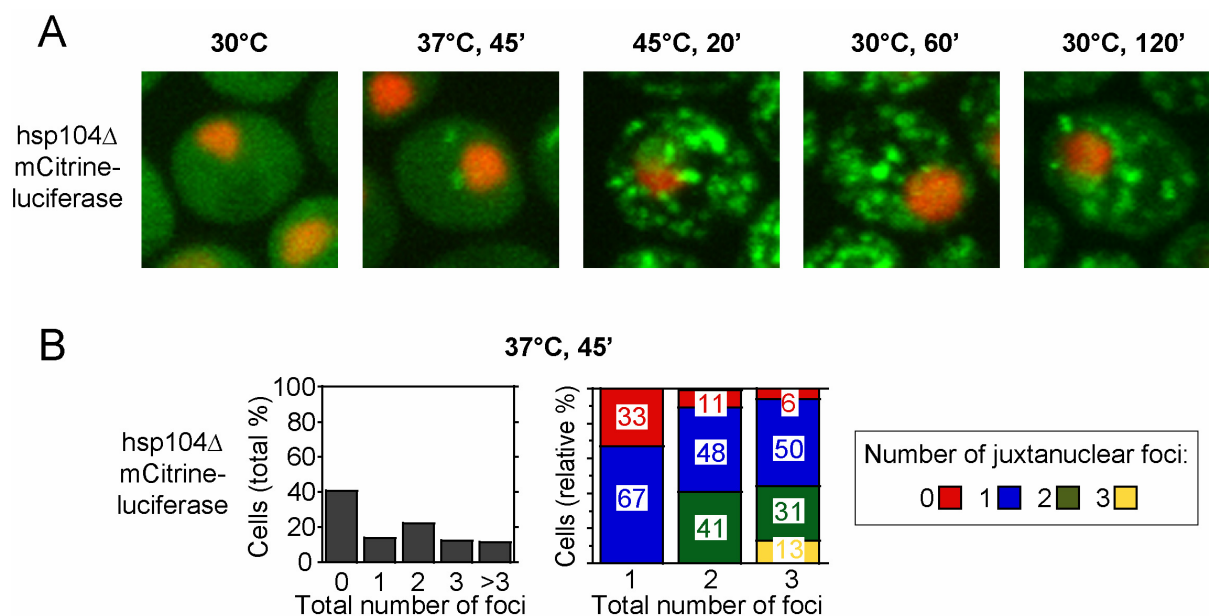


**Figure 5.30 Spatio-temporal organization of heat shock-induced protein aggregates in hsp104Δ cells.**

(A) Time-dependent changes in the localization of mCitrine-luciferase (green) in hsp104Δ cells at 30°C, after preconditioning at 37°C for 45 min, heat shock at 45°C for 20 min, and recovery at 30°C for 60 and 120 min. Nuclei were visualized by co-expressing HTB1-mCherry (red). (B) Number (dark grey columns) and localization (colored columns) of mCitrine-luciferase inclusions after the preconditioning period (37°C, 45 min). The color code deciphers foci localization. Red corresponds to zero juxtannuclear inclusions, blue to one, green to two, and yellow to three. The total number of foci per cell is depicted in all diagrams on the x-axis. Quantifications are based on the analysis of n = 100 cells.

### ***5.9 Following severe heat stress mCherry-VHL is not sorted to specific compartments***

Our observation that protein aggregates generated upon heat stress are rather randomly distributed throughout the yeast cell during both formation and disaggregation, appears at first glance to conflict the identification of specific deposition sites of misfolded proteins (JUNQ, IPOD) (Kaganovic et al., 2008). I here sought to compare the organization of mCherry-VHL during prolonged mild thermal stress and recovery from sublethal heat shock. At 30°C mCherry-VHL displayed a diffuse staining (Figure 5.31). In the presence of the proteasome inhibitor MG132 incubation at 37°C for 30 min induced formation of multiple cytosolic punctae (Figure 5.31 *top*). Prolonged incubation at 37°C (180 min) resulted in reduction of foci numbers, leaving cells with JUNQ and IPOD-like inclusions. In order to address mCherry-VHL localization in response to more severe thermal stress, I subjected proteasome-inhibited cells (+MG132) to sublethal heat shock (45°C, 20 min) and allowed recovery either at 30°C or 37°C for 180 min. Heat shock induced the formation of multiple mCherry-VHL foci distributed throughout the cytosol (Figure 5.31 *bottom*), reminiscent of mCitrine-luciferase and Hsp104-mCFP. Subsequent incubation at 30°C or 37°C for 180 min increased the juxtannuclear fraction of aggregates, but numerous inclusions remained dispersed in the cellular periphery, implying that distinct mCherry-VHL aggregation compartments do not form after heat shock. Taken together, these observations indicate that the applied stress condition has a profound impact on aggregate organization, since a simple sorting of mCherry-VHL, mCitrine-luciferase, and Hsp104-mCFP to JUNQ or IPOD-like deposition sites was no longer observed upon heat shock to 45°C.

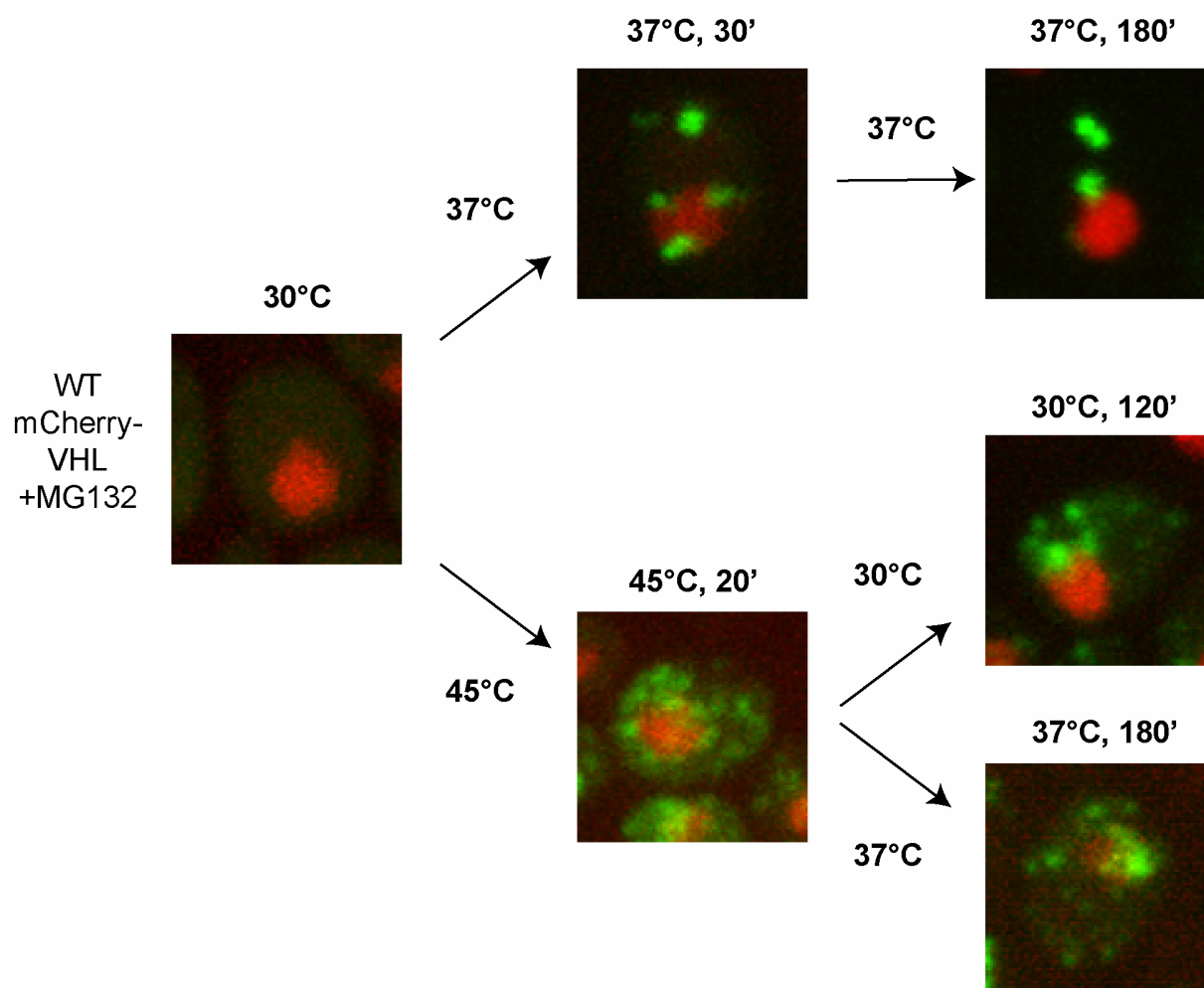


**Figure 5.31** Following heat shock mCherry-VHL is not sorted to distinct compartments.

Time-dependent changes in the localization of mCherry-VHL (green) at 30°C, after shift to 37°C for 30 and 180 min (top), or after heat shock (45°C, 20) and subsequent recovery at 30°C for 120 min or 37°C for 180 min (bottom). Before temperature shift, proteasomal degradation was blocked by addition of MG132. Nuclei were visualized by co-expressing HTB1-Cerulean (red).

### 5.10 Protein disaggregation does not rely on specific deposition sites

In order to gain insight into the dynamics of aggregate formation and solubilization, I performed time-lapse microscopy of single yeast cells expressing either mCitrine-luciferase or Hsp104-mCFP. Here, I had a major emphasis on the organization of aggregates during heat shock and the recovery phase at 30°C. Between 10 min and 20 min heat shock only minor movements of inclusions were monitored (Figure 5.32 A/B). During the first 30 min of recovery I observed a reduction of total foci numbers that was accompanied by an increase in fluorescent intensity of both remaining foci and background. Subsequently, the residual inclusions were progressively vanishing. Since reactivation of luciferase is largely completed within 30 min (Figure 5.29), I sought to obtain more detailed insight into the inclusion dynamics of this time interval. I performed single cell microscopy with 1 min time resolution, starting at 10 min recovery (Figure 5.33). Earlier time points could not be monitored due to an

unstable focus caused by the temperature shift from 45°C to 30°C. The higher time resolution revealed mobility of both juxtannuclear and peripheral inclusions. Since the aggregates were mostly randomly distributed throughout the reactivation phase, I conclude that sorting of aggregates to specific sites is not a prerequisite for Hsp104-mediated solubilization. Moreover, the intensity gain of inclusions during the reactivation interval indicates agglutination of aggregated proteins to form foci of greater size.

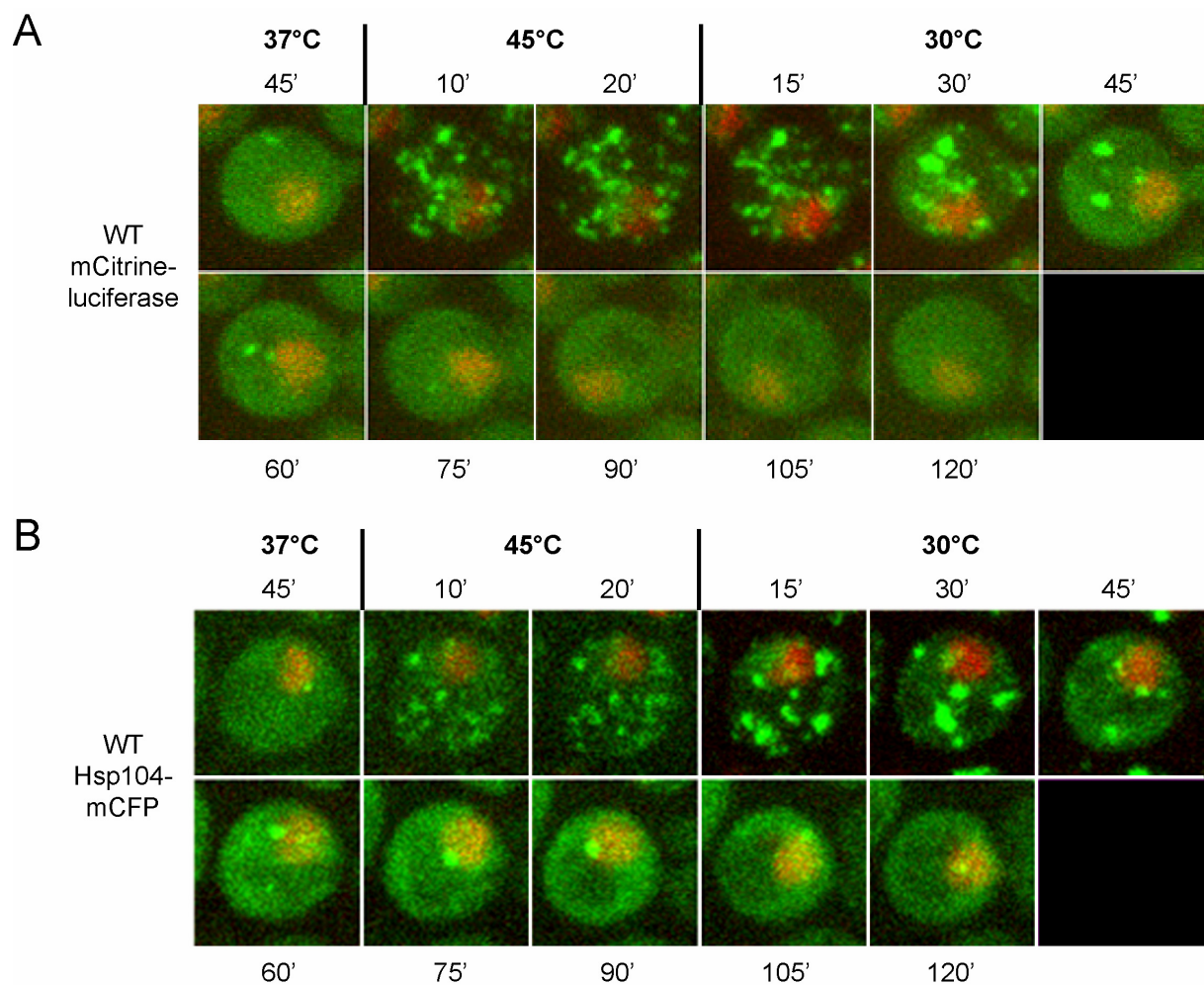


**Figure 5.32 Reactivation of protein aggregates does not require sorting to specific deposition sites.** Time-lapse microscopy of single wild-type (WT) cells expressing mCitrine-luciferase (A) or Hsp104-mCFP (B) (both green) at the indicated time points. Nuclei were visualized by co-expressing HTB1-mCherry (red).

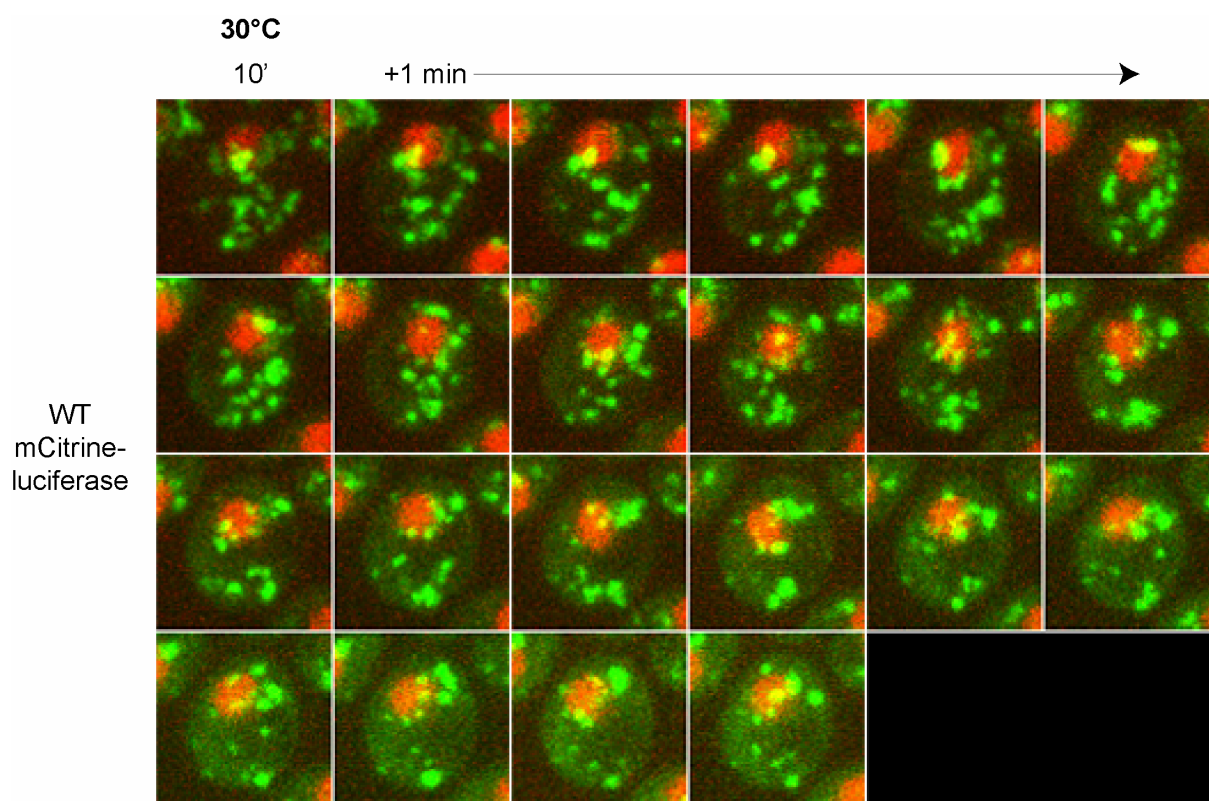


**Figure 5.33 Reactivation of protein aggregates does not require sorting to specific deposition sites.** Protein aggregates are mostly randomly distributed throughout the luciferase reactivation phase, which is completed within 30 min recovery (see Figure 5.29). Time-lapse microscopy pictures with 1 min time resolution, starting at 10 min recovery at 30°C, are displayed of a single wild-type (WT) cell expressing mCitrine-luciferase (green). Nuclei were visualized by co-expressing HTB1-mCherry (red).

### ***5.11 sHsps affect the refolding and organization of heat shock-induced aggregated proteins***

The *S. cerevisiae* sHsps have been shown to be involved in protein disaggregation (Hsp26) (Cashikar *et al.*, 2005; Haslbeck *et al.*, 2005b) and sequestering misfolded proteins in IPOD-like compartments (Hsp42) (this study). I therefore sought to gain insight into the role of Hsp26 and Hsp42 in the spatio-temporal organization of heat shock-induced protein aggregates. First, I compared the misfolding of mCitrine-luciferase in WT, hsp26 $\Delta$ , and hsp42 $\Delta$  cells. When following the refolding of aggregated mCitrine-luciferase during the recovery phase by measuring luciferase activity, I observed that an isogenic hsp26 $\Delta$  strain displayed slower refolding kinetics than WT cells, while hsp42 $\Delta$  showed normal refolding (Figure 5.34 A). This cannot be accounted to increased protein degradation, because hsp26 $\Delta$  cells displayed even slightly higher mCitrine-luciferase levels compared to WT cells at the end of the recovery period (Figure 5.34 B/C). Congruent to the slower luciferase refolding, hsp26 $\Delta$  cells, in comparison to WT, showed an increased number of remaining mCitrine-luciferase and Hsp104-mCFP foci after 60 min and 120 min recovery at 30°C (Figure 5.35,

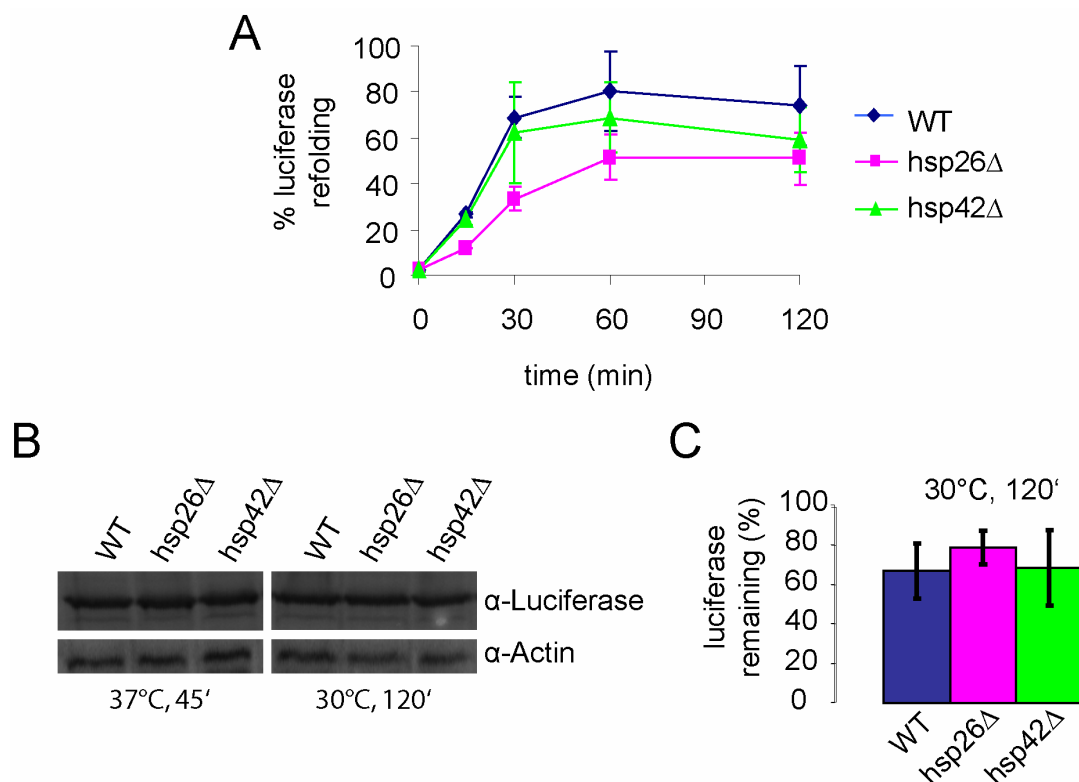


**Figure 5.34 Small heat shock proteins influence refolding, but not degradation, of heat shock-induced protein aggregates.**

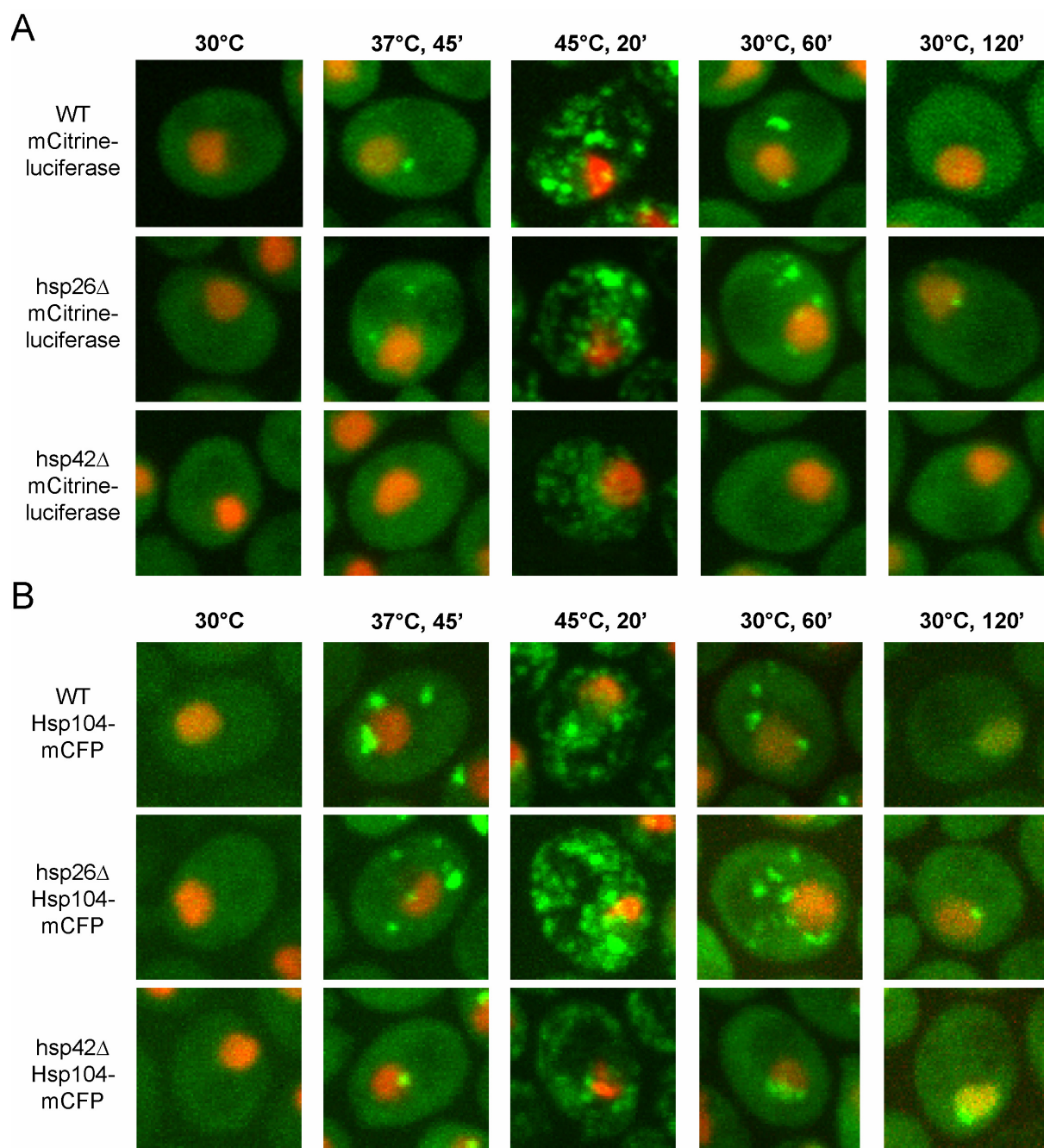
(A) The hsp26Δ strain displays slower luciferase refolding kinetics than wild-type (WT) cells, while the hsp42Δ strain shows normal refolding. Luciferase activity during the recovery period at 30°C is depicted in the isogenic WT (blue), hsp26Δ (pink), and hsp42Δ (green) strains. The luciferase activity before heat shock was set as 100%. *De novo* synthesis of mCitrine-luciferase was inhibited by addition of 10 μg/ml cycloheximide before heat shock. (B) mCitrine-luciferase levels are similar in the WT, hsp26Δ, and hsp42Δ strains after the preconditioning period (37°C, 45 min) and recovery at 30°C for 120 min, as monitored by western blot analysis. (C) Quantification of mCitrine-luciferase levels is depicted in WT (blue), hsp26Δ (orange), and hsp42Δ (yellow) cells after recovery at 30°C for 120 min. Luciferase levels after the preconditioning period (37°C, 45 min) were set as 100%.

Figure 5.36 A and Figure 5.37 A). Notably, in hsp42Δ cells no mCitrine-luciferase inclusions were found neither after preconditioning (37°C, 45 min) nor after 60 and 120 min recovery (30°C) (Figure 5.35 A and Figure 5.36 B). While heat shock induced the formation of multiple cytosolic mCitrine-luciferase inclusions in hsp42Δ cells, the foci appeared less condensed and intense. Heat shock still caused complete inactivation of luciferase in the hsp42Δ strain and resulted in the formation of pelletable mCitrine-luciferase aggregates (Figure 5.38 A), demonstrating that luciferase forms aggregates in hsp42Δ cells, which are, however, differently organized. After 60 and 120 min recovery, a minor fraction of luciferase was yet pelletable, similar to WT cells. However, in the WT strain aggregation foci were still detectable. I conclude that the mCitrine-luciferase aggregates in hsp42Δ cells, which remain throughout the recovery phase, are of smaller, sub-microscopic size. Alternatively, the detectable foci in WT cells could constitute only a minor fraction of total luciferase, such that

differences in pelletable luciferase were not detectable via Western blotting. The lack of detectable foci cannot be accounted to upregulated protein degradation, because *hsp42Δ* and WT cells displayed similar amounts of mCitrine-luciferase degradation (Figure 5.34 B/C). Neither can it be accounted to upregulation of the heat shock response, because WT and *hsp42Δ* cells expressed similar amounts of Hsp104 (Figure 5.38 B). In *hsp42Δ* cells complemented with Hsp42 expressed from its native promoter, peripheral mCitrine-luciferase aggregation foci were detectable after recovery at 30°C for 60 min (Figure 5.39 A). Moreover, knocking out *HSP42* in a different yeast strain (W303) resulted in disappearance of inclusions (Figure 5.39 B), demonstrating that the altered distribution of protein aggregates is directly caused by missing Hsp42.

To generalize my finding, I next monitored the generation and solubilization of heat stress-induced endogenous yeast aggregates stained by Hsp104-mCFP in *hsp42Δ* cells. After the preconditioning period, strongly reduced numbers of endogenous yeast aggregation foci were detectable in *hsp42Δ* cells in comparison to WT (Figure 5.35 B and Figure 5.37 B). Moreover, the foci localized almost exclusively juxtannuclear. Heat shock induced the formation of multiple cytosolic Hsp104-mCFP stained inclusions, the foci however appeared less condensed and intense. During recovery at 30°C, peripheral inclusions were more rapidly cleared in *hsp42Δ* cells than WT. Juxtannuclear inclusions were still detectable in roughly one third of the cells after 120 min recovery (30°C). *Hsp42Δ* cells therefore do not possess detectable inclusions that remain in the cellular periphery.

In order to gain insight into the organization dynamics of endogenous yeast aggregates in the WT and *hsp42Δ* strains, I performed time-lapse microscopy of single yeast cells expressing Hsp104-mCFP with 2 min time resolution. Since Hsp42 had no influence on the reactivation of luciferase, I here had a major emphasis on the organization of aggregates remaining after 30 min recovery at 30°C. In WT cells the agglutination of diverse inclusions into foci with increased fluorescent intensity was monitored, indicating fusion of smaller aggregates to larger ones (Figure 5.40 A), corroborating my earlier finding (Figure 5.32 and Figure 5.33). In *hsp42Δ* cells juxtannuclear accumulation of aggregates was accompanied by vanishing of peripheral foci (Figure 5.40 B), substantiating that Hsp42 is essential for the residence of protein inclusions in the cellular periphery.



**Figure 5.35 Small heat shock proteins influence the organization of heat shock-induced protein aggregates.**

Time-dependent changes in the localization of mCitrine-luciferase (A) or endogenous yeast aggregates stained by Hsp104-mCFP (B) (both green) in wild-type (WT), hsp26Δ, and hsp42Δ cells at 30°C, after preconditioning at 37°C for 45 min, heat shock at 45°C for 20 min, and recovery at 30°C for 60 and 120 min. Nuclei were visualized by co-expressing HTB1-mCherry (red).

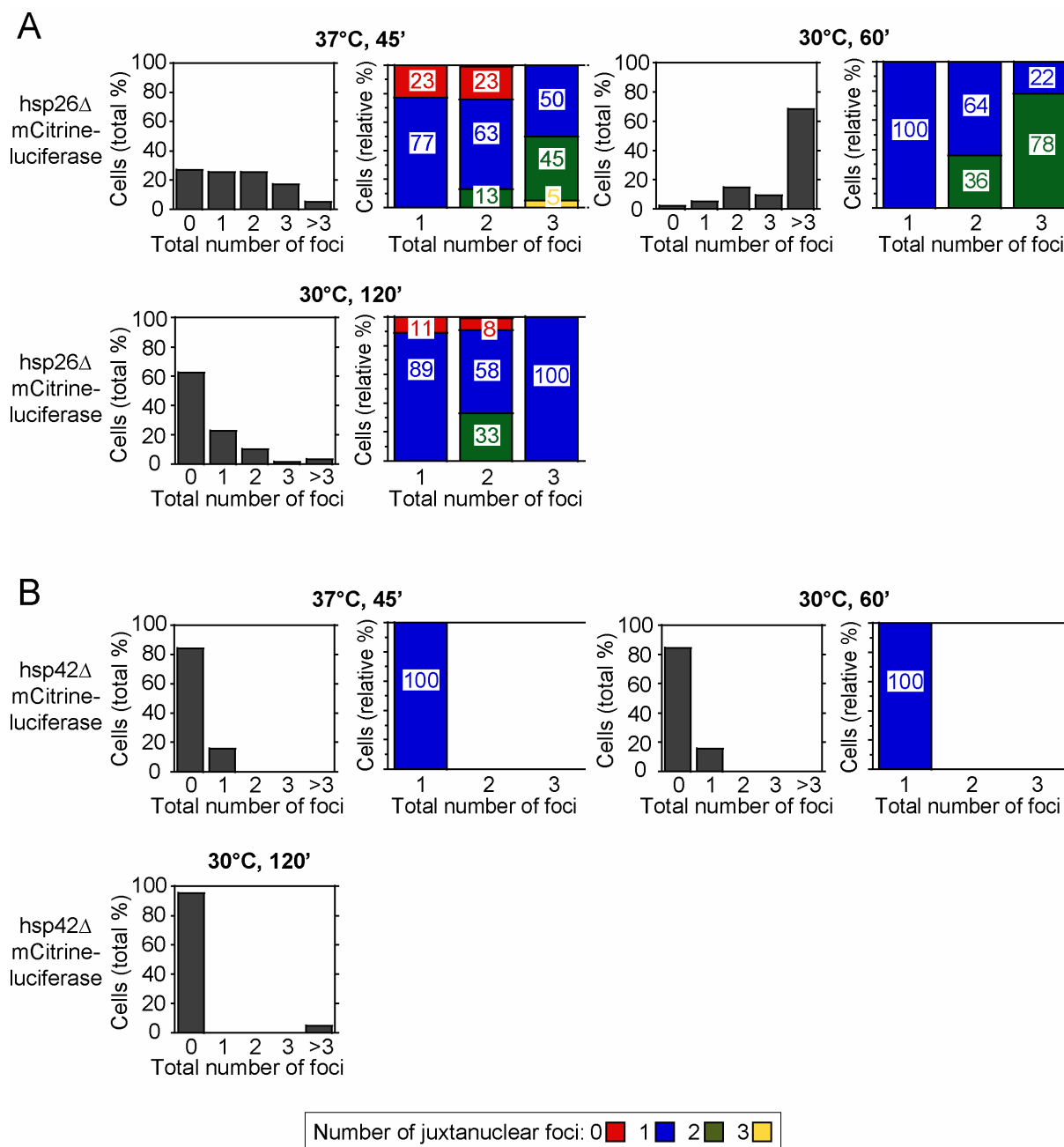


**Figure 5.36 Small heat shock proteins influence the organization of mCitrine-luciferase aggregates.**

Number (dark grey columns) and localization (colored columns) of mCitrine-luciferase inclusions in hsp26Δ (A) and hsp42Δ (B) cells after the preconditioning period (37°C, 45 min) and recovery at 30°C for 60 and 120 min. The color code deciphers foci localization. Red corresponds to zero juxtannuclear inclusions, blue to one, green to two, and yellow to three. The total number of foci per cell is depicted in all diagrams on the x-axis. Quantifications are based on the analysis of n = 100 cells.

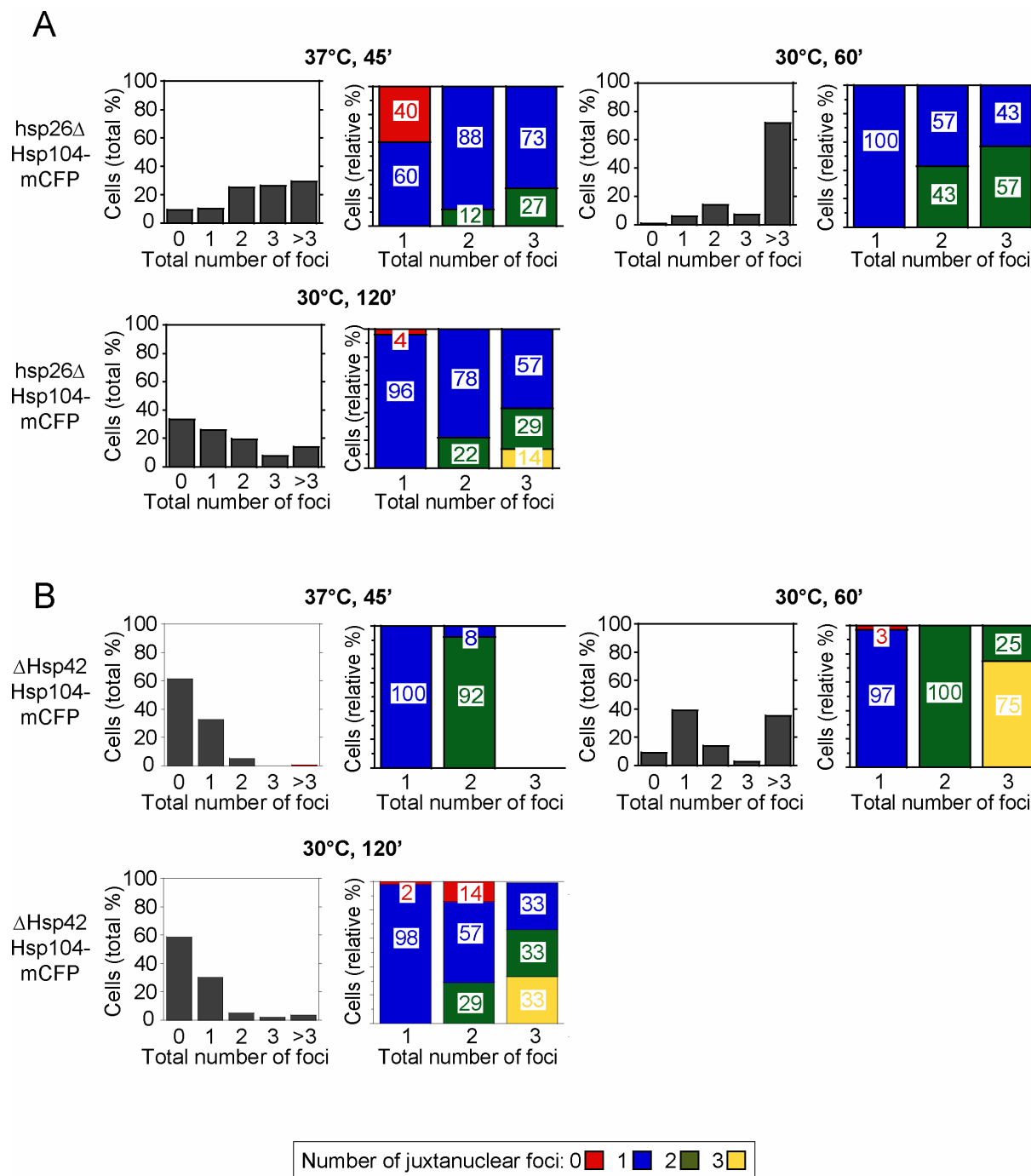


**Figure 5.37 Small heat shock proteins influence the organization of endogenous yeast aggregates stained by Hsp104-mCFP.**

Number (dark grey columns) and localization (colored columns) of Hsp104-mCFP stained inclusions in hsp26Δ (A) and hsp42Δ (B) cells after the preconditioning period (37°C, 45 min) and recovery at 30°C for 60 and 120 min. The color code deciphers foci localization. Red corresponds to zero juxtannuclear inclusions, blue to one, green to two, and yellow to three. The total number of foci per cell is depicted in all diagrams on the x-axis. Quantifications are based on the analysis of n = 100 cells.

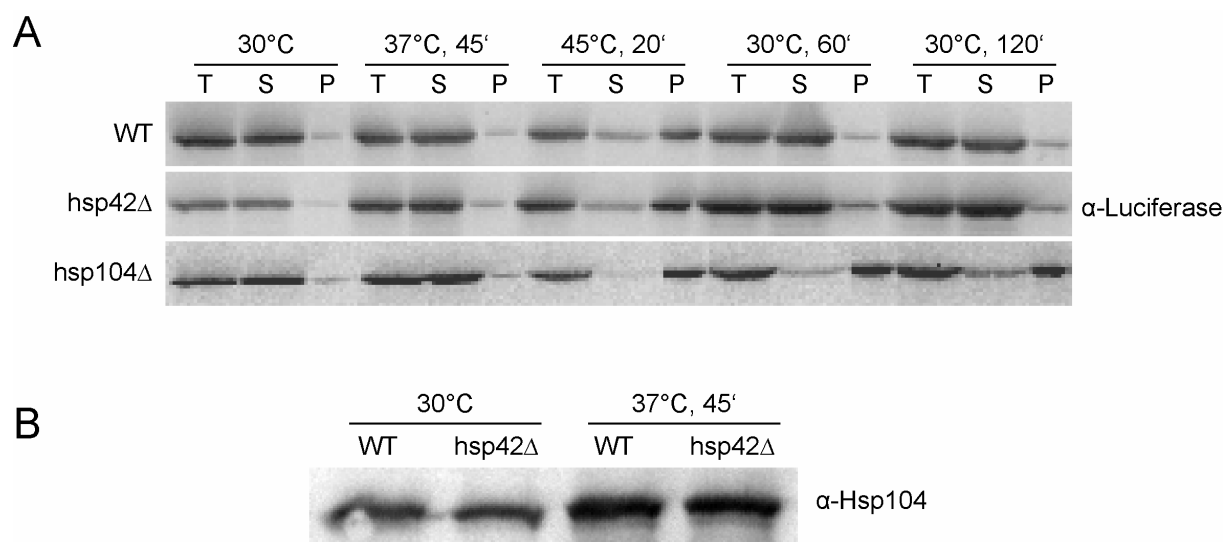


**Figure 5.38 mCitrine-luciferase solubility as well as Hsp104 expression levels are not altered in hsp42Δ cells.**

(A) mCitrine-luciferase solubility is similar in the WT and hsp42Δ strains. Solubility was assessed in wild-type (WT), hsp42Δ, and hsp104Δ cells at 30°C, after preconditioning at 37°C for 45 min, heat shock at 45°C for 20 min, and recovery at 30°C for 60 and 120 min. The solubility was determined by a supernatant-pellet assay described in materials and methods (paragraph 4.3.4). T = total lysate, S = supernatant, P = pellet. (B) Hsp104 expression levels are similar in WT and hsp42Δ cells at 30°C and after the preconditioning period (37°C, 45 min).

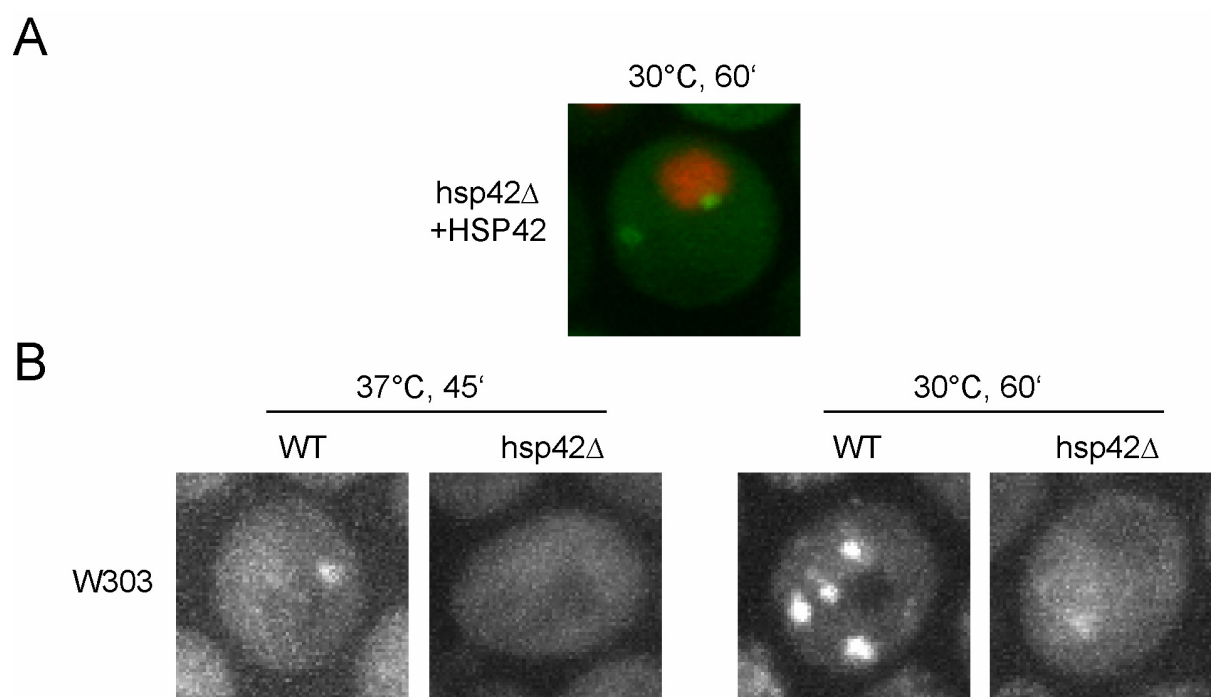


**Figure 5.39 The altered distribution of protein aggregates in hsp42Δ cells is directly caused by missing Hsp42.**

(A) Complementing the hsp42Δ strain with Hsp42 expressed from its native promoter induces reappearance of peripheral aggregation foci. Image of hsp42Δ cells expressing both mCitrine-luciferase (green) and Hsp42 is shown after recovery at 30°C for 60 min. Nuclei were visualized by co-expressing HTB1-mCherry (red). (B) Knocking out *HSP42* in a different yeast strain (W303) results in disappearance of peripheral inclusions. W303 WT and hsp42Δ cells expressing mCitrine-luciferase are depicted after the preconditioning period (37°C, 45 min) and recovery at 30°C for 60 min.

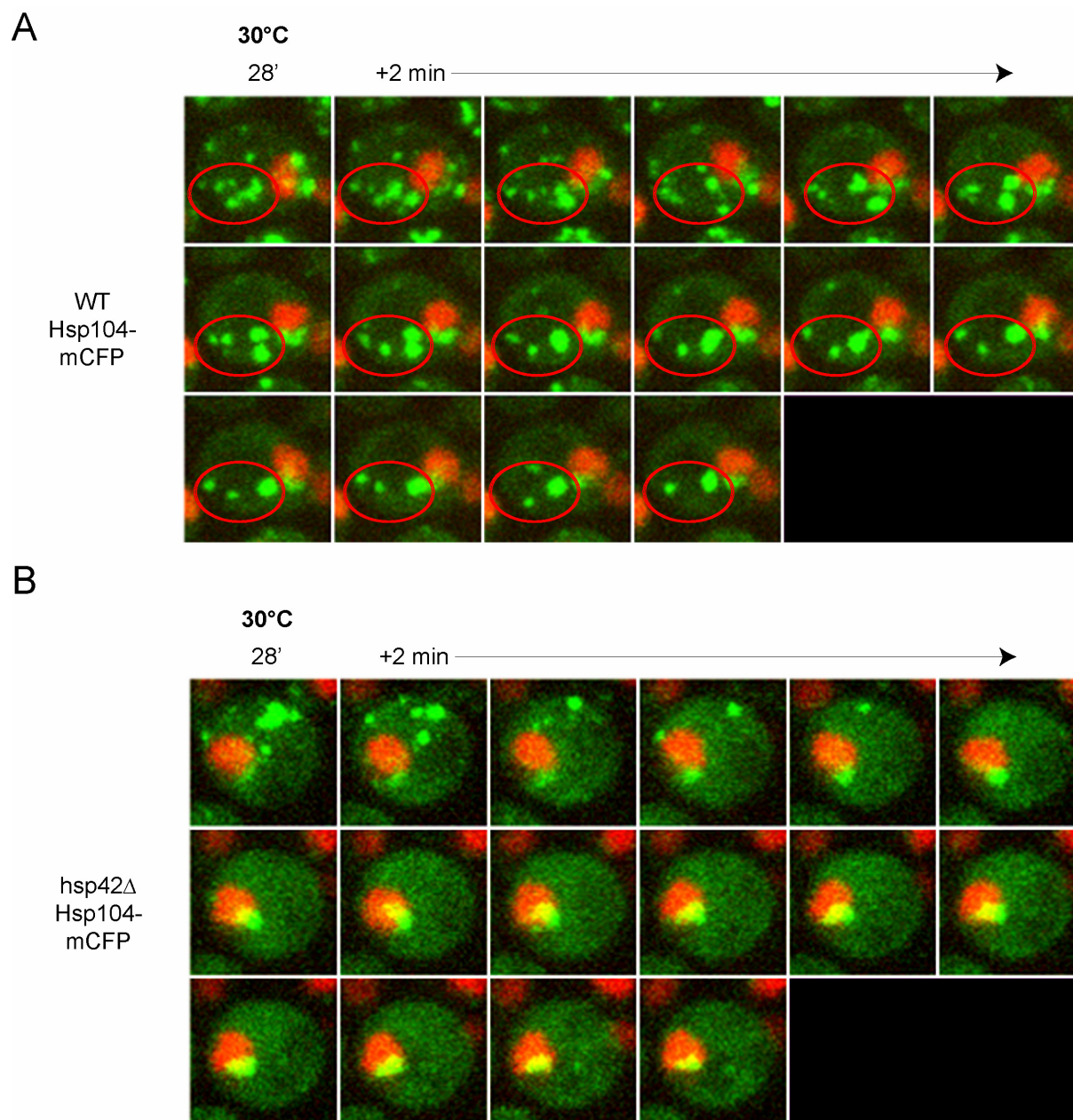


**Figure 5.40 Hsp42 is essential for the persistence of protein inclusions in the cellular periphery.**

Time-lapse microscopy pictures with 2 min time resolution, starting at 28 min recovery at 30°C, are shown of wild-type (WT) (A) and *hsp42Δ* (B) cells expressing Hsp104-mCFP (green). Nuclei were visualized by co-expressing HTB1-mCherry (red). In WT cells the agglutination of diverse foci into inclusions with increased fluorescent intensity (red circle) was monitored. In *hsp42Δ* cells juxtannuclear accumulation of aggregates was accompanied by vanishing of peripheral foci.

### ***5.12 Misfolded proteins accumulate at the nucleus in hsp42Δ cells irrespective of the aggregate load***

I next monitored the organization of aggregates in the presence of an inhibitor of proteasomal degradation (MG132). Blocking the proteasome greatly increased the number of Hsp104-mCFP foci in WT cells. After the preconditioning period and 120 min recovery, almost all WT cells carried aggregation foci (Figure 5.41 A/B). This is in contrast to cells with intact proteasomal degradation, where protein inclusions are cleared in more than 80 % of cells within 120 min recovery, indicating that proteasome inhibition increases the substrate load for the quality control system. To further challenge the hsp42Δ phenotype, I also applied heat stress in the hsp42Δ strain in the presence of MG132. Even the enhanced aggregate load did not result in the formation of stable peripheral inclusions in hsp42Δ cells and aggregates were exclusively observed as juxtannuclear foci after preconditioning and 120 min recovery (Figure 5.41 A/B). Notably, the juxtannuclear foci were maintained in 70 % of cells within 120 min recovery.

I also performed time-lapse microscopy of single cells expressing Hsp104-mCFP under such conditions (+ MG132) and followed the spatio-temporal organization of endogenous yeast aggregates during heat shock and subsequent recovery. In the WT strain aggregation foci were formed and pertained juxtannuclear and in the periphery (Figure 5.42 A). In the hsp42Δ strain aggregation foci were exclusively localizing to the nucleus within 30 min recovery (Figure 5.42 B). Remarkably, the intensity of the juxtannuclear-localized foci was greatly increased in comparison to hsp42Δ cells with intact proteasomal degradation. Taken together, misfolded proteins accumulate at the nucleus in the hsp42Δ strain irrespective of the aggregate load.

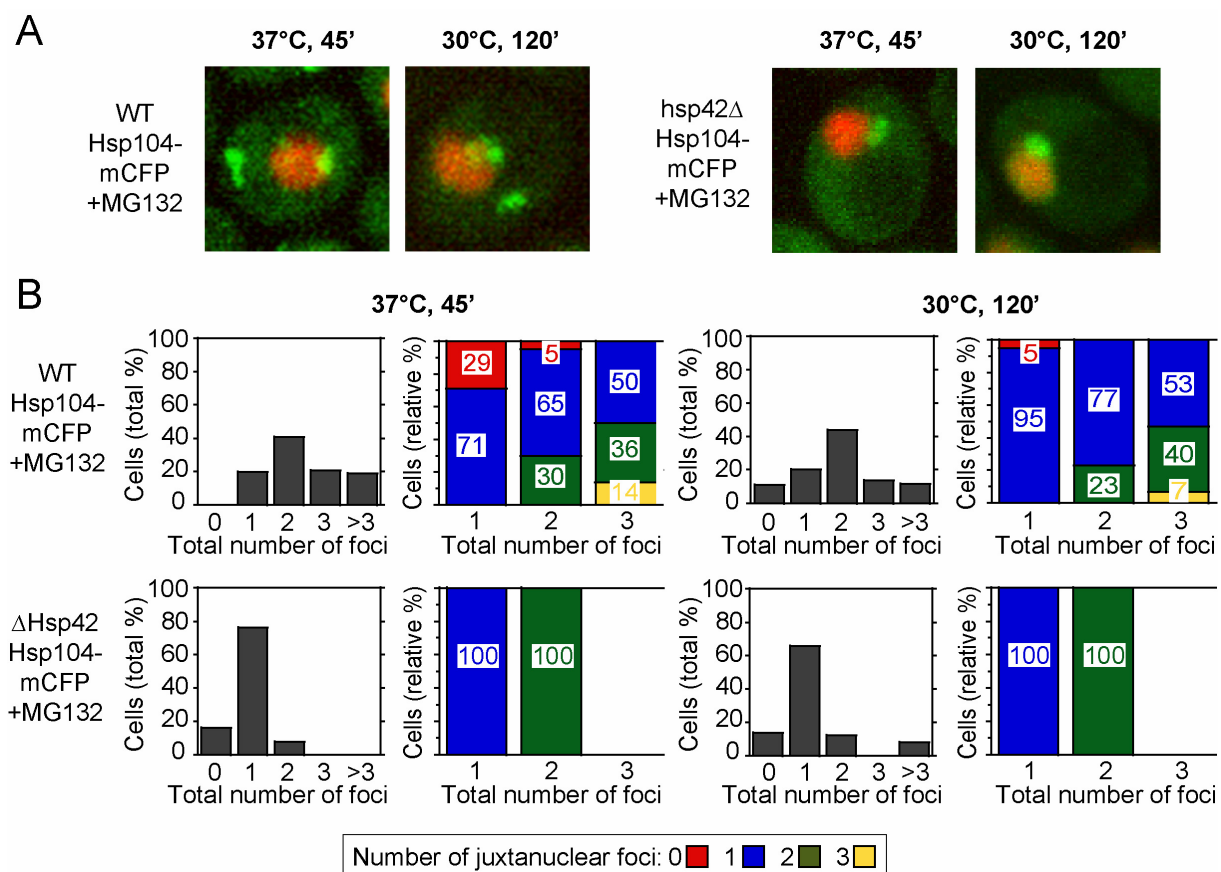


**Figure 5.41 Juxtannuclear accumulation of protein inclusions in *hsp42* $\Delta$  cells occurs irrespective of the aggregate load.**

(A) Number (dark grey columns) and localization (colored columns) of endogenous yeast aggregates stained by Hsp104-mCFP were monitored in wild-type (WT) and *hsp42* $\Delta$  cells after the preconditioning period (37°C, 45 min) and recovery at 30°C for 120 min. The proteasomal inhibitor MG132 was added before preconditioning. The color code deciphers foci localization. Red corresponds to zero juxtannuclear inclusions, blue to one, green to two, and yellow to three. The total number of foci per cell is depicted in all diagrams on the x-axis. Quantifications are based on the analysis of  $n = 100$  cells.

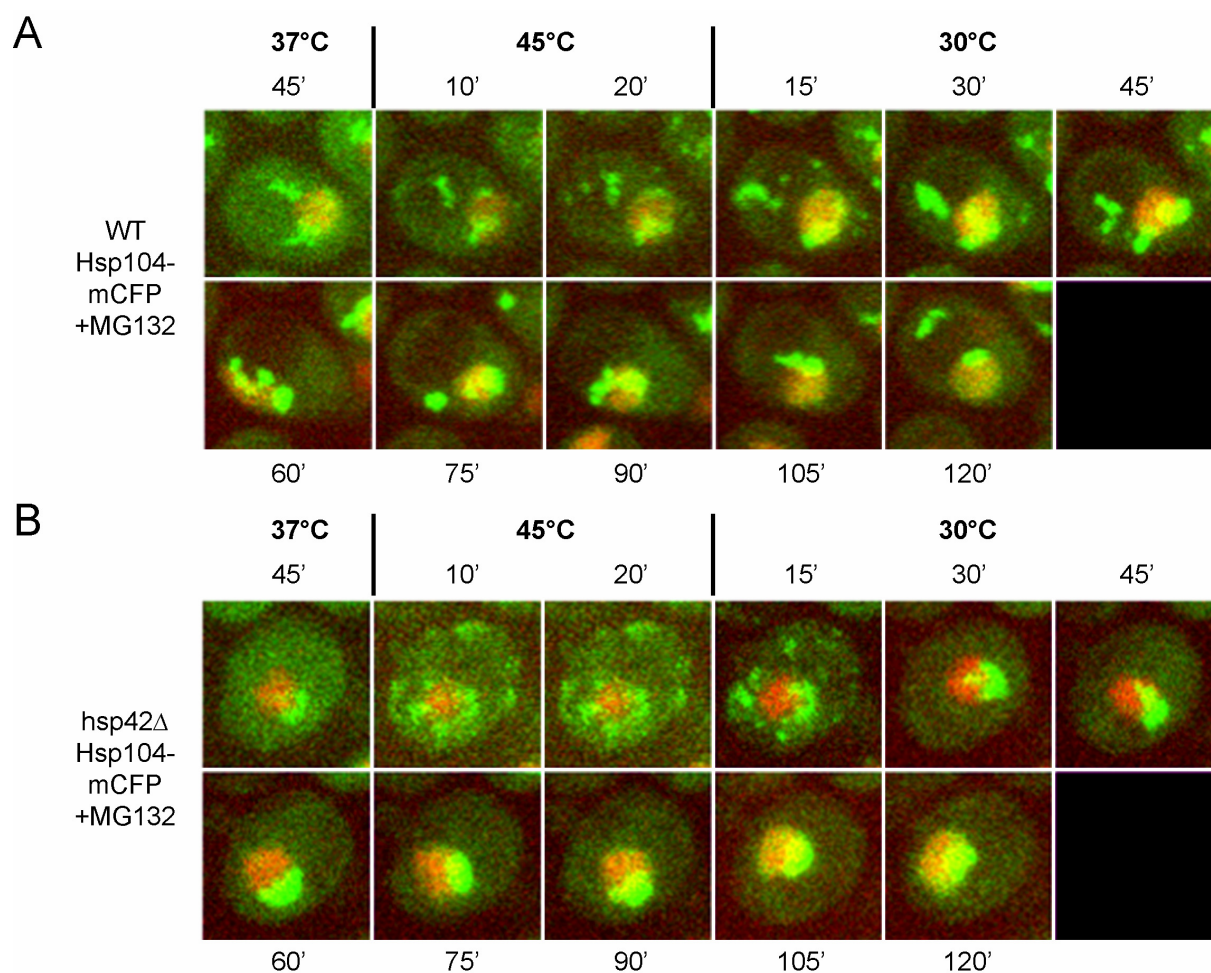


**Figure 5.42 Aggregation foci accumulate rapidly at the nucleus in *hsp42Δ* cells during blocked proteasomal degradation.**

Time-lapse microscopy pictures are shown of single wild-type (WT) (A) and *hsp42Δ* (B) cells expressing Hsp104-mCFP (green) at the indicated time period during heat shock and the recovery phase at 30°C. The proteasome inhibitor MG132 was added before preconditioning. Nuclei were visualized by co-expressing HTB1-mCherry (red).

### ***5.13 The actin cytoskeleton does not play a role in protein disaggregation***

The actin cytoskeleton is of crucial importance for aggregate partitioning to both the JUNQ and IPOD compartment (Figure 5.21). I therefore sought to determine whether it is also required for the resolubilization of heat-shock induced protein aggregates. For this purpose I followed Cerulean-luciferase and Hsp104-mCFP localization during heat shock and the subsequent recovery phase at 30°C in the presence of the actin-depolymerizing drug latrunculin A (LatA), which causes complete disruption of the yeast actin cytoskeleton (Ayscough *et al.*, 1997). The actin cytoskeleton was visualized via a genomic C-terminal fusion of mCitrine to Abp140 in Cerulean-luciferase expressing cells (Yang and Pon, 2002). While actin cables were present after heat shock and throughout the recovery phase in the DMSO-treated control cells, the LatA-treated cells displayed a completely disassembled actin cytoskeleton (Figure 5.43 A). Heat shock-induced Cerulean-luciferase and yeast endogenous aggregates stained via Hsp104-mCFP were however similar efficiently resolubilized in the presence and absence of LatA (Figure 5.43 A/B). The juxtannuclear persistence of Hsp104-stained aggregates in *hsp42Δ* cells was also independent of an intact actin cytoskeleton, because the presence of LatA did not influence the localization of misfolded proteins in the *hsp42Δ* strain (Figure 5.43 C). Therefore, the actin cytoskeleton seems of no importance for the disaggregation of protein inclusions.

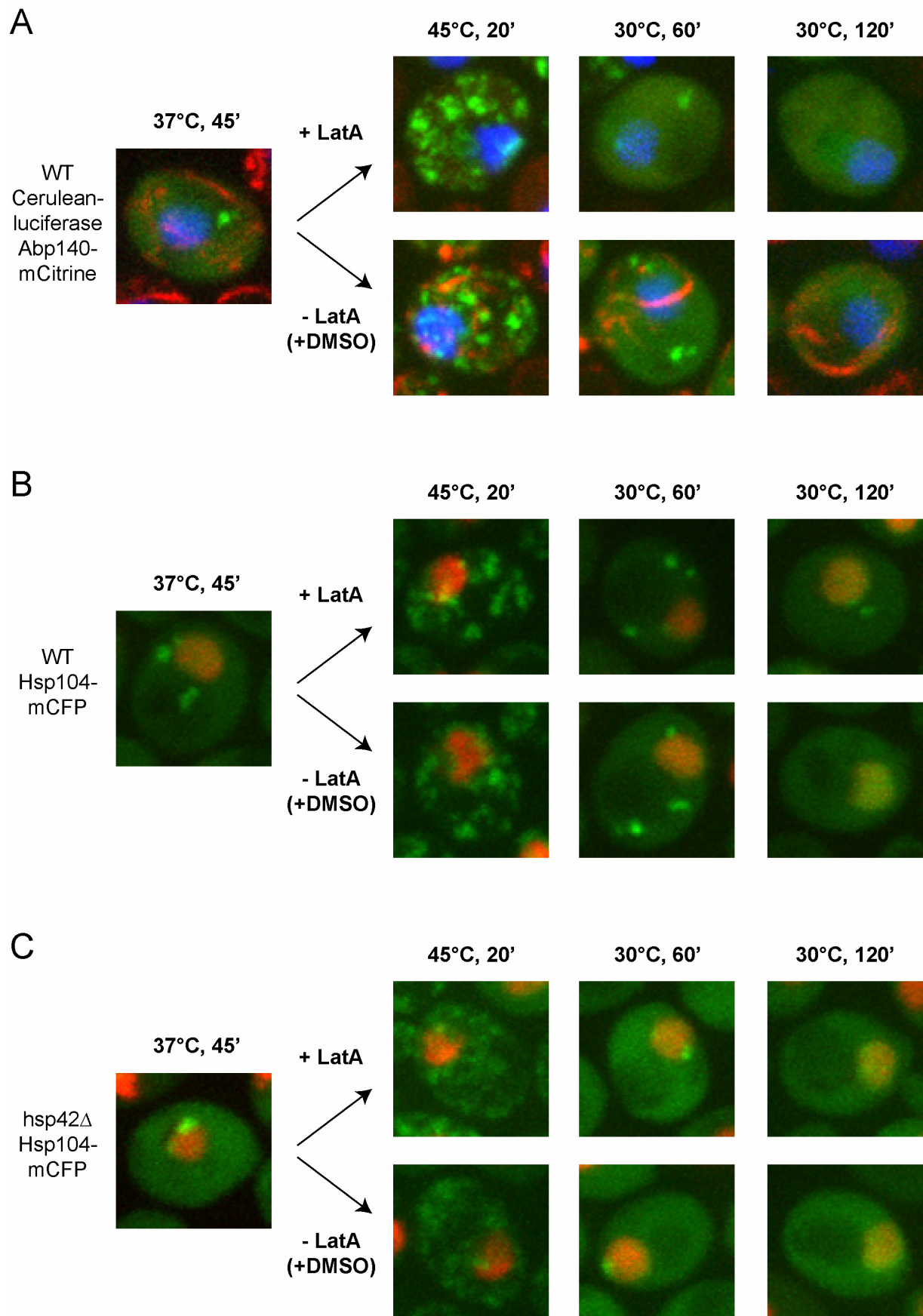


**Figure 5.43 The actin cytoskeleton is not required for protein disaggregation.**

(A) The clearance of heat shock-generated Cerulean-luciferase inclusions does not require actin polymerization. *S. cerevisiae* cells co-expressing Cerulean-luciferase (green) and Abp140-mCitrine (red), which binds actin cables and patches, were preconditioned at 37°C for 45 min, heat shocked at 45°C for 20 min, and allowed to recover at 30°C for 120 min. The actin-depolymerizing drug latrunculin A (LatA) was added prior to heat shock. Instead of LatA, control cells were treated with the same volume of DMSO. Nuclei were visualized by co-expressing HTB1-mCherry (blue). (B+C) The juxtannuclear persistence of Hsp104-mCFP foci in *hsp42Δ* cells does not require a functional actin cytoskeleton. Wild-type (WT) (B) and *hsp42Δ* (C) cells expressing Hsp104-mCFP (green) were treated as described in (A). Nuclei were visualized by co-expressing HTB1-mCherry (red).

**5.14 Protein inclusions are inherited asymmetrically**

Protein aggregates have been shown to be unequally partitioned between dividing cells (Fuentelba *et al.*, 2008; Lindner *et al.*, 2008; Aguilaniu *et al.*, 2003). We therefore sought to determine whether protein inclusions are segregated into daughters in *S. cerevisiae*. For that purpose time lapse microscopy of single cells was performed during the recovery period from heat shock. Interestingly, no novel buds were formed in cells until 45-60 min recovery (30°C), when most aggregation foci had successfully been cleared. Neither were pre-existing buds enlarged during this time interval. Once mitosis was started, the mCitrine-luciferase (data not shown) or Hsp104-mCFP stained foci, which were still remaining, were not segregated into daughters in all cells observed (Figure 5.44 A). Thus, WT cells keep their offspring devoid of visible protein inclusions. In order to monitor cells with a higher content of inclusions, we studied aggregate inheritance in *hsp26Δ* cells and could not observe aggregate partitioning into buds (Figure 5.44 B).

Aggregate clearance is nonetheless not a prerequisite for cell division, because the isogenic *hsp104Δ* strain, which had been heat shocked, still displayed mitosis. In contrast to WT cells, the cluttered protein aggregates in heat-shocked *hsp104Δ* cells entered the buds (Figure 5.44 C). However, if *hsp104Δ* cells were exposed to mild thermal stress (37°C, +MG132), the inclusions were not entering daughter cells (Figure 5.44 D). We conclude that sequestration of aggregated proteinaceous material into larger foci might ensure retention of protein aggregates in the mother cell and thus might contribute to rejuvenation of the progeny.

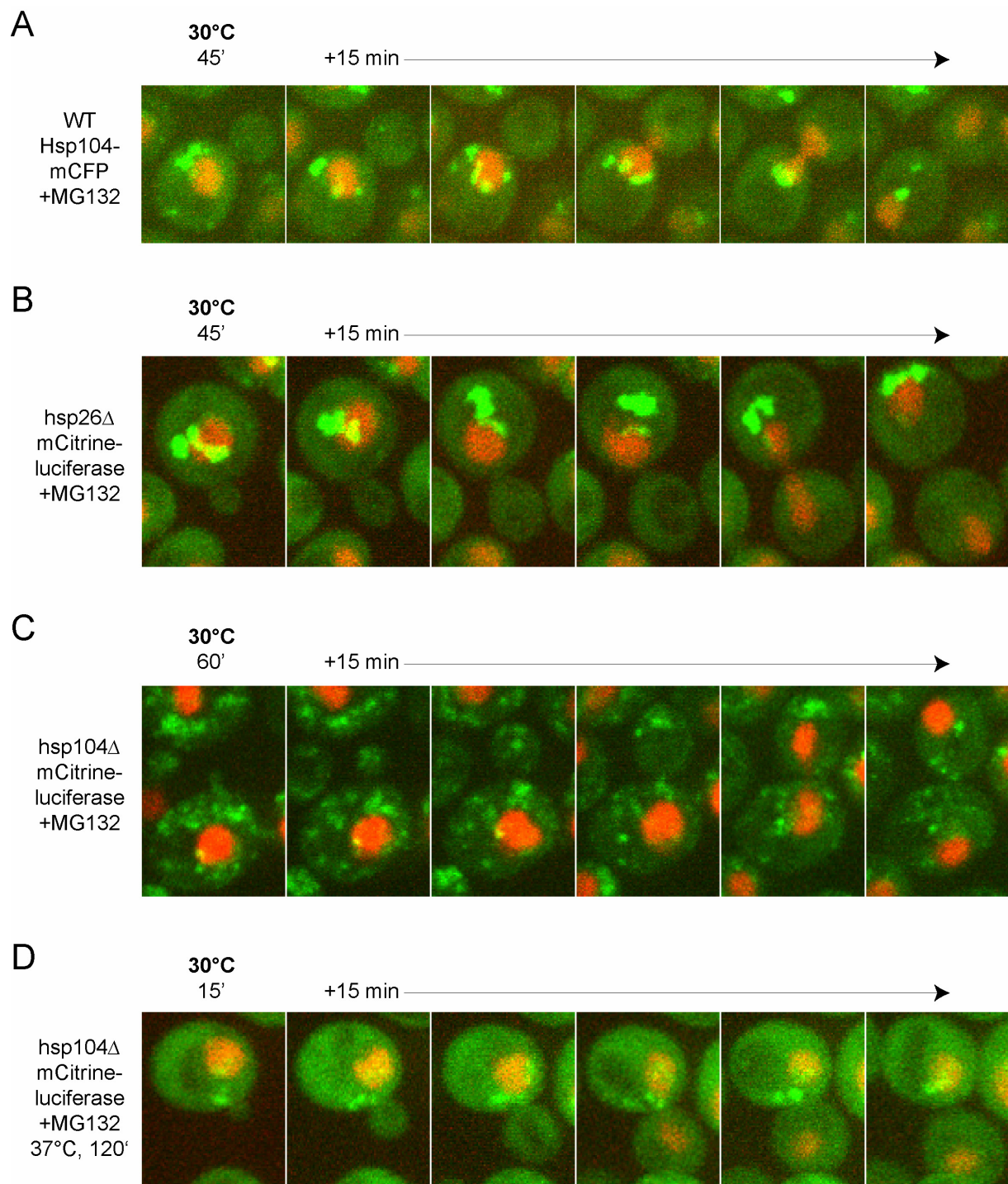


**Figure 5.44 Aggregation foci are inherited asymmetrically.**

*S. cerevisiae* wild-type (WT) cells expressing Hsp104-mCFP (A), and *hsp26Δ* (B) and *hsp104Δ* (C) cells expressing mCitrine-luciferase (green) were preconditioned at 37°C for 45 min, heat shocked at 45°C for 20 min, and allowed to recover at 30°C. Alternatively, *hsp104Δ* cells expressing mCitrine-luciferase were incubated at 37°C for 120 min and subsequently shifted to 30°C (D). Time-lapse microscopy pictures with 15 min time resolution, starting at the indicated time point of recovery at 30°C, are displayed. The proteasomal inhibitor MG132 was added before preconditioning (A-C) or shift to 37°C (D). Nuclei were visualized by co-expressing HTB1-mCherry (red).

### ***5.15 sHsps do not accelerate the velocity of thermal luciferase aggregation in vitro***

The results of the current study demonstrate an effect of *S. cerevisiae* sHsps on protein aggregate reactivation and localization. sHsps might therefore seed aggregation of their substrates. Since sHsps co-aggregate efficiently with non-native polypeptides, they could have a higher affinity for unfolded protein segments than other non-native polypeptides, which compete for binding to exposed hydrophobic regions. In order to determine whether sHsps actually accelerate the aggregation process of their substrates, I followed *in vitro* the aggregation kinetics of CFP- and YFP-luciferase in the presence and absence of sHsps. First, I established high-yield expression and purification protocols for Hsp26 and Hsp42 in *E. coli*. Both chaperones were N-terminally fused to a His<sub>6</sub>-SUMO tag. The His<sub>6</sub> tag facilitates purification with Ni-NTA chromatography and SUMO fusion leads to enhanced expression and solubility (Koken *et al.*, 1993). However, the high-yield protocol in *E. coli* that I established for Hsp42 did not generate functional chaperone (data not shown). On the other hand, testing Hsp26 chaperone activity in preventing the formation of light-scattering aggregates of malate dehydrogenase (MDH), I monitored an Hsp26 concentration dependent suppression of aggregation. Four times molar excess of Hsp26 prevented almost completely the formation of light scattering inclusions during MDH denaturation (Figure 5.45). The subsequent experiments were therefore carried out only with Hsp26.

Small protein inclusions formed at the beginning of the aggregation process do not contribute to light scattering at 600 nm. To establish a more sensitive assay for assessing protein aggregation, I cloned and purified CFP-luciferase and YFP-luciferase. Since the thermostable CFP and YFP moieties constitute an efficient FRET pair, the heat-induced aggregation kinetics of thermolabile luciferase could be monitored by following the FRET signal. Incubating an equimolar mix of the fusion proteins at 45°C generated upon CFP excitation a FRET signal, while, as expected, the CFP fluorescence was quenched (Figure 5.46 A). Surprisingly, carrying out the experiment in the presence of up to eight times molar excess of Hsp26 did not affect the FRET measurement (Figure 5.46 C). For that reason I monitored CFP-luciferase and YFP-luciferase prevention of aggregation in the presence of Hsp26, and did not find any effect of the chaperone on the formation of light scattering inclusions during heat denaturation of the luciferase fusion proteins (Figure 5.46 B). Consequently, *in vitro* luciferase constitutes a poor substrate for Hsp26. When testing a different sHsp, Hsp16.6 from the cyanobacterium *Synechocystis*, I observed an efficient prevention of light scattering

inclusion formation of the luciferase hybrid proteins (Figure 5.46 D). Hsp16.6 can thus modulate the aggregation process of the luciferase fusion proteins efficiently. However, no acceleration of the FRET process was examined in the presence of Hsp16.6 (Figure 5.46 E/F). Consequently, *in vitro* sHsps do not increase aggregation velocity in my technical setup.

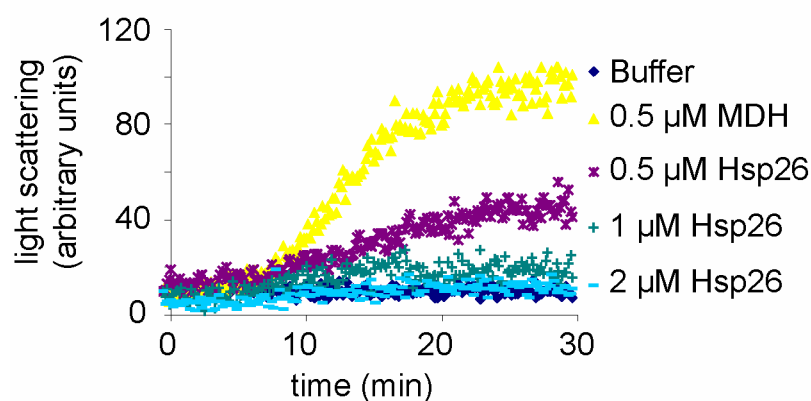


**Figure 5.45 Hsp26 influences the thermal aggregation of malate dehydrogenase.**

Influence of Hsp26 on the thermal aggregation of malate dehydrogenase (MDH). MDH (final concentration 0.5  $\mu\text{M}$ ) was diluted into a thermostatted solution (47°C) of 0.5  $\mu\text{M}$  (purple), 1  $\mu\text{M}$  (dark green), and 2  $\mu\text{M}$  (light blue) Hsp26. Spontaneous aggregation of MDH at 47°C in the absence of Hsp 26 is depicted in yellow. The signal of solely buffer is shown in dark blue. The kinetics of aggregation were determined by measuring the light scattering of the sample at 600 nm.

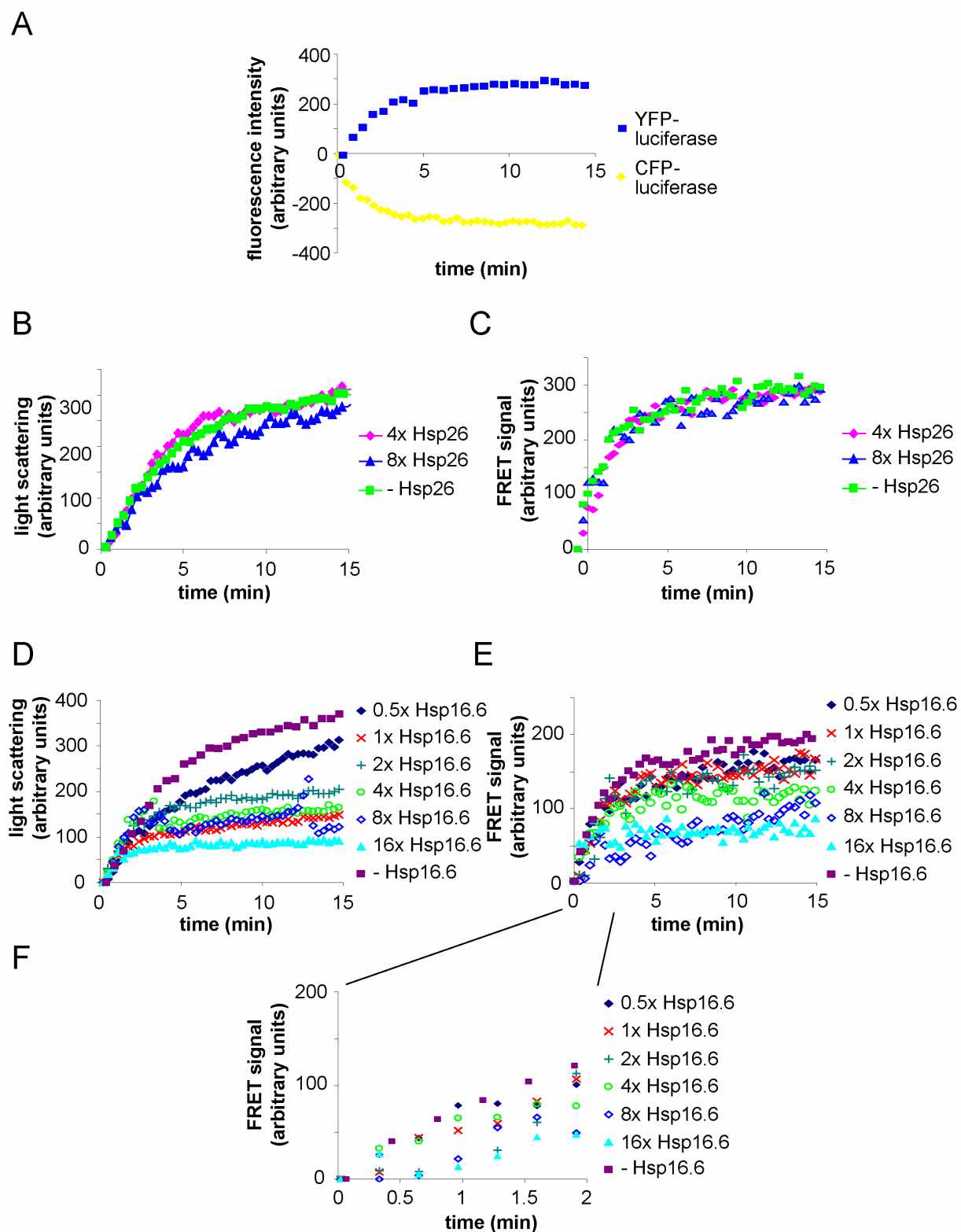


**Figure 5.46 sHsps do not accelerate the velocity of luciferase aggregation.**

(A) CFP- and YFP-luciferase fusion proteins constitute an efficient FRET pair. Equimolar amounts of CFP- and YFP-luciferase (final concentration each 0.5  $\mu\text{M}$ ) were diluted into thermostatted buffer (45°C). CFP- and YFP-luciferase fluorescence was monitored upon CFP excitation. Spontaneous aggregation of luciferase generates a FRET signal, i.e. an increase in YFP fluorescence and quenching of CFP fluorescence. (B+C) Hsp26 does not influence the thermal aggregation of CFP- and YFP-luciferase *in vitro*. CFP- and YFP-luciferase (final concentration each 0.5  $\mu\text{M}$ ) were diluted into a thermostatted solution (45°C) of molar 4 x (2  $\mu\text{M}$ , pink) and 8 x (4  $\mu\text{M}$ , blue) Hsp26. Spontaneous aggregation of CFP- and YFP-luciferase at 45°C in the absence of Hsp26 is depicted in green. The kinetics of aggregation were determined by measuring (B) the light scattering of the

---

sample at 600 nm and (C) the FRET signal (excitation of CFP and monitoring of YFP fluorescence). (D-F) *Synechocystis* Hsp16.6 prevents light scattering inclusion formation of CFP- and YFP-luciferase, but does not increase aggregation velocity. CFP- and YFP-luciferase (final concentration each 0.5  $\mu\text{M}$ ) were diluted into a thermostatted solution (45°C) of molar 0.5 x (0.5  $\mu\text{M}$ , dark blue), 1 x (1  $\mu\text{M}$ , red), 2 x (2  $\mu\text{M}$ , dark green), 4 x (4  $\mu\text{M}$ , light green), 8 x (8  $\mu\text{M}$ , blue), and 16 x (16  $\mu\text{M}$ , light blue) Hsp16.6. Spontaneous aggregation of CFP- and YFP-luciferase at 45°C in the absence of Hsp 16.6 is depicted in purple. The kinetics of aggregation were determined by measuring (D) the light scattering of the sample at 600 nm and (E+F) the FRET signal (excitation of CFP and monitoring of YFP fluorescence). (F) Enlargement of the first 2 min of the FRET measurement.

## 6. Discussion

### 6.1 *The small heat shock protein Hsp42 controls the spatio-temporal organization of misfolded proteins in S. cerevisiae*

I here analyzed the sorting of misfolded proteins in yeast cells during prolonged folding stress. In accordance with previous findings (Kaganovich *et al.*, 2008), I observed partitioning of different fluorescent aggregation reporters between juxtannuclear (JUNQ) and peripheral (IPOD) compartments in most cells. These compartments are suggested to fulfill different cellular functions. The JUNQ seems to predominantly harbor ubiquitylated substrates, potentially allowing for their rapid elimination by increasing the concentration of proteasomes at this site (Kaganovich *et al.*, 2008). In contrast, IPOD-like compartments are proposed to accumulate terminally misfolded and aggregated proteins, potentially protecting the cell from toxic protein species or facilitating aggregate clearance by either autophagy or dilution via cell division. Accordingly, mCherry-VHL molecules present in the JUNQ appear to be more mobile compared to those sequestered at IPOD-like compartments, in agreement with previous findings (Kaganovich *et al.*, 2008). On the other hand, return of yeast cells to physiological growth conditions allowed for Hsp104-dependent disintegration of the compartments (Figure 5.17, Figure 5.18 and Figure 5.19), indicating that the deposition of misfolded proteins at IPOD-like inclusions is not an irreversible event. This observation is consistent with the finding that the disaggregase Hsp104 binds to JUNQ and IPOD-like compartments (Kaganovich *et al.*, 2008).

Which cellular factors regulate the distribution of a misfolded substrate pool to the JUNQ and IPOD-like compartments? I performed a candidate approach and focused on the *S. cerevisiae* sHsps, namely Hsp26 and Hsp42, as they interact efficiently with aggregation-prone protein species (Haslbeck *et al.*, 2004a; Haslbeck *et al.*, 1999a). I speculated that their efficient coaggregation might additionally enable sHsps to function as sorting factors for protein aggregates. Indeed, I identified Hsp42 as an essential factor in the formation of IPOD-like inclusions (Figure 5.5). Misfolded proteins do not accumulate in peripheral inclusions in *hsp42Δ* cells, but seem to be re-directed to the JUNQ, as revealed by increased fluorescent intensity of juxtannuclear mCherry-VHL foci. Hsp42 exerts a specific function, because the second *S. cerevisiae* sHsp, Hsp26, did not affect aggregate sorting (Figure 5.5). Consistent with this observation Hsp26 was present in all visible inclusions whereas Hsp42 was only found in peripheral foci, but was absent from one juxtannuclear focus, suggesting that Hsp42 is

directly involved in targeting aggregation-prone proteins to peripheral sites (Figure 5.9). It is currently not evident which parameters prevent Hsp42 from association with JUNQ compartments. Substrate ubiquitylation has been previously shown to play a crucial role in targeting misfolded protein species to the JUNQ and might interfere with Hsp42 binding.

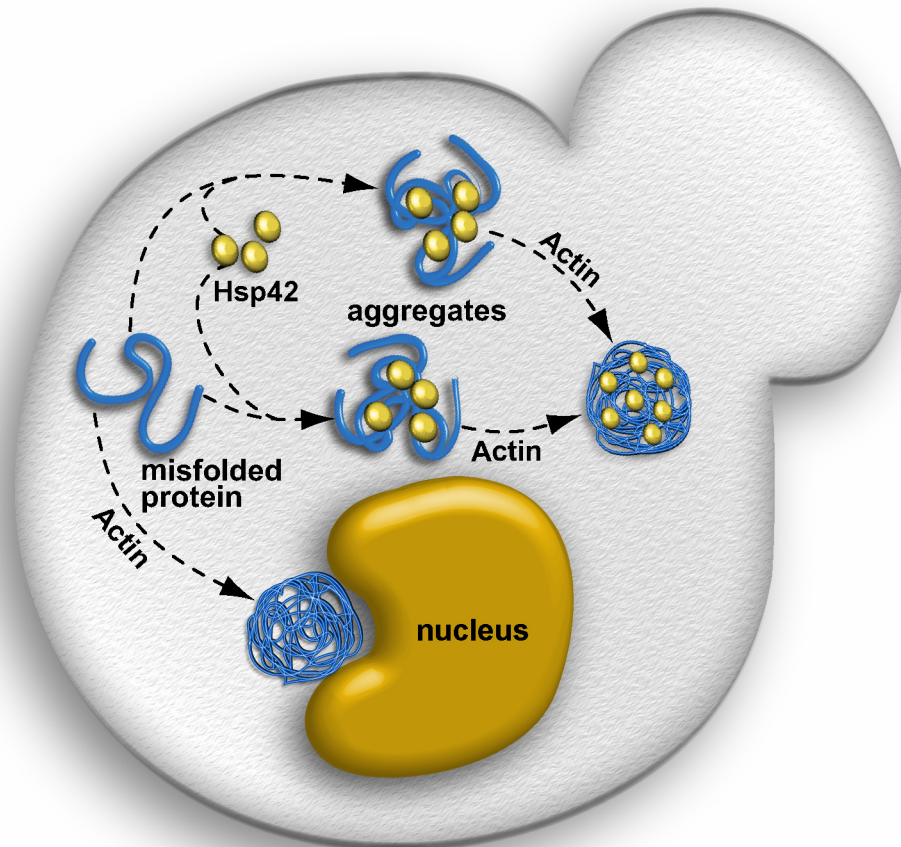


**Figure 6.1 Model of the Hsp42-dependent sorting of misfolded proteins during prolonged stress conditions.**

Hsp42 co-aggregates with misfolded proteins. The resulting complexes are sorted in an actin-dependent process to peripheral inclusions. Protein aggregates not harboring Hsp42 accumulate at the nucleus in a process that also requires the actin cytoskeleton.

The consequences of re-directing misfolded proteins exclusively to the juxtannuclear deposition sites in *hsp42Δ* cells are not evident. I noticed surprisingly that the JUNQ compartment of *hsp42Δ* cells showed a moderate increase in substrate mobility and was slightly more rapidly solubilized by Hsp104 (Figure 5.16 and Figure 5.17). These findings might suggest that the Hsp42-dependent sorting to peripheral compartments retards substrate resolubilization, thereby potentially reducing substrate load for the quality control system.

Since *hsp42Δ* cells do not exhibit a reported growth or viability phenotype, the consequences of controlling substrate flux into distinct compartments remain to be revealed.

Why does Hsp42, but not Hsp26, control aggregate sorting? Hsp26 represents a temperature-controlled chaperone that requires increased temperatures for activation, restricting its chaperone activity to particular stress conditions (Franzmann *et al.*, 2008; Haslbeck *et al.*, 1999a). In contrast, Hsp42 appears to be constitutively active, allowing it to associate with misfolded proteins generated upon folding stress conditions distinct from heat shock (Haslbeck *et al.*, 2004a). Furthermore, I identified the large NTD of Hsp42 as a key determinant in contributing functional specificity to the sHsp (Figure 5.12). The Hsp42ΔN deletion variant did not allow for the formation of IPOD-like inclusions. Since NTDs of sHsps also contribute to sHsp oligomerization and thus general functionality, I additionally transferred the Hsp42 NTD to Hsp26. This N42-Hsp26 chimera exhibited a gain-of-function phenotype, as it could partially restore the occurrence of IPOD-like inclusions. According to a key function of the Hsp42 NTD in aggregate sorting, Hsp42 deleted of its CTE (Hsp42ΔC) could restore occurrence of peripheral inclusions, in contrast to Hsp26, Hsp26 with the CTE of Hsp42 (Hsp26-C42), and Hsp42 possessing the Hsp26 NTD (N26-Hsp42). NTDs of sHsps have been demonstrated to mediate substrate interaction and sHsp oligomerization (Jaya *et al.*, 2009; Basha *et al.*, 2006; Stromer *et al.*, 2004). Interestingly, a role of NTDs beyond their contribution to the chaperone activity of sHsps has been noticed for *Synechocystis* Hsp16.6, which seems to exert an additional, yet unknown activity (Friedrich *et al.*, 2004). My findings illuminate a novel function of the Hsp42 NTD in controlling the distribution of aggregated proteins between distinct deposition sites. I speculate that at least parts of the elongated Hsp42 NTD are exposed at the surface of Hsp42/substrate complexes, even upon co-aggregation of Hsp42 with misfolded proteins. Such a scenario implies the existence of further, so far unknown, sorting factors that might bind to the Hsp42 NTD, thereby potentially linking protein inclusions to the actin cytoskeleton, which I have shown to be required for aggregate sorting (Figure 5.21). I also considered the possibility that Hsp42 might exert an indirect effect by stabilizing the actin cytoskeleton during stress conditions (Gu *et al.*, 1997). I did, however, not observe differences in the organization of the actin cytoskeleton in *hsp42Δ* cells when compared to WT cells at both physiological and folding stress conditions (Figure 5.23). Along the same line, formation of the juxtannuclear deposition sites was still possible in *hsp42Δ* cells, but not upon disruption of the actin cytoskeleton via addition of LatA (Figure 5.21), largely excluding that Hsp42 exerts its role by simply stabilizing the actin cytoskeleton.

Summarized, I unraveled a novel function of the sHsp family in controlling the cellular sorting of damaged proteins. In mammalian cells K63-linked polyubiquitylation of substrates is suggested to serve as a signal for aggregate sorting by mediating the binding of the adaptor protein HDAC6, which links the ubiquitylated substrate to the microtubule motor protein dynein (Olzmann and Chin, 2008; Kawaguchi *et al.*, 2003). The use of an incorporated sHsp as a specific sorting label for protein inclusions represents a novel strategy. Is this novel role of sHsps in controlling the cellular localization of aggregated proteins evolutionary conserved? In plant cells the formation of heat stress granules (HSG) depends on sHsp activity, supporting such conserved function (Miroshnichenko *et al.*, 2005). Mammalian cells have been reported to sequester misfolded proteins into two distinct compartments like yeast cells (Kaganovich *et al.*, 2008). Hsp42 homologs are, however, only present in closely related fungi, suggesting that Hsp42 function has been taken over by other family members. Intriguingly, the number of sHsp family members is strongly increased in higher eukaryotes (Haslbeck *et al.*, 2005a) and sHsp function is no longer restricted to protein folding stress, but is also linked to e.g. developmental processes and regulation of apoptosis (Heikkila, 2004; Arrigo, 2000). The evolutionary variability of N- and C-terminal extensions might enable sHsps to adopt novel functions, including the cellular sorting of aggregated proteins, thereby potentially taking over the function of *S. cerevisiae* Hsp42.

## **6.2 Stress conditions determine the organization of aggregated proteins**

Besides studying the fate of protein aggregates during prolonged thermal stress (37°C) in cells with blocked proteasomal protein degradation, I analyzed the spatio-temporal organization of aggregates during and after application of sublethal heat shock (45°C, 20 min). I focused on establishing an authentic experimental setup, utilizing physiological expression levels of reporter constructs and intact proteasomal degradation. Heat shock induced the formation of multiple aggregation foci that were distributed throughout the cell (Figure 5.25). No specific pattern of aggregate positioning was detected, suggesting that inclusion formation occurs at random localization. This agrees with electron microscopic studies, which have observed the appearance of large electron dense particles in the cytosol and nucleus after heat shock (Parsell *et al.*, 1994). The aggregation of proteins at random localization is likely explained by the severity of the heat shock, resulting in the massive generation of misfolded protein species, thus temporarily overwhelming the cellular protein quality control and sorting

machinery. As soon as stress is removed, proteins are started to be refolded in a process requiring Hsp104-dependent protein disaggregation (Figure 5.25 and Figure 5.30).

Is protein disaggregation coupled to specific localizations? Since aggregation foci remain distributed throughout the cytoplasm of the cell during the refolding phase (Figure 5.32 and Figure 5.33), protein disaggregation seems to occur *in situ*. This is further substantiated by the observation that a polymerized actin cytoskeleton is not required for the disaggregation process (Figure 5.43). These results appear to contrast previous findings showing prolonged mild thermal stress (37°C) to result in sorting of misfolded proteins to JUNQ and IPOD-like compartments in an actin cytoskeleton dependent manner (Figure 5.21) (Kaganovich *et al.*, 2008). When the JUNQ/IPOD substrate VHL is subjected to sublethal heat shock (45°C), it is no longer sorted to the distinct compartments, but rather forms multiple foci in the cytosol, which largely persist throughout the recovery phase (30°C) (Figure 5.31). I suggest that heat shock-induced protein misfolding exceeds the functional capacity of the cellular system for sorting misfolded proteins to JUNQ/IPOD-like compartments, resulting in protein aggregation at random position throughout the yeast cytosol. In consequence, the nature of applied stress determines the deposition sites of misfolded proteins.

Interestingly, disappearance of luciferase and Hsp104-stained aggregation foci during the recovery phase is accompanied by an increase in fluorescence intensity of remaining inclusions (Figure 5.32, Figure 5.33, and Figure 5.40), suggesting agglutination of protein aggregates. The agglutination process might be facilitated by the observed mobility of inclusions. Different mobility patterns between peripheral and juxtannuclear aggregates were monitored. While peripheral foci were able to move through the cell, juxtannuclear foci generally stayed at the nucleus. The cause of juxtannuclear inclusion immobility remains to be revealed.

In search of factors regulating protein aggregation and reactivation, I performed a candidate approach and focused on the *S. cerevisiae* sHsps, namely Hsp26 and Hsp42, which interact efficiently with aggregation-prone protein species and function as sorting factors for misfolded proteins. Indeed, I observed Hsp26 to be required for rapid reactivation of aggregated luciferase (Figure 5.34). In *hsp26*Δ cells the kinetics of luciferase enzymatic activity regain were slower during recovery from heat shock. Congruent to the slower luciferase refolding, a delayed disintegration of aggregation foci was detectable in *hsp26*Δ cells (Figure 5.35). These results agree with previous findings showing that Hsp26 renders aggregates more accessible to the disaggregation machinery (Hsp104/ Ssa1/Ydj1) (Cashikar *et al.*, 2005; Haslbeck *et al.*, 2005b).

In contrast to Hsp26, the absence of Hsp42 had no effect on the reactivation of aggregated luciferase (Figure 5.34). However, after the preconditioning period and 60 min recovery peripheral foci were virtually absent in *hsp42Δ* cells, while juxtannuclear inclusions were still detectable (Figure 5.35). This compares favorably to the observation that Hsp42 is essential for the formation of peripheral IPOD-like compartments (Figure 5.5). Notably, sublethal heat shock induced the formation of peripheral aggregation foci in *hsp42Δ* cells (Figure 5.35). The inclusions appeared, however, less condensed and intense, indicating that Hsp42 is co-aggregating with substrates and alters their morphology. During mild thermal stress conditions (37°C) protein inclusions form exclusively at the nucleus in *hsp42Δ* cells (Figure 5.8). The appearance of peripheral aggregation foci in the *hsp42Δ* strain points to temporal substrate overload of the cellular sorting system, thereby also resulting in protein aggregation at random positions in *hsp42Δ* cells.

Taken together, I here demonstrate that the actual stress condition has a profound influence on the deposition site of protein aggregates in yeast cells. Severe heat shock seems to overwhelm the cellular sorting system, which otherwise targets misfolded proteins to JUNQ/IPOD-like compartments, resulting in the deposition of protein aggregates at random localizations. Subsequent Hsp104-dependent solubilization of aggregates does not require an initial sorting of aggregates to distinct sites and, accordingly, takes place in the absence of a functional cytoskeleton. I also demonstrate a functional divergence between the *S. cerevisiae* sHsps during the aggregation and disaggregation process. While being not involved in the sorting of aggregated proteins, Hsp26 facilitates solubilization of aggregated proteins. In contrast, Hsp42 serves strictly as a sorting factor, but does not influence protein disaggregation. The cellular protein quality control machinery thus uses specialized sHsp types in the defense against misfolded protein species.

## 7. References

- Abelson, J.N., Guthrie, C., Fink, G. R. (ed.) (2003) *Guide to yeast genetics and molecular biology*. New York, NY: Academic Press Inc.
- Aguilaniu, H., Gustafsson, L., Rigoulet, M. and Nystrom, T. (2003) Asymmetric inheritance of oxidatively damaged proteins during cytokinesis. *Science*. **299**: 1751-1753.
- Anton, L.C., Schubert, U., Bacik, I., Princiotta, M.F., Wearsch, P.A., Gibbs, J., *et al* (1999) Intracellular localization of proteasomal degradation of a viral antigen. *J Cell Biol*. **146**: 113-124.
- Arrasate, M., Mitra, S., Schweitzer, E.S., Segal, M.R. and Finkbeiner, S. (2004) Inclusion body formation reduces levels of mutant huntingtin and the risk of neuronal death. *Nature*. **431**: 805-810.
- Arrigo, A.P. (2000) sHsp as novel regulators of programmed cell death and tumorigenicity. *Pathol Biol (Paris)*. **48**: 280-288.
- Ayscough, K.R., Stryker, J., Pokala, N., Sanders, M., Crews, P. and Drubin, D.G. (1997) High rates of actin filament turnover in budding yeast and roles for actin in establishment and maintenance of cell polarity revealed using the actin inhibitor latrunculin A. *J Cell Biol*. **137**: 399-416.
- Ban, N., Nissen, P., Hansen, J., Capel, M., Moore, P.B. and Steitz, T.A. (1999) Placement of protein and RNA structures into a 5 Å-resolution map of the 50S ribosomal subunit. *Nature*. **400**: 841-847.
- Basha, E., Friedrich, K.L. and Vierling, E. (2006) The N-terminal arm of small heat shock proteins is important for both chaperone activity and substrate specificity. *J Biol Chem*. **281**: 39943-39952.
- Basha, E., Lee, G.J., Demeler, B. and Vierling, E. (2004) Chaperone activity of cytosolic small heat shock proteins from wheat. *Eur J Biochem*. **271**: 1426-1436.
- Bedford, L., Hay, D., Devoy, A., Paine, S., Powe, D.G., Seth, R., *et al* (2008) Depletion of 26S proteasomes in mouse brain neurons causes neurodegeneration and Lewy-like inclusions resembling human pale bodies. *J Neurosci*. **28**: 8189-8198.
- Ben-Zvi, A.P. and Goloubinoff, P. (2002) Proteinaceous infectious behavior in non-pathogenic proteins is controlled by molecular chaperones. *J Biol Chem*. **277**: 49422-49427.
- Benaroudj, N., Zwickl, P., Seemuller, E., Baumeister, W. and Goldberg, A.L. (2003) ATP hydrolysis by the proteasome regulatory complex PAN serves multiple functions in protein degradation. *Mol Cell*. **11**: 69-78.
- Bence, N.F., Sampat, R.M. and Kopito, R.R. (2001) Impairment of the ubiquitin-proteasome system by protein aggregation. *Science*. **292**: 1552-1555.
- Bennett, E.J., Bence, N.F., Jayakumar, R. and Kopito, R.R. (2005) Global impairment of the ubiquitin-proteasome system by nuclear or cytoplasmic protein aggregates precedes inclusion body formation. *Mol Cell*. **17**: 351-365.

- Bjorkoy, G., Lamark, T., Brech, A., Outzen, H., Perander, M., Overvatn, A., *et al* (2005) p62/SQSTM1 forms protein aggregates degraded by autophagy and has a protective effect on huntingtin-induced cell death. *J Cell Biol.* **171**: 603-614.
- Brady, J.P., Garland, D., Douglas-Tabor, Y., Robison, W.G., Jr., Groome, A. and Wawrousek, E.F. (1997) Targeted disruption of the mouse alpha A-crystallin gene induces cataract and cytoplasmic inclusion bodies containing the small heat shock protein alpha B-crystallin. *Proc Natl Acad Sci U S A.* **94**: 884-889.
- Candido, E.P. (2002) The small heat shock proteins of the nematode *Caenorhabditis elegans*: structure, regulation and biology. *Prog Mol Subcell Biol.* **28**: 61-78.
- Carrio, M.M. and Villaverde, A. (2005) Localization of chaperones DnaK and GroEL in bacterial inclusion bodies. *J Bacteriol.* **187**: 3599-3601.
- Cashikar, A.G., Duennwald, M. and Lindquist, S.L. (2005) A chaperone pathway in protein disaggregation. Hsp26 alters the nature of protein aggregates to facilitate reactivation by Hsp104. *J Biol Chem.* **280**: 23869-23875.
- Cheng, G., Basha, E., Wysocki, V.H. and Vierling, E. (2008) Insights into small heat shock protein and substrate structure during chaperone action derived from hydrogen/deuterium exchange and mass spectrometry. *J Biol Chem.* **283**: 26634-26642.
- Chiti, F. and Dobson, C.M. (2006) Protein misfolding, functional amyloid, and human disease. *Annu Rev Biochem.* **75**: 333-366.
- Ciechanover, A. (1994) The ubiquitin-proteasome proteolytic pathway. *Cell.* **79**: 13-21.
- Cotto, J.J. and Morimoto, R.I. (1999) Stress-induced activation of the heat-shock response: cell and molecular biology of heat-shock factors. *Biochem Soc Symp.* **64**: 105-118.
- de Groot, N.S. and Ventura, S. (2006) Protein activity in bacterial inclusion bodies correlates with predicted aggregation rates. *J Biotechnol.* **125**: 110-113.
- de Groot, N.S., Sabate, R. and Ventura, S. (2009) Amyloids in bacterial inclusion bodies. *Trends Biochem Sci.* **34**: 408-416.
- Dobson, C.M. (2003) Protein folding and misfolding. *Nature.* **426**: 884-890.
- Doglia, S.M., Ami, D., Natalello, A., Gatti-Lafranconi, P. and Lotti, M. (2008) Fourier transform infrared spectroscopy analysis of the conformational quality of recombinant proteins within inclusion bodies. *Biotechnol J.* **3**: 193-201.
- Dougan, D.A., Mogk, A., Zeth, K., Turgay, K. and Bukau, B. (2002) AAA+ proteins and substrate recognition, it all depends on their partner in crime. *FEBS Lett.* **529**: 6-10.
- Dragovic, Z., Broadley, S.A., Shomura, Y., Bracher, A. and Hartl, F.U. (2006) Molecular chaperones of the Hsp110 family act as nucleotide exchange factors of Hsp70s. *Embo J.* **25**: 2519-2528.
- Edskes, H.K., Gray, V.T. and Wickner, R.B. (1999) The [URE3] prion is an aggregated form of Ure2p that can be cured by overexpression of Ure2p fragments. *Proc Natl Acad Sci U S A.* **96**: 1498-1503.

Ehrnsperger, M., Graber, S., Gaestel, M. and Buchner, J. (1997) Binding of non-native protein to Hsp25 during heat shock creates a reservoir of folding intermediates for reactivation. *Embo J.* **16**: 221-229.

Ehrnsperger, M., Lilie, H., Gaestel, M. and Buchner, J. (1999) The dynamics of Hsp25 quaternary structure. Structure and function of different oligomeric species. *J Biol Chem.* **274**: 14867-14874.

Ellis, J. (1987) Proteins as molecular chaperones. *Nature.* **328**: 378-379.

Erjavec, N. and Nystrom, T. (2007) Sir2p-dependent protein segregation gives rise to a superior reactive oxygen species management in the progeny of *Saccharomyces cerevisiae*. *Proc Natl Acad Sci U S A.* **104**: 10877-10881.

Erjavec, N., Larsson, L., Grantham, J. and Nystrom, T. (2007) Accelerated aging and failure to segregate damaged proteins in Sir2 mutants can be suppressed by overproducing the protein aggregation-remodeling factor Hsp104p. *Genes Dev.* **21**: 2410-2421.

Fandrich, M. (2007) On the structural definition of amyloid fibrils and other polypeptide aggregates. *Cell Mol Life Sci.* **64**: 2066-2078.

Fink, A.L. (1998) Protein aggregation: folding aggregates, inclusion bodies and amyloid. *Fold Des.* **3**: R9-23.

Fortun, J., Dunn, W.A., Jr., Joy, S., Li, J. and Notterpek, L. (2003) Emerging role for autophagy in the removal of aggresomes in Schwann cells. *J Neurosci.* **23**: 10672-10680.

Franzmann, T.M., Menhorn, P., Walter, S. and Buchner, J. (2008) Activation of the chaperone Hsp26 is controlled by the rearrangement of its thermosensor domain. *Mol Cell.* **29**: 207-216.

Franzmann, T.M., Wuhr, M., Richter, K., Walter, S. and Buchner, J. (2005) The activation mechanism of Hsp26 does not require dissociation of the oligomer. *J Mol Biol.* **350**: 1083-1093.

Friedrich, K.L., Giese, K.C., Buan, N.R. and Vierling, E. (2004) Interactions between small heat shock protein subunits and substrate in small heat shock protein-substrate complexes. *J Biol Chem.* **279**: 1080-1089.

Fuentealba, L.C., Eivers, E., Geissert, D., Taelman, V. and De Robertis, E.M. (2008) Asymmetric mitosis: Unequal segregation of proteins destined for degradation. *Proc Natl Acad Sci U S A.* **105**: 7732-7737.

Gaestel, M. (2002) sHsp-phosphorylation: enzymes, signaling pathways and functional implications. *Prog Mol Subcell Biol.* **28**: 151-169.

Garcia-Fruitos, E., Gonzalez-Montalban, N., Morell, M., Vera, A., Ferraz, R.M., Aris, A., *et al* (2005) Aggregation as bacterial inclusion bodies does not imply inactivation of enzymes and fluorescent proteins. *Microb Cell Fact.* **4**: 27.

Garcia-Mata, R., Gao, Y.S. and Sztul, E. (2002) Hassles with taking out the garbage: aggravating aggresomes. *Traffic.* **3**: 388-396.

- Garcia-Mata, R., Bebok, Z., Sorscher, E.J. and Sztul, E.S. (1999) Characterization and dynamics of aggresome formation by a cytosolic GFP-chimera. *J Cell Biol.* **146**: 1239-1254.
- Gavin, R.H. (ed.) (2009) *Cytoskeleton Methods and Protocols, 2nd ed.* New York, NY: Humana Press.
- Glover, J.R. and Lindquist, S. (1998) Hsp104, Hsp70, and Hsp40: a novel chaperone system that rescues previously aggregated proteins. *Cell.* **94**: 73-82.
- Goldberg, A.L. (1995) Functions of the proteasome: the lysis at the end of the tunnel. *Science.* **268**: 522-523.
- Goldberg, A.L. (2003) Protein degradation and protection against misfolded or damaged proteins. *Nature.* **426**: 895-899.
- Gragerov, A.I., Martin, E.S., Krupenko, M.A., Kashlev, M.V. and Nikiforov, V.G. (1991) Protein aggregation and inclusion body formation in *Escherichia coli* rpoH mutant defective in heat shock protein induction. *FEBS Lett.* **291**: 222-224.
- Groll, M., Bajorek, M., Kohler, A., Moroder, L., Rubin, D.M., Huber, R., *et al* (2000) A gated channel into the proteasome core particle. *Nat Struct Biol.* **7**: 1062-1067.
- Gu, J., Emerman, M. and Sandmeyer, S. (1997) Small heat shock protein suppression of Vpr-induced cytoskeletal defects in budding yeast. *Mol Cell Biol.* **17**: 4033-4042.
- Haley, D.A., Horwitz, J. and Stewart, P.L. (1998) The small heat-shock protein, alphaB-crystallin, has a variable quaternary structure. *J Mol Biol.* **277**: 27-35.
- Hanahan, D. (1983) Studies on transformation of *Escherichia coli* with plasmids. *J Mol Biol.* **166**: 557-580.
- Hara, T., Nakamura, K., Matsui, M., Yamamoto, A., Nakahara, Y., Suzuki-Migishima, R., *et al* (2006) Suppression of basal autophagy in neural cells causes neurodegenerative disease in mice. *Nature.* **441**: 885-889.
- Haslbeck, M., Franzmann, T., Weinfurter, D. and Buchner, J. (2005a) Some like it hot: the structure and function of small heat-shock proteins. *Nat Struct Mol Biol.* **12**: 842-846.
- Haslbeck, M., Miess, A., Stromer, T., Walter, S. and Buchner, J. (2005b) Disassembling protein aggregates in the yeast cytosol. The cooperation of Hsp26 with Ssa1 and Hsp104. *J Biol Chem.* **280**: 23861-23868.
- Haslbeck, M., Braun, N., Stromer, T., Richter, B., Model, N., Weinkauff, S. and Buchner, J. (2004a) Hsp42 is the general small heat shock protein in the cytosol of *Saccharomyces cerevisiae*. *Embo J.* **23**: 638-649.
- Haslbeck, M., Ignatiou, A., Saibil, H., Helmich, S., Frenzl, E., Stromer, T. and Buchner, J. (2004b) A domain in the N-terminal part of Hsp26 is essential for chaperone function and oligomerization. *J Mol Biol.* **343**: 445-455.
- Haslbeck, M., Walke, S., Stromer, T., Ehrnsperger, M., White, H.E., Chen, S., *et al* (1999a) Hsp26: a temperature-regulated chaperone. *Embo J.* **18**: 6744-6751.

- Haslbeck, M., Walke, S., Stromer, T., Ehrnsperger, M., White, H.E., Chen, S., *et al* (1999b) Hsp26: a temperature-regulated chaperone. *EMBO J.* **18**: 6744-6751.
- Haslberger, T., Weibezahn, J., Zahn, R., Lee, S., Tsai, F.T., Bukau, B. and Mogk, A. (2007) M domains couple the ClpB threading motor with the DnaK chaperone activity. *Mol Cell.* **25**: 247-260.
- Haslberger, T., Zdanowicz, A., Brand, I., Kirstein, J., Turgay, K., Mogk, A. and Bukau, B. (2008) Protein disaggregation by the AAA+ chaperone ClpB involves partial threading of looped polypeptide segments. *Nat Struct Mol Biol.* **15**: 641-650.
- Heikkila, J.J. (2004) Regulation and function of small heat shock protein genes during amphibian development. *J Cell Biochem.* **93**: 672-680.
- Henderson, K.A. and Gottschling, D.E. (2008) A mother's sacrifice: what is she keeping for herself? *Curr Opin Cell Biol.* **20**: 723-728.
- Holmberg, C.I., Staniszewski, K.E., Mensah, K.N., Matouschek, A. and Morimoto, R.I. (2004) Inefficient degradation of truncated polyglutamine proteins by the proteasome. *Embo J.* **23**: 4307-4318.
- Horwitz, J. (1992) Alpha-crystallin can function as a molecular chaperone. *Proc Natl Acad Sci U S A.* **89**: 10449-10453.
- Ishikawa, T., Beuron, F., Kessel, M., Wickner, S., Maurizi, M.R. and Steven, A.C. (2001) Translocation pathway of protein substrates in ClpAP protease. *Proc Natl Acad Sci U S A.* **98**: 4328-4333.
- Iwata, A., Riley, B.E., Johnston, J.A. and Kopito, R.R. (2005) HDAC6 and microtubules are required for autophagic degradation of aggregated huntingtin. *J Biol Chem.* **280**: 40282-40292.
- Jaya, N., Garcia, V. and Vierling, E. (2009) Substrate binding site flexibility of the small heat shock protein molecular chaperones. *Proc Natl Acad Sci U S A.* **106**: 15604-15609.
- Jeong, H., Then, F., Melia, T.J., Jr., Mazzulli, J.R., Cui, L., Savas, J.N., *et al* (2009) Acetylation targets mutant huntingtin to autophagosomes for degradation. *Cell.* **137**: 60-72.
- Johnston, J.A., Ward, C.L. and Kopito, R.R. (1998) Aggresomes: a cellular response to misfolded proteins. *J Cell Biol.* **143**: 1883-1898.
- Johnston, J.A., Illing, M.E. and Kopito, R.R. (2002) Cytoplasmic dynein/dynactin mediates the assembly of aggresomes. *Cell Motil Cytoskeleton.* **53**: 26-38.
- Junn, E., Lee, S.S., Suhr, U.T. and Mouradian, M.M. (2002) Parkin accumulation in aggresomes due to proteasome impairment. *J Biol Chem.* **277**: 47870-47877.
- Kabani, M., Beckerich, J.M. and Brodsky, J.L. (2002) Nucleotide exchange factor for the yeast Hsp70 molecular chaperone Ssa1p. *Mol Cell Biol.* **22**: 4677-4689.
- Kaganovich, D., Kopito, R. and Frydman, J. (2008) Misfolded proteins partition between two distinct quality control compartments. *Nature.* **454**: 1088-1095.

- Kahle, P.J. and Haass, C. (2004) How does parkin ligate ubiquitin to Parkinson's disease? *EMBO Rep.* **5**: 681-685.
- Kappe, G., Leunissen, J.A. and de Jong, W.W. (2002) Evolution and diversity of prokaryotic small heat shock proteins. *Prog Mol Subcell Biol.* **28**: 1-17.
- Kawaguchi, Y., Kovacs, J.J., McLaurin, A., Vance, J.M., Ito, A. and Yao, T.P. (2003) The deacetylase HDAC6 regulates aggresome formation and cell viability in response to misfolded protein stress. *Cell.* **115**: 727-738.
- Kennedy, B.K., Austriaco, N.R., Jr. and Guarente, L. (1994) Daughter cells of *Saccharomyces cerevisiae* from old mothers display a reduced life span. *J Cell Biol.* **127**: 1985-1993.
- Kim, K.K., Kim, R. and Kim, S.H. (1998) Crystal structure of a small heat-shock protein. *Nature.* **394**: 595-599.
- Kirkin, V., McEwan, D.G., Novak, I. and Dikic, I. (2009a) A role for ubiquitin in selective autophagy. *Mol Cell.* **34**: 259-269.
- Kirkin, V., Lamark, T., Sou, Y.S., Bjorkoy, G., Nunn, J.L., Bruun, J.A., *et al* (2009b) A role for NBR1 in autophagosomal degradation of ubiquitylated substrates. *Mol Cell.* **33**: 505-516.
- Kisselev, A.F., Akopian, T.N. and Goldberg, A.L. (1998) Range of sizes of peptide products generated during degradation of different proteins by archaeal proteasomes. *J Biol Chem.* **273**: 1982-1989.
- Koken, M.H., Odijk, H.H., van Duin, M., Fornerod, M. and Hoeijmakers, J.H. (1993) Augmentation of protein production by a combination of the T7 RNA polymerase system and ubiquitin fusion: overproduction of the human DNA repair protein, ERCC1, as a ubiquitin fusion protein in *Escherichia coli*. *Biochem Biophys Res Commun.* **195**: 643-653.
- Komatsu, M., Waguri, S., Chiba, T., Murata, S., Iwata, J., Tanida, I., *et al* (2006) Loss of autophagy in the central nervous system causes neurodegeneration in mice. *Nature.* **441**: 880-884.
- Kopito, R.R. (2000) Aggresomes, inclusion bodies and protein aggregation. *Trends Cell Biol.* **10**: 524-530.
- Korolchuk, V.I., Mansilla, A., Menzies, F.M. and Rubinsztein, D.C. (2009) Autophagy inhibition compromises degradation of ubiquitin-proteasome pathway substrates. *Mol Cell.* **33**: 517-527.
- Koteiche, H.A. and McHaourab, H.S. (2003) Mechanism of chaperone function in small heat-shock proteins. Phosphorylation-induced activation of two-mode binding in alphaB-crystallin. *J Biol Chem.* **278**: 10361-10367.
- Krobitsch, S. and Lindquist, S. (2000) Aggregation of huntingtin in yeast varies with the length of the polyglutamine expansion and the expression of chaperone proteins. *Proc Natl Acad Sci U S A.* **97**: 1589-1594.
- Krueger-Naug, A.M., Plumier, J.C., Hopkins, D.A. and Currie, R.W. (2002) Hsp27 in the nervous system: expression in pathophysiology and in the aging brain. *Prog Mol Subcell Biol.* **28**: 235-251.

- Laskowska, E., Bohdanowicz, J., Kuczynska-Wisnik, D., Matuszewska, E., Kedzierska, S. and Taylor, A. (2004) Aggregation of heat-shock-denatured, endogenous proteins and distribution of the IbpA/B and Fda marker-proteins in *Escherichia coli* WT and grpE280 cells. *Microbiology*. **150**: 247-259.
- Lee, D.H. and Goldberg, A.L. (1998) Proteasome inhibitors: valuable new tools for cell biologists. *Trends Cell Biol.* **8**: 397-403.
- Lee, S., Owen, H.A., Prochaska, D.J. and Barnum, S.R. (2000) HSP16.6 is involved in the development of thermotolerance and thylakoid stability in the unicellular cyanobacterium, *Synechocystis* sp. PCC 6803. *Curr Microbiol.* **40**: 283-287.
- Liberek, K., Marszalek, J., Ang, D., Georgopoulos, C. and Zylicz, M. (1991) *Escherichia coli* DnaJ and GrpE heat shock proteins jointly stimulate ATPase activity of DnaK. *Proc Natl Acad Sci U S A.* **88**: 2874-2878.
- Lindner, A.B., Madden, R., Demarez, A., Stewart, E.J. and Taddei, F. (2008) Asymmetric segregation of protein aggregates is associated with cellular aging and rejuvenation. *Proc Natl Acad Sci U S A.* **105**: 3076-3081.
- Liu, L., Ghosh, J.G., Clark, J.I. and Jiang, S. (2006) Studies of alphaB crystallin subunit dynamics by surface plasmon resonance. *Anal Biochem.* **350**: 186-195.
- Lowe, J., McDermott, H., Pike, I., Spendlove, I., Landon, M. and Mayer, R.J. (1992) alpha B crystallin expression in non-lenticular tissues and selective presence in ubiquitylated inclusion bodies in human disease. *J Pathol.* **166**: 61-68.
- Lum, R., Tkach, J.M., Vierling, E. and Glover, J.R. (2004) Evidence for an unfolding/threading mechanism for protein disaggregation by *Saccharomyces cerevisiae* Hsp104. *J Biol Chem.* **279**: 29139-29146.
- Maisonneuve, E., Ezraty, B. and Dukan, S. (2008) Protein aggregates: an aging factor involved in cell death. *J Bacteriol.* **190**: 6070-6075.
- Maniatis, T., Sambrook, J., Fritsch, E. F. (ed.) (1989) *Molecular cloning: a laboratory manual, 2nd ed.* Cold Spring Harbor, NY: Cold Spring Harbor Laboratory Press.
- Martin-Aparicio, E., Yamamoto, A., Hernandez, F., Hen, R., Avila, J. and Lucas, J.J. (2001) Proteasomal-dependent aggregate reversal and absence of cell death in a conditional mouse model of Huntington's disease. *J Neurosci.* **21**: 8772-8781.
- McCarty, J.S., Buchberger, A., Reinstein, J. and Bukau, B. (1995) The role of ATP in the functional cycle of the DnaK chaperone system. *J Mol Biol.* **249**: 126-137.
- McClellan, A.J., Scott, M.D. and Frydman, J. (2005) Folding and quality control of the VHL tumor suppressor proceed through distinct chaperone pathways. *Cell.* **121**: 739-748.
- Meriin, A.B., Zhang, X., He, X., Newnam, G.P., Chernoff, Y.O. and Sherman, M.Y. (2002) Huntington toxicity in yeast model depends on polyglutamine aggregation mediated by a prion-like protein Rnq1. *J Cell Biol.* **157**: 997-1004.
- Miroshnichenko, S., Tripp, J., Nieden, U., Neumann, D., Conrad, U. and Manteuffel, R. (2005) Immunomodulation of function of small heat shock proteins prevents their assembly

- into heat stress granules and results in cell death at sublethal temperatures. *Plant J.* **41**: 269-281.
- Mogk, A., Schmidt, R. and Bukau, B. (2007) The N-end rule pathway for regulated proteolysis: prokaryotic and eukaryotic strategies. *Trends Cell Biol.* **17**: 165-172.
- Mogk, A., Schlieker, C., Friedrich, K.L., Schonfeld, H.J., Vierling, E. and Bukau, B. (2003) Refolding of substrates bound to small Hsps relies on a disaggregation reaction mediated most efficiently by ClpB/DnaK. *J Biol Chem.* **278**: 31033-31042.
- Morell, M., Bravo, R., Espargaro, A., Sisquella, X., Aviles, F.X., Fernandez-Busquets, X. and Ventura, S. (2008) Inclusion bodies: specificity in their aggregation process and amyloid-like structure. *Biochim Biophys Acta.* **1783**: 1815-1825.
- Mortimer, R.K. and Johnston, J.R. (1959) Life span of individual yeast cells. *Nature.* **183**: 1751-1752.
- Muchowski, P.J. and Wacker, J.L. (2005) Modulation of neurodegeneration by molecular chaperones. *Nat Rev Neurosci.* **6**: 11-22.
- Nakatogawa, H., Suzuki, K., Kamada, Y. and Ohsumi, Y. (2009) Dynamics and diversity in autophagy mechanisms: lessons from yeast. *Nat Rev Mol Cell Biol.* **10**: 458-467.
- Nucifora, F.C., Jr., Sasaki, M., Peters, M.F., Huang, H., Cooper, J.K., Yamada, M., *et al* (2001) Interference by huntingtin and atrophin-1 with cbp-mediated transcription leading to cellular toxicity. *Science.* **291**: 2423-2428.
- Nystrom, T. (2005) Role of oxidative carbonylation in protein quality control and senescence. *Embo J.* **24**: 1311-1317.
- Ogura, T. and Wilkinson, A.J. (2001) AAA+ superfamily ATPases: common structure--diverse function. *Genes Cells.* **6**: 575-597.
- Olzmann, J.A. and Chin, L.S. (2008) Parkin-mediated K63-linked polyubiquitylation: a signal for targeting misfolded proteins to the aggresome-autophagy pathway. *Autophagy.* **4**: 85-87.
- Ortega, J., Singh, S.K., Ishikawa, T., Maurizi, M.R. and Steven, A.C. (2000) Visualization of substrate binding and translocation by the ATP-dependent protease, ClpXP. *Mol Cell.* **6**: 1515-1521.
- Pandey, U.B., Nie, Z., Batlevi, Y., McCray, B.A., Ritson, G.P., Nedelsky, N.B., *et al* (2007) HDAC6 rescues neurodegeneration and provides an essential link between autophagy and the UPS. *Nature.* **447**: 859-863.
- Pankiv, S., Clausen, T.H., Lamark, T., Brech, A., Bruun, J.A., Outzen, H., *et al* (2007) p62/SQSTM1 binds directly to Atg8/LC3 to facilitate degradation of ubiquitylated protein aggregates by autophagy. *J Biol Chem.* **282**: 24131-24145.
- Parsell, D.A., Kowal, A.S., Singer, M.A. and Lindquist, S. (1994) Protein disaggregation mediated by heat-shock protein Hsp104. *Nature.* **372**: 475-478.
- Patino, M.M., Liu, J.J., Glover, J.R. and Lindquist, S. (1996) Support for the prion hypothesis for inheritance of a phenotypic trait in yeast. *Science.* **273**: 622-626.

- Piel, M., Meyer, P., Khodjakov, A., Rieder, C.L. and Bornens, M. (2000) The respective contributions of the mother and daughter centrioles to centrosome activity and behavior in vertebrate cells. *J Cell Biol.* **149**: 317-330.
- Pierpaoli, E.V., Sandmeier, E., Baici, A., Schonfeld, H.J., Gisler, S. and Christen, P. (1997) The power stroke of the DnaK/DnaJ/GrpE molecular chaperone system. *J Mol Biol.* **269**: 757-768.
- Powers, E.T., Morimoto, R.I., Dillin, A., Kelly, J.W. and Balch, W.E. (2009) Biological and chemical approaches to diseases of proteostasis deficiency. *Annu Rev Biochem.* **78**: 959-991.
- Queitsch, C., Hong, S.W., Vierling, E. and Lindquist, S. (2000) Heat shock protein 101 plays a crucial role in thermotolerance in Arabidopsis. *Plant Cell.* **12**: 479-492.
- Rajan, R.S., Illing, M.E., Bence, N.F. and Kopito, R.R. (2001) Specificity in intracellular protein aggregation and inclusion body formation. *Proc Natl Acad Sci U S A.* **98**: 13060-13065.
- Ratajczak, E., Zietkiewicz, S. and Liberek, K. (2009) Distinct activities of Escherichia coli small heat shock proteins IbpA and IbpB promote efficient protein disaggregation. *J Mol Biol.* **386**: 178-189.
- Raviol, H., Sadlish, H., Rodriguez, F., Mayer, M.P. and Bukau, B. (2006) Chaperone network in the yeast cytosol: Hsp110 is revealed as an Hsp70 nucleotide exchange factor. *Embo J.* **25**: 2510-2518.
- Rebollo, E., Sampaio, P., Januschke, J., Llamazares, S., Varmark, H. and Gonzalez, C. (2007) Functionally unequal centrosomes drive spindle orientation in asymmetrically dividing Drosophila neural stem cells. *Dev Cell.* **12**: 467-474.
- Renkawek, K., de Jong, W.W., Merck, K.B., Frenken, C.W., van Workum, F.P. and Bosman, G.J. (1992) alpha B-crystallin is present in reactive glia in Creutzfeldt-Jakob disease. *Acta Neuropathol.* **83**: 324-327.
- Rizzo, M.A., Springer, G.H., Granada, B. and Piston, D.W. (2004) An improved cyan fluorescent protein variant useful for FRET. *Nat Biotechnol.* **22**: 445-449.
- Rokney, A., Shagan, M., Kessel, M., Smith, Y., Rosenshine, I. and Oppenheim, A.B. (2009) E. coli transports aggregated proteins to the poles by a specific and energy-dependent process. *J Mol Biol.* **392**: 589-601.
- Rubinsztein, D.C. (2006) The roles of intracellular protein-degradation pathways in neurodegeneration. *Nature.* **443**: 780-786.
- Rujano, M.A., Bosveld, F., Salomons, F.A., Dijk, F., van Waarde, M.A., van der Want, J.J., et al (2006) Polarised asymmetric inheritance of accumulated protein damage in higher eukaryotes. *PLoS Biol.* **4**: e417.
- Rusan, N.M. and Peifer, M. (2007) A role for a novel centrosome cycle in asymmetric cell division. *J Cell Biol.* **177**: 13-20.
- Saint-Ruf, C., Taddei, F. and Matic, I. (2004) Stress and survival of aging Escherichia coli rpoS colonies. *Genetics.* **168**: 541-546.

- Sanchez, Y. and Lindquist, S.L. (1990) HSP104 required for induced thermotolerance. *Science*. **248**: 1112-1115.
- Schmidt, R., Bukau, B. and Mogk, A. (2009) Principles of general and regulatory proteolysis by AAA+ proteases in Escherichia coli. *Res Microbiol*. **160**: 629-636.
- Schroder, H., Langer, T., Hartl, F.U. and Bukau, B. (1993) DnaK, DnaJ and GrpE form a cellular chaperone machinery capable of repairing heat-induced protein damage. *Embo J*. **12**: 4137-4144.
- Sheff, M.A. and Thorn, K.S. (2004) Optimized cassettes for fluorescent protein tagging in Saccharomyces cerevisiae. *Yeast*. **21**: 661-670.
- Sikorski, R.S. and Hieter, P. (1989) A system of shuttle vectors and yeast host strains designed for efficient manipulation of DNA in Saccharomyces cerevisiae. *Genetics*. **122**: 19-27.
- Singh, S.K., Grimaud, R., Hoskins, J.R., Wickner, S. and Maurizi, M.R. (2000) Unfolding and internalization of proteins by the ATP-dependent proteases ClpXP and ClpAP. *Proc Natl Acad Sci U S A*. **97**: 8898-8903.
- Singhvi, A. and Garriga, G. (2009) Asymmetric divisions, aggresomes and apoptosis. *Trends Cell Biol*. **19**: 1-7.
- Specht, S., Miller, S., Mogk, A., Bukau, B. (2010).
- Squier, T.C. (2001) Oxidative stress and protein aggregation during biological aging. *Exp Gerontol*. **36**: 1539-1550.
- Stearns, T. (2001) Centrosome duplication. a centriolar pas de deux. *Cell*. **105**: 417-420.
- Stefani, M. and Dobson, C.M. (2003) Protein aggregation and aggregate toxicity: new insights into protein folding, misfolding diseases and biological evolution. *J Mol Med*. **81**: 678-699.
- Stromer, T., Ehrnsperger, M., Gaestel, M. and Buchner, J. (2003) Analysis of the interaction of small heat shock proteins with unfolding proteins. *J Biol Chem*. **278**: 18015-18021.
- Stromer, T., Fischer, E., Richter, K., Haslbeck, M. and Buchner, J. (2004) Analysis of the regulation of the molecular chaperone Hsp26 by temperature-induced dissociation: the N-terminal domain is important for oligomer assembly and the binding of unfolding proteins. *J Biol Chem*. **279**: 11222-11228.
- Szabo, A., Langer, T., Schroder, H., Flanagan, J., Bukau, B. and Hartl, F.U. (1994) The ATP hydrolysis-dependent reaction cycle of the Escherichia coli Hsp70 system DnaK, DnaJ, and GrpE. *Proc Natl Acad Sci U S A*. **91**: 10345-10349.
- Tan, J.M., Wong, E.S., Kirkpatrick, D.S., Pletnikova, O., Ko, H.S., Tay, S.P., *et al* (2008) Lysine 63-linked ubiquitylation promotes the formation and autophagic clearance of protein inclusions associated with neurodegenerative diseases. *Hum Mol Genet*. **17**: 431-439.

- Tessarz, P., Schwarz, M., Mogk, A. and Bukau, B. (2009) The yeast AAA+ chaperone Hsp104 is part of a network that links the actin cytoskeleton with the inheritance of damaged proteins. *Mol Cell Biol.* **29**: 3738-3745.
- Theysen, H., Schuster, H.P., Packschies, L., Bukau, B. and Reinstein, J. (1996) The second step of ATP binding to DnaK induces peptide release. *J Mol Biol.* **263**: 657-670.
- Van Montfort, R., Slingsby, C. and Vierling, E. (2001a) Structure and function of the small heat shock protein/alpha-crystallin family of molecular chaperones. *Adv Protein Chem.* **59**: 105-156.
- van Montfort, R.L., Basha, E., Friedrich, K.L., Slingsby, C. and Vierling, E. (2001b) Crystal structure and assembly of a eukaryotic small heat shock protein. *Nat Struct Biol.* **8**: 1025-1030.
- Venkatraman, P., Wetzel, R., Tanaka, M., Nukina, N. and Goldberg, A.L. (2004) Eukaryotic proteasomes cannot digest polyglutamine sequences and release them during degradation of polyglutamine-containing proteins. *Mol Cell.* **14**: 95-104.
- Ventura, S. and Villaverde, A. (2006) Protein quality in bacterial inclusion bodies. *Trends Biotechnol.* **24**: 179-185.
- Verhoef, L.G., Lindsten, K., Masucci, M.G. and Dantuma, N.P. (2002) Aggregate formation inhibits proteasomal degradation of polyglutamine proteins. *Hum Mol Genet.* **11**: 2689-2700.
- Waelter, S., Boeddrich, A., Lurz, R., Scherzinger, E., Lueder, G., Lehrach, H. and Wanker, E.E. (2001) Accumulation of mutant huntingtin fragments in aggresome-like inclusion bodies as a result of insufficient protein degradation. *Mol Biol Cell.* **12**: 1393-1407.
- Webb, J.L., Ravikumar, B., Atkins, J., Skepper, J.N. and Rubinsztein, D.C. (2003) Alpha-Synuclein is degraded by both autophagy and the proteasome. *J Biol Chem.* **278**: 25009-25013.
- Weber-Ban, E.U., Reid, B.G., Miranker, A.D. and Horwich, A.L. (1999) Global unfolding of a substrate protein by the Hsp100 chaperone ClpA. *Nature.* **401**: 90-93.
- Weibezahn, J., Schlieker, C., Tessarz, P., Mogk, A. and Bukau, B. (2005) Novel insights into the mechanism of chaperone-assisted protein disaggregation. *Biol Chem.* **386**: 739-744.
- Weibezahn, J., Tessarz, P., Schlieker, C., Zahn, R., Maglica, Z., Lee, S., *et al* (2004) Thermotolerance requires refolding of aggregated proteins by substrate translocation through the central pore of ClpB. *Cell.* **119**: 653-665.
- Wetzel, R. (1994) Mutations and off-pathway aggregation of proteins. *Trends Biotechnol.* **12**: 193-198.
- White, H.E., Orlova, E.V., Chen, S., Wang, L., Ignatiou, A., Gowen, B., *et al* (2006) Multiple distinct assemblies reveal conformational flexibility in the small heat shock protein Hsp26. *Structure.* **14**: 1197-1204.
- Wickner, S., Maurizi, M.R. and Gottesman, S. (1999) Posttranslational quality control: folding, refolding, and degrading proteins. *Science.* **286**: 1888-1893.

Wigley, W.C., Fabunmi, R.P., Lee, M.G., Marino, C.R., Muallem, S., DeMartino, G.N. and Thomas, P.J. (1999) Dynamic association of proteasomal machinery with the centrosome. *J Cell Biol.* **145**: 481-490.

Winkler, J., Seybert, A., König, K., Pruggnaller, K., Haselmann, U., Sourjik, V., Weiss, M., Frangakis, A.S., Mogk, A. and Bukau, B. (2010) Quantitative and spatio-temporal features of protein aggregation in *E. coli* and consequences on protein quality control and cellular aging. In *Submitted*, pp. -.

Wojcik, C., Schroeter, D., Wilk, S., Lamprecht, J. and Paweletz, N. (1996) Ubiquitin-mediated proteolysis centers in HeLa cells: indication from studies of an inhibitor of the chymotrypsin-like activity of the proteasome. *Eur J Cell Biol.* **71**: 311-318.

Wooten, M.W., Geetha, T., Babu, J.R., Seibenhener, M.L., Peng, J., Cox, N., *et al* (2008) Essential role of sequestosome 1/p62 in regulating accumulation of Lys63-ubiquitylated proteins. *J Biol Chem.* **283**: 6783-6789.

Yamashita, Y.M., Mahowald, A.P., Perlin, J.R. and Fuller, M.T. (2007) Asymmetric inheritance of mother versus daughter centrosome in stem cell division. *Science.* **315**: 518-521.

Yang, H.C. and Pon, L.A. (2002) Actin cable dynamics in budding yeast. *Proc Natl Acad Sci U S A.* **99**: 751-756.

## 8. Abbreviations

AAA+	ATPases associated with a variety of cellular activities
ADP	adenosine diphosphate
ATP	adenosine triphosphate
bp	base-pair
<i>C. elegans</i>	<i>Caenorhabditis elegans</i>
CHX	cycloheximide
CFP	cyan fluorescent protein
CTE	C-terminal extension
dd	double-distilled
DMSO	dimethylsulfoxide
DNA	deoxyribonucleic acid
dNTPs	deoxyribonucleic triphosphate
DTT	dithiothreitol
<i>E. coli</i>	<i>Escherichia coli</i>
EDTA	ethylenediaminetetraacetic acid
EtOH	ethanol
FLIP	Fluorescence Loss in Photobleaching
FRET	Fluorescence Energy Transfer
hr	hour
Hsp	heat shock protein
IPOD	insoluble protein deposit
JUNQ	juxtannuclear quality control
kDa	kilo Dalton
LatA	latrunculin A
M	molar
MDH	malate dehydrogenase
min	minutes
$\mu$ M	micromolar
mM	millimolar
nm	nanometer
nt	nucleotides
NTD	N-terminal domain

PAGE	polyacrylamide gel electrophoresis
PBS	phosphate-buffered saline
PCR	polymerase chain reaction
psi	pounds per square inch
PVDF	polyvinylidene fluoride
RNA	ribonucleic acid
rpm	revolutions per minute
S	Svedberg unit
sec	seconds
<i>S. cerevisiae</i>	<i>Saccharomyces cerevisiae</i>
SDS	sodium dodecyl sulfate
sHsp	small heat shock protein
UV	ultraviolet
v/v	volume (of solute) per volume (of solvent)
WT	wild type
w/v	weight (of solute) per volume (of solvent)
YFP	yellow fluorescent protein

## 9. Acknowledgements

Bernd, I would like to express my gratitude to you for giving me the opportunity to perform my Ph.D. studies in your laboratory. Deciding between Zurich University and your group, I'm very happy to have accepted your offer. Your enthusiastic leadership has had profound impact on the outcome of this work. Besides your intellectual input, I would also like to thank you for always being a very kind boss and competitive volleyball partner.

Axel, I'm very grateful for your constant support and friendship. You helped shaping a great part of my project. I really appreciate your permanent availability to discuss latest results (in both science and soccer) and plan experiments. I would like to express my gratitude for your assistance while writing the publications and dissertation and would like to thank you for rapid and high quality corrections.

Prof. Elmar Schiebel, I would like to thank you for fruitful and inspiring discussion and ideas regarding the cytoskeleton part of my project. Moreover, I'm grateful to you for being the co-referee of this study.

Jens, I would like to thank you for discussion, inspiring ideas, and proof reading of the manuscript.

Lab members, I gladly express my gratitude to you for providing advice, discussion, and reagents for the experimental work. I also thank you for the fun atmosphere and being friendly companions in and outside the lab. I'd especially like to thank: the "Clp" and "Yeast" groups for scientific exchange, ideas, and discussion as well as fun (beach-)volleyball games, watching soccer evenings, Kubb and table tennis championships, lunch breaks with detailed analysis of every major sports event, handball championship afternoons, and board game evenings among other things; Regina for help regarding whatever experimental issue; Ronny for being a nice and helpful roommate; Stephi for the fruitful collaboration.

I acknowledge Ulrike Engel and Christian Ackermann of the Nikon Imaging Center Heidelberg for the great help in performing microscopy and support in data analysis, Holger Lorenz for microscopy support, and Yves-Michel Cully for help with the model.

I'm grateful to the Stiftung Stipendien-Fonds of the Verbandes der Chemischen Industrie e.V. for providing me with the Chemistry Fund – Ph.D. Fellowship.

Meine Familie, ihr seit das Rückgrat, ohne das ich mich nicht fortbewegen könnte. Ihr gewährt mir jederzeit bedingungslose Unterstützung. Ich danke euch für Rückhalt, auf den ich jederzeit zurückgreifen kann. Ich habe mich stets gefreut, wenn ich euch endlich wieder einmal in Berlin besuchen konnte oder ihr nach Heidelberg gereist seid.

Meine Eltern, ich danke euch dafür, dass ihr mich bis jetzt bei jeder Entscheidung unterstützt habt, egal in welche Richtung sie auch gegangen sein mag. Man kann sich Eltern wie euch nur wünschen. Jan, Miri, Leo und Lilly, ich danke euch für viel Liebe und ein vierfach warmes Willkommen bei jedem Berlinbesuch. Til, ich habe mich sehr über deine regelmäßigen Besuche gefreut und dafür, dass du deine Hand jederzeit für mich ins Feuer legen würdest, wenn es denn nötig wäre. Tobi, es ist toll, dass du nur einen Katzensprung entfernt wohnst und wir so viele schöne Tage miteinander teilen konnten, sei es denn nun bei vielfältigen Sportarten, Brettspielen, Pokerspielen, Radfahren und vielem mehr. Meine Großeltern Specht, so aufgeschlossene und liebevolle Großeltern wie euch kann man sich nur wünschen. Oma Sommerfeld, ich danke dir für großzügige Unterstützung und die kulinarischen Freuden während meiner Berlinaufenthalte.

Aga, auch wenn der Tag noch so lang war im Labor oder einfach alles schief ging, ich hatte und habe immer einen Lichtblick, auf den ich mich zu Hause freuen konnte und kann. Ich danke dir für die Unterstützung, zeitweilige Nachsicht und einfühlsame Partnerschaft. Aga meiner Seele und Aga meines Herzens.